Volume 21 | Suppl. 1 | January 2019
ISSN 1099-5129 (Print)
ISSN 1532-2092 (Online)
academic.oup.com/europace

EHRA
European Heart Rhythm Association

EP Europace

Supplements

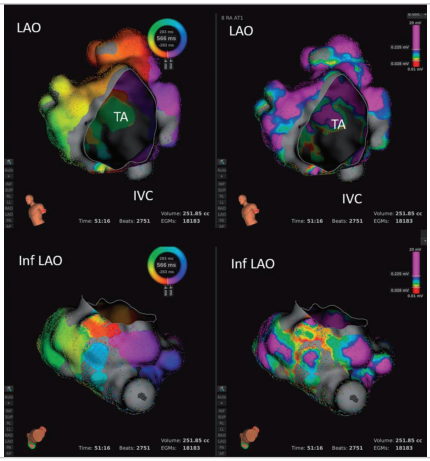

CTI re-entry in a patient with mitral atresia, a common atrium, and previous ablation. See figure legend on page i47.

- Advanced Mapping Capabilities

Member of the ESC Journal Family

OXFORD UNIVERSITY PRESS

ESC European Society of Cardiology

EP-614903-AA

EP — Europace

https://academic.oup.com/europace

EP-614903-AA

Advanced Mapping Capabilities

Guest Editors

Sabine Ernst

Stephan Willems

This supplement was supported by an unrestricted grant from the Boston Scientific.

EP-614903-AA

Aims and Scope

EP — Europace — The **Euro**pean Journal of **P**acing, **A**rrhythmias and **C**ardiac **E**lectrophysiology of the European Heart Rhythm Association and the European Society of Cardiology. The journal aims to provide an avenue of communication of top quality European and international original scientific work and reviews in the fields of Arrhythmias, Pacing and Cellular Electrophysiology. The 2012 impact factor of EP is 2.765. The Journal offers the reader a collection of contemporary original peer-reviewed papers, invited papers and editorial comments together with book reviews and correspondence. The journal is affiliated with the Working Groups on e-Cardiology and Cardiac Cellular Electrophysiology of the European Society of Cardiology.

A subscription to *EP — Europace* comprises 12 issues (plus *EP — Europace Supplements*). All prices include postage, and for subscribers outside the UK delivery is by Standard Air. Advance Access contains papers that have reached corrected proof stage, but have not yet been included within an issue. Advance Access is updated daily.

Annual subscription rate (Volume 21, 12 issues + supplements, 2019)
Institutional
Academic/Non profit only - print and online: £1273.00/$2420.00/€1910.00
Academic/Non profit only - online only: £944.00/$1794.00/€1416.00
Academic/Non profit only - print only: £1171.00/$2226.00/€1757.00
Corporate - print and online: £1624.00/$3085.00/€2436.00
Corporate - online only: £1180.00/$2242.00/€1770.00
Corporate - print only: £1497.00/$2843.00/€2244.00
Personal
Print edition and individual online access: £328.00/$623.00/€492.00
Please note: US$ rate applies to US & Canada, Euros applies to Europe, UK£ applies to UK and Rest of World.

There may be other subscription rates available; for a complete listing please visit https://academic.oup.com/europace/subscribe.

Full prepayment, in the correct currency, is required for all orders. Orders are regarded as firm and payments are not refundable. Subscriptions are accepted and entered on a complete volume basis. Claims cannot be considered more than FOUR months after publication or date of order, whichever is later. All subscriptions in Canada are subject to GST. Subscriptions in the EEC may be subject to European VAT. If registered, please supply details to avoid unnecessary charges. For subscriptions that include online versions, a proportion of the subscription price may be subject to UK VAT. Personal rate subscriptions are only available if payment is made by personal cheque or credit card and delivery is to a private address.

The current year and two previous years' issues are available from Oxford University Press. Previous volumes can be obtained from the Periodicals Service Company at http://www.periodicals.com/oxford.html or Periodicals Service Company, 11 Main Street, Germantown, NY 12526, USA. E-mail: psc@periodicals.com. Tel: (518) 537-4700. Fax: (518) 537-5899.

For further information, please contact: Journals Customer Service Department, Oxford University Press, Great Clarendon Street, Oxford OX2 6DP, UK. E-mail: jnls.cust.serv@oup.com. Tel (and answerphone outside normal working hours): + 44 (0)1865 353907. Fax: + 44 (0)1865 353485. **In the US, please contact:** Journals Customer Service Department, Oxford University Press, 2001 Evans Road, Cary, NC 27513, USA. E-mail: jnlorders@oup.com. Tel (and answerphone outside normal working hours): 800 852 7323 (toll-free in USA/Canada). Fax: 919 677 1714. **In Japan, please contact:** Journals Customer Services, Oxford Journals, Oxford University Press, 4-5-10-8F, Shiba, Minato-ku, Tokyo, 108-8386, Japan. E-mail: custserv.jp@oup.com. Tel: + 81 3 5444 5858. Fax: + 81 3 3454 2929.

Methods of payment. Payment may be made: by cheque (to Oxford University Press, Cashiers Office, Great Clarendon Street, Oxford, OX2 6DP, UK); by bank transfer [to Barclays Bank Plc, Oxford Office, Oxford (bank sort code 20-65-18) (UK); overseas only Swift code BARC GB22 (GB£ Sterling Account no. 70299332, IBAN GB89BARC20651870299332; US$ Dollars Account no. 66014600, IBAN GB27BARC20651866014600; EU€ EURO Account no. 78923655, IBAN GB16BARC20651878923655]; or by credit card (Mastercard, Visa, Switch or American Express).

EP — Europace (ISSN 1099-5129) is published monthly by Oxford University Press, Oxford, UK and distributed in the USA by Central Mailing Services c/o UKP Worldwide, 1637 Stelton Road B2, Piscataway, NJ 08854. The US annual subscription price is $2843. Airfreight and mailing in the USA by agent named Central Mailing Services c/o UKP Worldwide, 1637 Stelton Road B1-2, Piscataway, NJ 08854. Periodicals postage paid at Piscataway, NJ and additional mailing offices.

US POSTMASTER: send address changes to *EP — Europace*, Oxford University Press, Central Mailing Services c/o UKP Worldwide, 1637 Stelton Road B1-2, Piscataway, NJ 08854.

Subscription records are maintained at Oxford University Press, Great Clarendon Street, Oxford, OX2 6DP, UK.

Environmental and ethical policies
Oxford Journals, a division of Oxford University Press, is committed to working with the global community to bring the highest quality research to the widest possible audience. Oxford Journals will protect the environment by implementing environmentally friendly policies and practices wherever possible. Please see https://academic.oup.com/journals/pages/about_us/ethical_policies for further information on environmental and ethical policies.

Supplements, reprints and corporate sales
For requests from industry and companies regarding supplements, bulk article reprints, sponsored subscriptions, translation opportunities for previously published material, and corporate online opportunities, please e-mail special.sales@oup.com, fax: + 44 (0)1865 353774 or visit http://www.oupmediainfo.com/#!/reprints-eprints.

Digital object identifier (DOI)
For information about DOIs and to resolve them, please visit http://www.doi.org/

Permissions
For information on how to request permissions to reproduce articles/information from this journal, please visit https://academic.oup.com/journals/pages/access_purchase/rights_and_permissions.

Advertising
Advertising, inserts and artwork enquiries should be addressed to: Advertising and Special Sales, Oxford Journals, Oxford University Press, Great Clarendon Street, Oxford OX2 6DP, UK. Tel: + 44 (0)1865 354767; Fax: + 44 (0)1865 353774; E-mail: jnlsadvertising@oup.com.

Instructions for authors
Full instructions for manuscript preparation and submission can be found through the *EP — Europace* home page at: https://academic.oup.com/europace.

Drug disclaimer
The mention of trade names, commercial products or organizations, and the inclusion of advertisements in the journal does not imply endorsement by *EP — Europace*, the editors, the editorial board, Oxford University Press or the organization to which the authors are affiliated. The editors and publishers have taken all reasonable precautions to verify drug names and doses, the results of experimental work and clinical findings published in the journal. The ultimate responsibility for the use and dosage of drugs mentioned in the Journal and in interpretation of published material lies with the medical practitioner, and the editors and publisher cannot accept liability for damages arising from any error or omissions in the journal. Please inform the editors of any errors.

Material disclaimer
The opinions expressed in *EP — Europace* are those of the authors and contributors, and do not necessarily reflect those of the European Heart Rhythm Association, the European Society of Cardiology, the editors, the editorial board, Oxford University Press or the organization to which the authors are affiliated.

Society
All members of national cardiac societies in Europe, ESC Associations, Working Groups, and Councils are automatically members of the European Society of Cardiology and are entitled to receive the journal at the special reduced rate.

For European Society of Cardiology and European Heart Rhythm Association Members prices: visit https://www.escardio.org/The-ESC/Membership.

Typeset by Cenveo Publisher Services, Bangalore, India.
Printed by Bell and Bain Ltd., Glasgow on acid-free paper.

EP — Europace

Volume 21 No. S1 January 2019

INTRODUCTION

EDITORIAL

REVIEWS

CLINICAL RESEARCH

Open Access Paper

ESC European Society of Cardiology
Europace (2019) **21**, i1
doi:10.1093/europace/euy123

Introduction for high-density mapping supplement

Sabine Ernst (Guest Editor)[1]* and Stephan Willems (Co-Guest Editor)[2]

[1]Royal Brompton Hospital, National Heart and Lung Institute, Imperial College, Sydney Street, SW3 6NP, London, UK; and [2]Universitaetsklinikum Eppdendorf, Martinistr. 52, 20251 Hamburg, Germany

Dear reader,

In 2017, during the European Heart Rhythm Association (EHRA) annual congress in Vienna a symposium entitled 'New therapy opportunities thanks to advanced mapping capabilities—what does the real world's data tell us?' was held that focused on the use of the novel 3D high-resolution mapping system Rhythmia (Boston Scientific). This educational event was extremely well received, and the discussion of the various presentations was very lively. Most presentations concentrated on specific arrhythmias such as atrial fibrillation ablation, post-atrial fibrillation atrial tachycardia, or ventricular tachycardia in various patient cohorts. As an additional format, an 'Experts on the spot' symposium was staged on the role of high-resolution mapping for pulmonary vein isolation, both moderated and presented by Dres. Ullah and Jilek. They jointly present here their take home messages of their conversation (link to the manuscript).

Of course, not all questions could be answered or even just addressed during the 'live' session and sometimes tricks and learning points are best communicated in writing. Moreover, we also encouraged the authors of this supplements to submit movie clips to support their manuscripts. They could be reviewed and downloaded on the Europace website (https://academic.oup.com/europace).

As the chairpersons of the symposium, we approached both the Editor-in-Chief of Europace and Boston Scientific as the commercial sponsor to propose this supplement, which could ideally serve as a reference for users to guide them in their own procedures. Specific advices, such as setting the confidence level according to the signal noise level, using fill thresholds and 'uncovering' signals in scar areas may help to succeed in challenging cases. If this supplement on high-resolution mapping can help with this endeavour even only a little bit, then authors and editors would be very pleased indeed!

We hope you have an enjoyable time reading this supplement

Sabine Ernst

Stephan Willems

* Corresponding author. Tel: +44 207 351 8612; fax: +44 207 351 8634. *E-mail address*: s.ernst@rbht.nhs.uk

ESC European Society of Cardiology
Europace (2019) **21**, i2–i3
doi:10.1093/europace/euy240

EDITORIAL

Advanced mapping capabilities 2018—summary: are we working towards more personalized ablation strategies?

Sabine Ernst[1]* and Stephan Willems[2]

[1]Royal Brompton and Harefield NHS Foundation Trust, Imperial College, Sydney Street, London, SW3 6NP, UK; and [2]Universitaetsklinikum Eppendorf, Martinistr. 52, 20251 Hamburg, Germany

We started our journey on high-density mapping (HDM) with an insight on how to identify conduction gaps in previously applied pulmonary vein (PV) isolation. A substantial number of atrial fibrillation (AF) patients have to represent themselves for 'touch-up' procedures as PV reconnection is still the prevailing problem of after any type of ablation energy including balloons [e.g. cryo, laser, or radiofrequency (RF) current]. Bolao and colleagues shared their approach to gap identification and furthered our knowledge on gap dimensions.[1] Using the HDM system, fast acquisition and automatic annotation of the electrical information has been demonstrated. Having more information of the antral PV activation allows differentiation of both atrial and PV potentials. Using the basket mapping catheter, activation during different pacing manoeuvres can be easily and quasi-simultaneously tested, which facilitates ultimately to locate conduction patterns. This information let to a significantly shorter overall RF delivery time and also shortened the overall procedure time. There was also a trend to significantly better outcome, albeit non-statistically significant despite the use of non-contact force equipped ablation catheters in the treatment arm as compared to a historic control of the same operator. Larger, multicentre trials are clearly necessary with accurate patient sample sizes to confirm this finding.

In the second manuscript, two experienced electrophysiologists debated the role of the atrial myocardium as the substrate for maintenance of AF vs. trigger initiation from the PVs.[2] Their dialogue was illustrated by deliberations on the various studies from conventional mapping and ablation techniques. Using the HDM, identification of the individual myocardial substrate should be facilitated and thereby truly allowing to personalize the AF ablation strategy. This may be especially important in patients with persistent or longstanding-persistent AF or patients with significantly enlarged atria. However, the step from individual substrate identification to delivery of the 'winning' ablation strategy is obviously still a challenge, but due to the small electrode sizes low-amplitude voltage areas should be much easier to identify. Whether this level of detail provides an incremental benefit for strategies involving scar ablation is an area of future investigation and has to date not been demonstrated.

Latcu and colleagues reported very insightful and instructive on how to take advantage of the high resolution mapping capabilities in identifying atrial tachycardia substrates mostly after extensive AF ablation.[3] As substrate modification by linear lesions and other non-PV isolation techniques are applied in many non-paroxysmal AF patients, the incidence of iatrogenic atrial tachycardia has risen exponentially. Mapping of these atrial tachycardias can be a great challenge and identification of micro-reentry and bystander areas can be difficult if lower resolution systems are employed.

Bourier and colleagues demonstrated that the HDM system could successfully be applied to ventricular arrhythmia.[4] This information is compared to the information obtained from the gold standards of CARTO or ENSITE sequential mapping systems. They carefully reviewed the published evidence for catheter ablation of ventricular tachycardia using high resolution mapping techniques and highlighted the different electrcardiogram characteristics when mapping is performed using small mapping electrodes in comparison to the standard mapping and ablation tip. In addition, they emphasized the advantage of 3D image integration to identify 'anatomical' substrates rather than only 'functional' substrates.

All HDM-guided procedures listed the lack of appropriate lesion assessment as one of the leading problems in ablation for both atrial and ventricular arrhythmias. Gunawardene and colleagues reported on their single centre pilot experience with local impedance (LI) measurements from a novel ablation catheter and compared the results to the conventional impedance displayed at the RF generator (GI).[5] The catheter tip is equipped with three additional electrodes that allow recording of nearfield impedance, which changes characteristically once RF energy is delivered into the myocardium. Depending on baseline LI, an appropriate drop in LI of about 13 Ω seems to predict good lesion formation, whilst fluctuating LI is characteristic for poor catheter stability and thereby poorer lesion formation. In both settings, the changes in LI are more pronounced then in GI. However, due to the overall small sample size and the explorative nature of a pilot trial, no final claim of improved effectiveness especially in low voltage areas can be made at this point in time.

The opinions expressed in this article are not necessarily those of the Editors of *Europace* or of the European Society of Cardiology.

* Corresponding author. Tel: +44 20 7351 8612; fax: +44 20 7351 8629. E-mail address: s.ernst@rbht.nhs.uk

The authors point out that the multicentre LOCALIZE trial has already been initiated, which will address this issue in greater detail.

Catheter ablation of atrial tachycardia in patients with congenital heart disease poses a number of challenges including the identification of previously acquired surgical scars and/or previous ablation attempts. Another challenge is the sheer size of the atrial chambers which makes any sequential mapping attempt more difficult. With the multitude of potential substrates, these patients are typically plagued by multiple atrial tachycardias which Ernst *et al.* attempted to address in a sequential fashion.[6] Recommendations for scar settings and 3D image integration are reviewed, cautioning the expectations at least for the present.

We hope this variety of contributions from several groups will provide further insights into contemporary HDM and ablation in order to improve our understanding of complex tachyarrhythmias and help to overcome hurdles still preventing us from successful treatment of these entities. Thus, this supplement may represent a small step towards more personalized strategies in this setting.

Conflict of interest: S.E. received honoraria from Boston Scientific, Stereotaxis and Biosense Webster and has research collaborations with Baylis Medical, Medilumics and Catheter Precision. S.W.: none declared.

References

1. García-Bolao I, Ballesteros G, Ramos Ardanaz P, Vives E, Neglia R, Menéndez D *et al.* Do 'difficult to identify' pulmonary vein connections explain continuing high recurrence rates after atrial fibrillation ablation? *Europace* 2019;**21**(Suppl 1): i4–11.
2. Jilek C, Ullah W. Pulmonary vein reconnections or substrate in the left atrium: what is the reason for atrial fibrillation recurrences? A dialogue on a pressing clinical situation. *Europace* 2019;**21**(Suppl 1):i12–20.
3. Latçu DG, Bun S-S, Arroyo RC, Wedn AM, Benaich FA, Hasni K *et al.* Scar identification, quantification, and characterization in complex atrial tachycardia: a path to targeted ablation? *Europace* 2019;**21**(Suppl 1):i21–6.
4. Bourier F, Martin R, Martin CA, Takigawa M, Kitamura T, Frontera A *et al.* Is it feasible to offer 'targeted ablation' of ventricular tachycardia circuits with better understanding of isthmus anatomy and conduction characteristics? *Europace* 2019; **21**(Suppl 1):i27–33.
5. Gunawardene M, Münkler P, Eickholt C, Akbulak RÖ, Jularic M, Klatt N *et al.* A novel assessment of local impedance during catheter ablation: initial experience in humans comparing local and generator measurements. *Europace* 2019; **21**(Suppl 1):i34–42.
6. Ernst S, Cazzoli I, Guarguagli S. An initial experience of high-density mapping-guided ablation in a cohort of patients with adult congenital heart disease. *Europace* 2019;**21**(Suppl 1):i43–53.

ESC European Society of Cardiology
Europace (2019) **21**, i4–i11
doi:10.1093/europace/euy177

REVIEW

Do 'difficult to identify' pulmonary vein connections explain continuing high recurrence rates after atrial fibrillation ablation?

Ignacio García-Bolao[1]*, Gabriel Ballesteros[1], Pablo Ramos Ardanaz[1], Enrique Vives[1], Renzo Neglia[1], Diego Menéndez[1], Ane Erkiaga Aio[2], and Ana de la Fuente[1]

[1]Department of Cardiology and Cardiovascular Surgery, Clínica Universidad de Navarra, Avenida Pío XII, 36 (31008) Pamplona, Spain; and [2]Rhythmia Field Clinical Specialist, Boston Scientific Corporation, Madrid, Spain

Received 3 April 2018; editorial decision 27 June 2018; accepted 3 July 2018

Despite the emerging technical evolution of the last two decades, the primary success rate of single-procedure pulmonary vein isolation (PVI), the cornerstone for any atrial fibrillation ablation procedure, is highly variable ranging from 53% to 92%. The recent development of ultra-high-density electroanatomic mapping systems, capable of acquiring and annotating multiple electrograms, with high spatiotemporal precision, which are processed by automated algorithms to generate activation and substrate maps to support and guide ablation procedures, has opened a new stage in cardiac electrophysiology. In this article, we review the existing evidence on the utility of high-density mapping on catheter-based PVI, the possibility to detect pulmonary vein potentials that remain undetected when using a standard approach and its potential relevance to the clinical outcome, and how this new technology is providing novel pathophysiological insights on complete PVI and atrial fibrillation ablation outcomes.

Keywords Atrial fibrillation ablation • Redo atrial fibrillation ablation • Pulmonary vein isolation • High-density mapping • Rhythmia™ mapping system • Orion™ mapping catheter

Introduction

For many highly symptomatic atrial fibrillation (AF) patients catheter ablation offers the most efficacious option for maintaining sinus rhythm when antiarrhythmic drugs (AADs) have been ineffective, are contraindicated, or cannot be tolerated.[1,2] Large-scale observational studies, randomized controlled trials, and meta-analysis have confirmed the superiority of catheter ablation in maintaining sinus rhythm (success 66–89% with catheter ablation vs. 9–58% with AAD), as well as improving symptoms, exercise capacity, and quality of life.[3–11] Accordingly, catheter ablation has moved from an 'experimental therapy' to the standard of care for sinus rhythm maintenance for both paroxysmal and persistent AF specially for operators and sites that maintain high annual procedure volumes and optimal technical competence for AF ablation.[1,2] However, enthusiasm for ablation approach is somehow limited for long-term outcomes data. For example, in the randomized RAAFT-2 trial,[11] among patients with paroxysmal AF without previous AAD treatment, ablation compared with antiarrhythmic drugs resulted in a lower rate of recurrent atrial tachyarrhythmias at 2 years, but recurrence was documented in approximately 50% of patients.

Complete pulmonary vein isolation (PVI) on the atrial level is the keystone and best documented target for catheter ablation. Pulmonary vein isolation can be achieved by point-by-point radiofrequency (RF) ablation, linear lesions encircling the pulmonary veins [both guided by conventional circular mapping catheters (CMC) and non-fluoroscopic mapping systems],[11–13] or cryoballoon ablation (with a modified spiral mapping catheter),[14,15] with similar clinical outcomes. Pulmonary vein isolation was initially tested in patients with paroxysmal AF but appears to be non-inferior to more extensive ablation even in persistent AF patients.[16] Moreover, complete electrical isolation of the pulmonary veins (PVs) with documented entrance and/or exit block has better rhythm outcomes than incomplete isolation.[17]

Leaving aside the possibility of performing other AF ablation additional strategies, PV re-isolation is a standard and mandatory

* Corresponding author. Tel: +34 948 255 400; fax: +34 948 296 500. *E-mail address*: igarciab@unav.es

technique in redo procedures. Lack of detection PV reconnection may occur due to inadequate strategy for mapping the PV, insufficient attempts at mapping it or due to inappropriate tools for assessing PVI. The recent development of ultra-high-density electroanatomic mapping (HDM) systems, capable of acquiring and annotating multiple electrograms, which are processed by automated algorithms to generate activation and substrate maps to support and guide ablation procedures, has opened a new stage in cardiac electrophysiology. These systems are capable to rapidly and automatically acquire maps with high spatiotemporal precision, without the need for extensive manual annotation, through the combination of catheters with small and closely spaced electrodes in combination with dedicated mapping platforms.[18]

In this article, we are going to review the existing evidence on the utility of HDM on catheter-based PVI and how this new technology is providing novel pathophysiological insights on complete PVI and AF ablation outcomes.

Pulmonary vein isolation and atrial fibrillation ablation outcomes

Pulmonary veins are not only the area of initiation but also of maintenance of AF in a large number of patients, and sustained PV tachycardia initiated by pulmonary venous ectopy is the dominant mechanism.[19–21] For this reason, current guidelines state that ablation strategies targeting the PVs or PV antra are the cornerstone for most AF ablation procedures and, if the PVs are targeted, complete electric isolation and elimination of all PV potentials should be the main goal in overcoming the arrhythmia.[1,2] This approach is supported not only from all randomized clinical trials, but also from experimental research. Although AF recurrence after catheter ablation may not only be due to non-durable PV isolation, in the absence of other obvious trigger areas, re-isolation is mandatory and is part of common practice.

In the Gap-AF-AFNET trial,[17] Kuck *et al.*, assessed the impact of complete vs. incomplete circumferential lines around the pulmonary veins during catheter ablation of paroxysmal AF. Using a classical approach [conventional non-fluoroscopic mapping systems and some form of variable-loop circular mapping catheters (CMC) to assess electrical PVI], they nicely shown the superiority of complete PVI over incomplete PVI with respect to AF recurrence within 3 months. In a cohort of 233 patients, AF recurred in 62.2% of patients completely isolated and in 79.2% of patients left with an intended persistent gap ($P < 0.001$), for a difference in favour of complete PVI of 17.1% (95% confidence interval 5.3–28.9%).

Moreover, the correlation between PV reconnection and AF recurrence after the index procedure underlines the important role of the PVs in the pathophysiology of AF. Patients with AF recurrences almost always have conduction gaps, as shown in multiple observational and experimental studies, and closure of these conduction gaps with RF current led to re-isolation of the PVs with fewer AF recurrences.[22–25]

For all these reasons, PVI is now widely accepted as the cornerstone of AF ablation procedures. According to the ESC guidelines, electrical isolation of the PVs is recommended during all AF ablation procedures (Class I, level of evidence A) and elimination or dissociation of all the PV potentials recorded from a CMC should be the primary endpoint for AF ablation procedures.[1,2]

Assessing pulmonary vein isolation in clinical practice

Pulmonary vein isolation is traditionally achieved by RF energy or by single-shot techniques such as cryoballoon ablation. With both strategies, the complex 3D structure of the PVs and the geometry of PV ostia led to the development of mapping-guided PV isolation as a more effective diagnostic tool to assess PVI by using CMC. The importance of using a CMC for assessing isolation of the PV antrum on the outcome of the PVI procedure has been clearly established and it is widely considered as the gold standard procedure for testing entrance and exit block.[26,27]

However, the systematic use of standard CMC to assess PVI has obvious limitations and pitfalls.[28] Some anatomical reasons might explain suboptimal identification of PVP's (pulmonary vein potentials). For instance, due to the different takeoffs of the PVs, CMC is usually obliquely oriented with the anterior part of the mapping catheter being positioned more profoundly within the vein and the posterior part more atrially situated. Similarly, the bottom of the CMC is typically deeper within the superior PVs, whereas the opposite is true for the inferior PVs. This poor wall contact affects both the sensing features of the catheter, to assess entrance block, as well as the pacing capabilities, to assess local PV capture and exit block. Also, wide funnel that is often observed in the upper PVs may lead to a mismatch between CMC and the PV. Such a lack of contact may result in inferior results. For all these anatomical reasons, leaving undiagnosed remnants of unisolated muscular tissue is a common issue of CMCs, even after careful supplementary exploration and targeted ablation.[28] Secondly, the right inferior PV may, on occasion, present difficulties in achieving a stable position with the CMC. Complete catheterization of the left inferior PV with the CMC can be also challenging in some cases. Thirdly, discrimination of near-field PV potentials from far-field extra-PV potentials can be challenging with conventional CMC even after careful pacing manoeuvres. Finally, and looking specifically at single-shot systems, there are obvious weaknesses and 'roughness' of some of their diagnostic features, which are somehow dictated by their own design (fixed-curve CMCs, too distal PV mapping, limited number of electrodes, etc).[29,30]

High-density mapping to detect pulmonary vein potentials

With contemporary technology, some PV potentials may remain undetected. Meissner *et al.*[31] recently demonstrated the superiority of a high-density basket catheter (High-Density Mesh Mapper) in identifying PVP's that an octapolar single-shot CMC was not be able to identify, both before and after cryoballoon ablation. In a series of 24 patients, they identified an average of 83.6 ± 4.8 PVPs in all four PVs (this meant 20.9 ± 10.5 PVPs/per single PV per patient in the HDM group, 14.5 ± 1.3 PVPs/in all four PVs, and 3.6 ± 2.7 PVPs/per

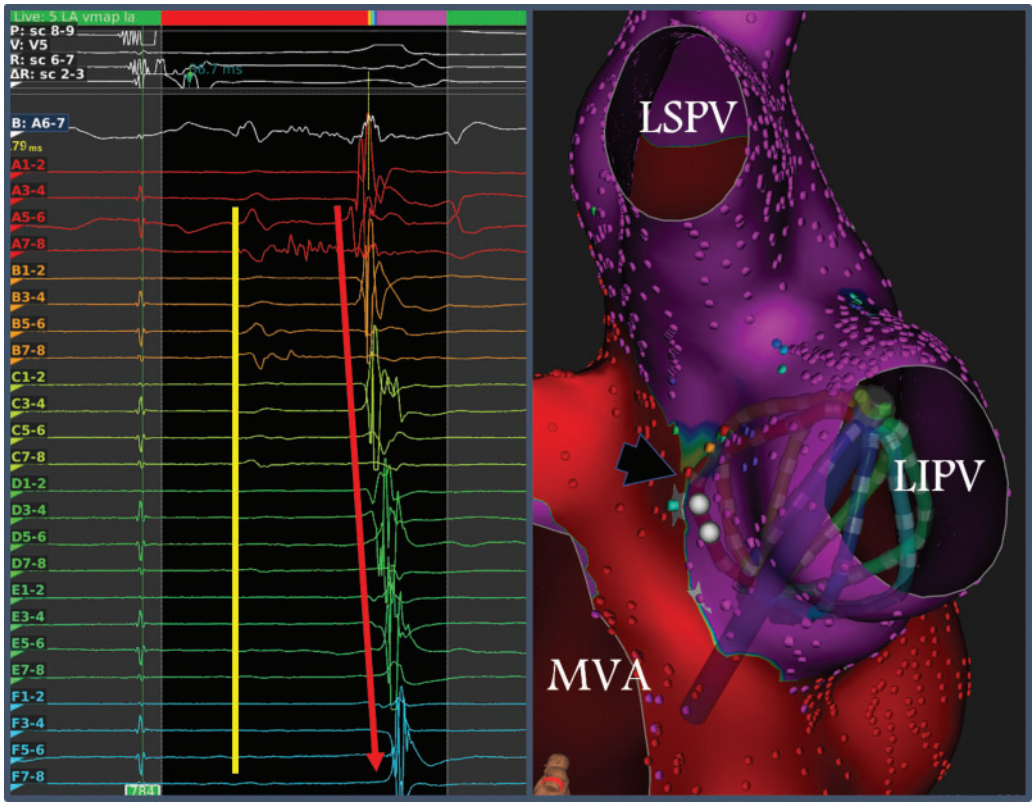

Figure 1 Example electrograms (left panel) recorded with the Orion catheter inside the LIPV (right panel). With no need for catheter manipulations or stimulation manoeuvres, recordings from a single spline can distinguish PV potentials, which propagate from proximal to distal (red arrow), from 'far-field' potentials, which are simultaneous (yellow line). The PV reconnection gap at the anterosuperior level of the venous antrum can be observed (black arrowhead). LIPV, left inferior pulmonary vein; LSPV, left superior pulmonary vein; MVA, mitral valve anulus; PV, pulmonary vein.

single PV per patient in the cryo group) before ablation, thereby leading to a significant difference in the identification of PVPs per PV quadrant. Of 384 PV quadrants/24 patients analysed, the HDM identified a significantly higher number of PVPs compared with cryo (279 vs. 192 quadrants, respectively, $P < 0.05$).

Using a different approach, Anter *et al.*[32] showed the superiority of a HDM strategy in detecting PVPs compared with a standard CMC. In their study, they used the Rhythmia mapping system, a new system capable of rapid and high-resolution electroanatomical and activation mapping paired with the Orion mini-basket catheter. The mini-basket catheter consists of eight splines, each containing eight small (0.4 mm^2 each) electrodes with an interelectrode spacing of 2.5 mm measured from centre to centre. The mini-basket is expandable to a nominal equatorial diameter of 18 mm and a maximal diameter of 22 mm. In 12 patients undergoing PVI using Rhythmia, the Orion and a conventional CMC (20 electrodes, each with a surface area of 1 mm^2, recording bipolar electrograms with an interelectrode spacing of 3 mm) were placed simultaneously at the left atrium-PV junction for baseline and post-PVI signal assessment. The main finding of this study was that after PVI, concordance between the catheters was only 68%. Discordance in all cases resulted from loss of PV potentials on the CMC with persistence of PV potentials on the mini-basket catheter. In 9 of 13 PVs (69%), these potentials represented true PV potentials that were exclusively recorded with the smaller and closely spaced mini-basket electrodes. The authors also reported a 31% of PVP overestimation related to neighbouring structures using the Orion catheter, so this possibility should always be ruled out by stimulation manoeuvres and analysis of the potential propagation as previously described.[33] In this head-to-head comparison, overestimation of PVI was more frequent with the CMC (20.8% vs. 0% of the PVs).

The potential advantages of a closely spaced multielectrode system with a basket configuration and HDM features are varied and can mainly be explained by both the catheter construction itself and the anatomical aspects of the PVs (*Table 1*). The smaller and closer interelectrode spacing are subjected to less signal averaging and cancellation effects, thus recording higher bipolar voltage amplitude. This could potentially explain the improved sensitivity of the mini-basket catheter in detecting PV potentials after RF ablation, while these are no longer identified with a standard CMC. Also, the increased mapping resolution, potentially identifying surviving bundles that may correspond to gaps in the ablation line may be advantageous for mapping scar areas or acutely ablated tissue.[32] Moreover, the combination of transverse and longitudinal mapping that can provide multiple transverse planes of activation at different levels could better detect PV potentials from muscular sleeves, could help to further discriminate far-field from

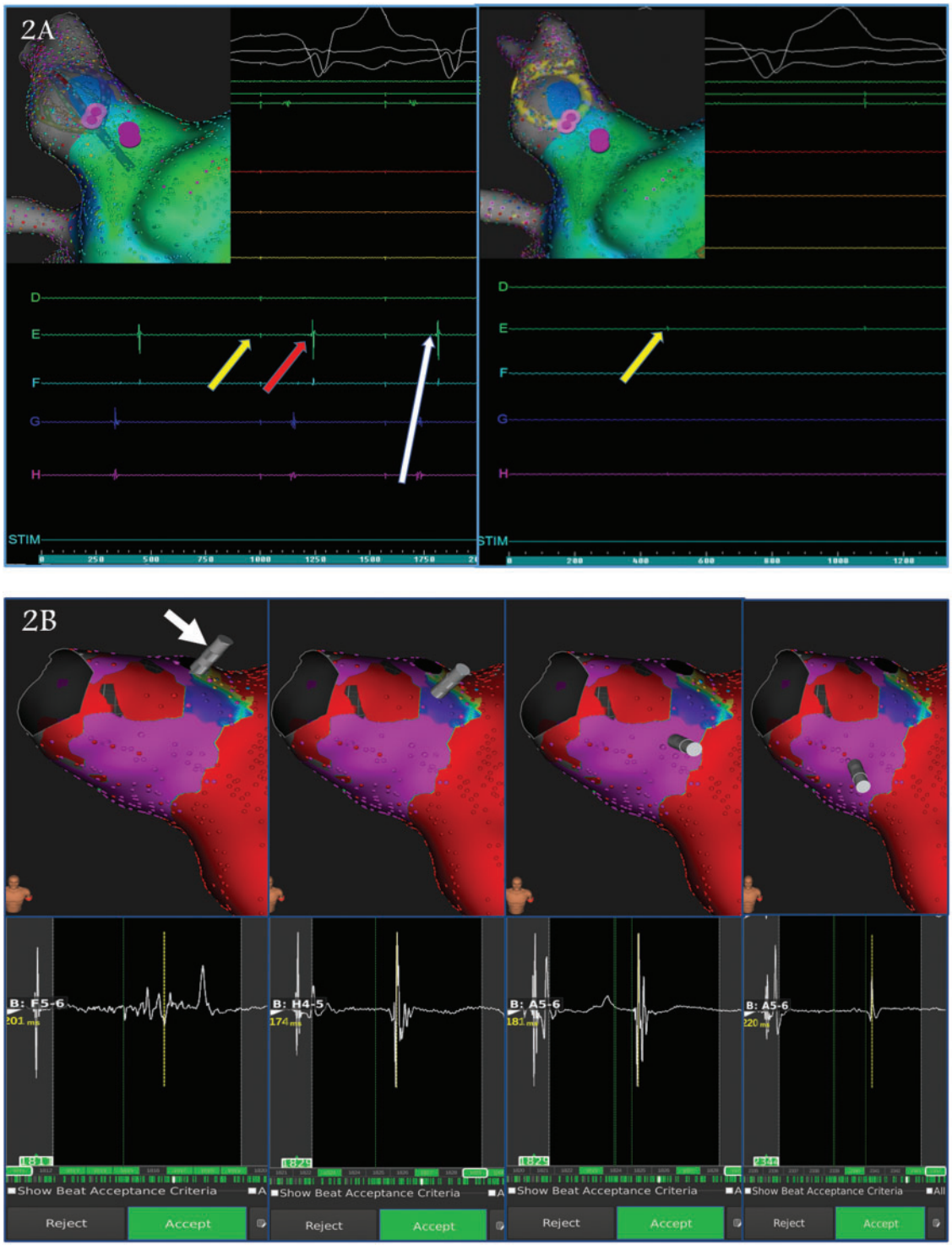

Figure 2 (*A*) Reconnection of right superior PV in a patient with a prior cryoablation procedure. Left panel: electrograms observed within the vein using the IntellaMap Orion catheter. Right panel: electrograms observed within the vein using a circular multipolar catheter. An atrial pacing spike (yellow arrows) can be seen in both. With the Orion catheter it is possible to observe PV electrograms (red arrow) with the characteristic progression of near-field signals (white arrow). It was not possible to appreciate these signals with a circular mapping catheter, even after several attempts at repositioning the catheter. A new isolation was achieved after a focal application of radiofrequency. (*B*) The progression of the electrical front can also be observed with the virtual robing prove (white arrow) after the acquisition of the map. PV, pulmonary vein. Modified from García-Bolao *et al.*[33]

Table 1 Potential advantages of the mini-basket with closely spaced electrodes architecture vs. a conventional CMC for assessing PVI

Small, closely spaced electrodes that allow better discrimination of near-field PV potentials from far-field extra-PV potentials.
Combination of transverse and longitudinal mapping that can provide multiple transverse planes of activation at different levels.
High definition activation entrance and exit maps (useful for gap detection).
Easier recognition of PV-to-LA block (higher chance to achieve local PV capture due to a closer apposition of the electrodes against the PV wall).
Speed/easy to use in the LA-PV's.
High anatomical accuracy.
Easier access to the early branching pattern in all PV's.
Precise definition of the PV's ostia.
Tagging transeptal puncture and mapping interatrial septum.
Possibility to use abbreviated high-density maps of the PV's and LA-PV junction.

CMC, circular mapping catheter; LA, left atrium; PV, pulmonary vein; PVI, pulmonary vein isolation.

near-field potentials (*Figures 1 and 2*) and avoids underdetection of potentials caused by the orientation of the wavefront. The latter can be more difficult with a CMC, although it can be mitigated by pacing manoeuvres from different points of the atrium.

High-density mapping for pulmonary vein isolation

There are several observational studies assessing the acute safety, effectiveness, clinical use and short-term outcomes of HDM with the Rhythmia System, and the Orion mini-basket catheter on AF ablation (*Table 2*). Although most of these studies showed that the system is fast, safe, and clinically useful, there is no long-term clinical assessment of the performance of this strategy. All these clinical studies covered a wide spectrum of AF presentations, including paroxysmal, persistent and long-standing persistent arrhythmias, and *de novo* as well as redo procedures, all of them sharing the common endpoint of PVI.

In a preliminary observation, Kosiuk *et al.*[34] studied 36 consecutive patients with paroxysmal or persistent AF undergoing *de novo* or repeat AF ablation, in which left atrial electroanatomical maps were acquired with a mini-basket (14 patients) or with a system-specific, magnet-enabled ablation catheter (22 patients), both with the Rhythmia HDM system. Maps acquired with mini-basket required significantly shorter mapping time and had higher point density, while procedural and fluoroscopy time was higher in the mini-basket group. Procedural endpoints and complications rates were similar in both groups.

Rottner *et al.*[35] studied 37 PVI patients with paroxysmal and persistent AF treated with the Rhythmia compared with 37 patients using conventional mapping with the Carto. They observed a significantly longer total mapping time ($P = 0.001$), with similar total ablation time ($P = 0.707$), total procedure duration ($P = 0.99$), and acute PVI success between both groups. During follow-up, 84.8% of patients remained free from any AF/AT-recurrence using Carto vs. 88.2% when using Rhythmia ($P = 0.53$). The authors conclude that Rhythmia was proved to be effective and well applicable for PVI, but more long-term data would be mandatory before final conclusions could be drawn.

Our group[33] reported data on 62 paroxysmal and persistent consecutive AF patients who underwent a PVI procedure with Rhythmia and Orion catheter. We compared this prospective cohort to a historical retrospective sample of 62 consecutive patients treated by the same operator with a conventional mapping system (Ensite Velocity) with a standard CMC. In this study, the number of intracardiac electrograms per map was significantly higher in Rhythmia procedures (12 125 ± 2826 vs. 133 ± 21 with Velocity; $P < 0.001$), with no significant differences in the total procedure time or the number of complications. Interestingly, the Orion catheter was placed for mapping in more PVs when compared with the standard CMC (99.5% vs. 95.61%; $P = 0.04$) although there were no significant differences in the percentage of PV isolation between the two groups. To note, in redo procedures, an ablation gap could be identified on the activation map in 67% of the reconnected PVs compared to only 40% in the control group; $P = 0.042$, which suggested the greater electroanatomical definition of HDM when compared with the standard approach.

In a subsequent work from our group,[36] 108 consecutive patients with a previous PVI procedure were included in a non-randomized study that assessed the recognition of reconnection gaps in PV by means of HDM (with the analysis of the activation map and the propagation pattern) (*Figure 3*) compared with a control group that received conventional non-fluoroscopic guidance with CMC by the same principal operator. Among the HDM group, adequate recognition of reconnection gaps (predefined as the electrical isolation of the vein or a delay of the PV electrograms equal to or greater than 10 ms with a change in the activation pattern of the CMC/Orion equatorial electrograms after a single focal application of RF) was obtained in 60.99% of the reconnected PVs (86 of 141), a figure significantly higher than that achieved with analysis of CMC recorded signals (39.66%, 48 of 121; $P = 0.001$). The number of applications and total RF time were also significantly lower in the HDM group (12.46 ± 6.1 vs. 15.63 ± 7.7 and 7.61 ± 3 vs. 9.29 ± 5; $P = 0.02$, and $P = 0.03$, respectively). At the 6-month follow-up, a non-statistically significant reduction in AF recurrence was found (8 patients, 14.8% for the HDM group, vs. 16 patients, 29.6% for the CMC group; $P = 0.104$). This fact has to be assessed with caution, since the study did not have enough

Table 2 Studies assessing the acute safety, effectiveness, clinical use, and short-term outcomes of HDM with the Rhythmia System

	Randomization	Comparison groups	*n* (study/control)	AF type	HDM (points/mapping time)	Main findings
Kosiuk *et al.*[34]	No	HDM with Orion vs. HDM with abl	36 (14/22)	Paroxysmal 39% Persistent 61%	Orion: 8832/7.9 min Abl: 4460/18.8 min	• Shorter mapping time and higher point density in Orion group but, higher procedural and fluoroscopy time
Rottner *et al.*[31]	Yes	HDM (Rhythmia) vs. point-by-point (Carto)	74 (37/37)	Paroxysmal 44% Persistent 56%	8365/23.2 min	• Longer mapping (12 vs. 23 min) and fluoroscopy time (12 vs. 21 min) and more RF applications (25 vs. 35) with Rhythmia • No difference in procedure duration, acute success, complications, and AF recurrence rate
Ballesteros *et al.*[32]	No	Rhythmia vs. Ensite Velocity	142 (62/62)	Paroxysmal 61% Persistent 39%	12 125/18 min	• AF ablation guided by Rhythmia System is safe without prolongation of total procedural time • The Orion catheter allows selective catheterization of a higher number of PV's as compared with a CMC • HDM seems superior to CMC activation pattern in PV gap recognition
García-Bolao *et al.*[33]	No	HDM (Rhythmia) vs. conventional NFNS with a CMC	108 (54/54)	Only redo procedures Paroxysmal 75% Persistent 25%	13425/19.4 min	• HD activation maps allows greater precision in the identification of reconnection gaps in PV, which resulted in lower radiofrequency time for the new isolation • HD voltage map alone does not have enough precision to recognize the gaps

abl, magnet-enabled ablation catheter; AF, atrial fibrillation; CMC, circular mapping catheter; HD, high density; HDM, high-density mapping; NFNS, non-fluoroscopic navigation system; Orion, Orion catheter; PV, pulmonary veins; RF, radiofrequency.

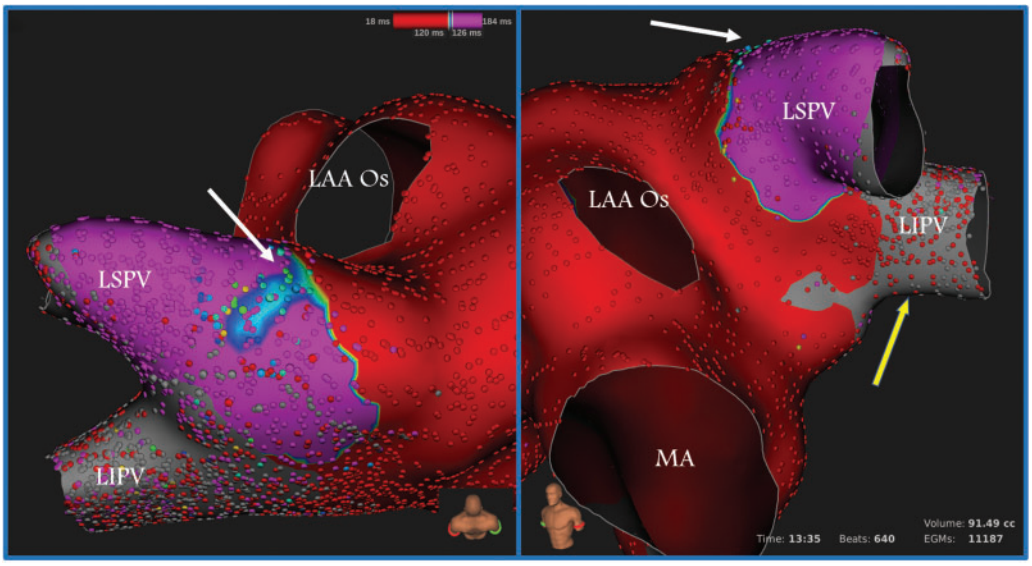

Figure 3 Activation map during recognition of the reconnection gap of the left superior pulmonary vein from superior (left panel) and left anterior oblique (right panel) views. A reconnection gap can be observed in the superior region (white arrow). The map also shows that the left inferior pulmonary vein remains isolated (yellow arrow). Map time: 13 min and 35 s. LAA Os, left atrial appendage ostium; LIPV, left inferior pulmonary vein; LSPV, left superior pulmonary vein; MA, mitral annulus. Modified from García-Bolao *et al.*[33]

statistical power to detect small differences and the therapeutic approach in the HDM group was performed without contact sensor technology. Interestingly, although no significant differences were observed in the baseline characteristics of the two groups regarding age, sex, CHA_2DS_2-VASc score or type of index procedure, a higher percentage of reconnected PV was observed among the HDM group (63.8% vs. 56%, $P = 0.09$), that could imply a greater sensitivity of the Orion catheter when detecting remnants of unisolated PV tissue that cannot be detected with conventional CMC, a fact that is in concordance with the findings observed in Anter's study.[32]

More recently, Segerson *et al.*[37] underwent a study on 150 patients (39 redo and 111 *de novo* procedures) undergoing HDM-guided PVI and subsequent concealed low-voltage signals mapping and ablation against a historical series of 452 control patients who underwent traditional PVI alone. During mean follow-up of 320 days, after controlling for baseline characteristics, the HDM group exhibited hazard ratio of 0.19 in freedom from AF ($P < 0.001$). *De novo* patients exhibited hazard ratio of 0.44 relative to redo patients in the HDM-guided group. Both subgroups exhibited significantly lower event rates compared with controls in log-rank test analysis ($P < 0.001$). According to their results, ablation of these targets, interpreted by the authors as vulnerabilities in antral lesion sets, that is to say, residual low-voltage propagation within the PV antra after PVI was achieved, appears to significantly improve freedom from AF compared with PVI alone.

Conclusions

High-density mapping allows for more accurate identification of PVPs detecting potentials that remain undetected when using standard approaches. In our experience it shows some advantages in PVI validation, especially evident in cases of PV with low or very proximal potentials, small veins, veins with non-circumferential muscular sleeves and generally in all redo procedures. Observational studies have shown that PVI with this approach is feasible and safe and one case-control study showed a significant freedom from AF ablating vulnerabilities in atrial lesions sets detected by HDM compared with the standard mapping approach. However, up to date, the long-term clinical benefit of HDM for PVI has not been proven in a head-to-head comparison and should be addressed in prospective and randomized clinical trials.

Conflict of interest: I.G.-B. has received consultant, proctoring and speaker's fees from Boston Scientific Corporation and St. Jude Medical. The rest of the authors have no conflict to declare.

References

1. Andrade JG, Macle L, Nattel S, Verma A, Cairns J. Contemporary atrial fibrillation management: a comparison of the current AHA/ACC/HRS, CCS, and ESC guidelines. *Can J Cardiol* 2017;**33**:965–76.
2. Kirchhof P, Benussi S, Kotecha D, Ahlsson A, Atar D, Casadei B *et al.* 2016 ESC Guidelines for the management of atrial fibrillation developed in collaboration with EACTS. *Europace* 2016;**18**:1609–78.
3. Mont L, Bisbal F, Hernandez-Madrid A, Perez-Castellano N, Vinolas X, Arenal A *et al.* Catheter ablation vs. antiarrhythmic drug treatment of persistent atrial fibrillation: a multicentre, randomized, controlled trial (SARA study). *Eur Heart J* 2014;**35**:501–7.
4. Hakalahti A, Biancari F, Nielsen JC, Raatikainen MJ. Radiofrequency ablation vs. antiarrhythmic drug therapy as first line treatment of symptomatic atrial fibrillation: systematic review and meta-analysis. *Europace* 2015;**17**:370–8.
5. Calkins H, Kuck KH, Cappato R, Brugada J, Camm AJ, Chen SA *et al.* 2012 HRS/EHRA/ECAS expert consensus statement on catheter and surgical ablation of atrial fibrillation: recommendations for patient selection, procedural techniques, patient management and follow-up, definitions, end-points, and research trial design. *Europace* 2012;**14**:528–606.
6. Wazni OM, Marrouche NF, Martin DO, Verma A, Bhargava M, Saliba W *et al.* Radiofrequency ablation vs antiarrhythmic drugs as first-line treatment of symptomatic atrial fibrillation: a randomized trial. *JAMA* 2005;**293**:2634–40.

7. Oral H, Pappone C, Chugh A, Good E, Bogun F, Pelosi F Jr *et al*. Circumferential pulmonary-vein ablation for chronic atrial fibrillation. *N Engl J Med* 2006;**354**: 934–41.
8. Stabile G, Bertaglia E, Senatore G, De Simone A, Zoppo F, Donnici G *et al*. Catheter ablation treatment in patients with drug-refractory atrial fibrillation: a prospective, multi-centre, randomized, controlled study (Catheter Ablation For The Cure Of Atrial Fibrillation Study). *Eur Heart J* 2006;**27**:216–21.
9. Calkins H, Reynolds MR, Spector P, Sondhi M, Xu Y, Martin A *et al*. Treatment of atrial fibrillation with antiarrhythmic drugs or radiofrequency ablation: two systematic literature reviews and meta-analyses. *Circ Arrhythm Electrophysiol* 2009; **2**:349–61.
10. Wilber DJ, Pappone C, Neuzil P, De Paola A, Marchlinski F, Natale A *et al*. Comparison of antiarrhythmic drug therapy and radiofrequency catheter ablation in patients with paroxysmal atrial fibrillation: a randomized controlled trial. *JAMA* 2010;**303**:333–40.
11. Morillo CA, Verma A, Connolly SJ, Kuck KH, Nair GM, Champagne J *et al*. RAAFT-2 Investigators. Radiofrequency ablation vs antiarrhythmic drugs as first-line treatment of paroxysmal atrial fibrillation (RAAFT-2): a randomized trial. *JAMA* 2014;**311**:692–700.
12. McLellan AJ, Ling LH, Azzopardi S, Lee GA, Lee G, Kumar S *et al*. A minimal or maximal ablation strategy to achieve pulmonary vein isolation for paroxysmal atrial fibrillation: a prospective multi-centre randomized controlled trial (the Minimax study). *Eur Heart J* 2015;**36**:1812–21.
13. Verma A, Sanders P, Macle L, Deisenhofer I, Morillo CA, Chen J *et al*. Substrate and Trigger Ablation for Reduction of Atrial Fibrillation Trial-Part II (STAR AF II): design and rationale. *Am Heart J* 2012;**164**:1–6.
14. Luik A, Radzewitz A, Kieser M, Walter M, Bramlage P, Hormann P *et al*. Cryoballoon versus open irrigated radiofrequency ablation in patients with paroxysmal atrial fibrillation: the prospective, randomized, controlled, noninferiority FreezeAF study. *Circulation* 2015;**132**:1311–9.
15. Kuck KH, Brugada J, Furnkranz A, Metzner A, Ouyang F, Chun KR *et al*. Cryoballoon or radiofrequency ablation for paroxysmal atrial fibrillation. *N Engl J Med* 2016;**374**:2235–45.
16. Verma A, Jiang CY, Betts TR, Chen J, Deisenhofer I, Mantovan R *et al*. Approaches to catheter ablation for persistent atrial fibrillation. *N Engl J Med* 2015;**372**:1812–22.
17. Kuck KH, Hoffmann BA, Ernst S, Wegscheider K, Treszl A, Metzner A *et al*. Impact of complete versus incomplete circumferential lines around the pulmonary veins during catheter ablation of paroxysmal atrial fibrillation: results from the Gap-Atrial Fibrillation-German Atrial Fibrillation Competence Network 1 Trial. *Circ Arrhythm Electrophysiol* 2016;**9**:e003337.
18. Nakagawa H, Ikeda A, Sharma T, Lazzara R, Jackman WM. Rapid high resolution electroanatomical mapping: evaluation of a new system in a canine atrial linear lesion model. *Circ Arrhythm Electrophysiol* 2012;**5**:417–24.
19. Haïssaguerre M, Jaïs P, Shah DC, Takahashi A, Hocini M, Quiniou G *et al*. Spontaneous initiation of atrial fibrillation by ectopic beats originating in the pulmonary veins. *N Engl J Med* 1998;**339**:659–66.
20. Haïssaguerre M, Shah DC, Jaïs P, Hocini M, Yamane T, Deisenhofer I *et al*. Electrophysiological breakthroughs from the left atrium to the pulmonary veins. *Circulation* 2000;**102**:2463–5.
21. Oral H, Scharf C, Chugh A, Hall B, Cheung P, Good E *et al*. Catheter ablation for paroxysmal atrial fibrillation: segmental pulmonary vein ostial ablation versus left atrial ablation. *Circulation* 2003;**108**:2355–60.
22. Mesas CE, Augello G, Lang CC, Gugliotta F, Vicedomini G, Sora N *et al*. Electroanatomic remodeling of the left atrium in patients undergoing repeat pulmonary vein ablation: mechanistic insights and implications for ablation. *J Cardiovasc Electrophysiol* 2006;**17**:1279–85.
23. Sauer WH, McKernan ML, Lin D, Gerstenfeld EP, Callans DJ, Marchlinski FE. Clinical predictors and outcomes associated with acute return of pulmonary vein conduction during pulmonary vein isolation for treatment of atrial fibrillation. *Heart Rhythm* 2006;**3**:1024–8.
24. Stabile G, Turco P, La RV, Nocerino P, Stabile E, De Simone A. Is pulmonary vein isolation necessary for curing atrial fibrillation? *Circulation* 2003;**108**:657–60.
25. Ouyang F, Antz M, Ernst S, Hachiya H, Mavrakis H, Deger FT *et al*. Recovered pulmonary vein conduction as a dominant factor for recurrent atrial tachyarrhythmias after complete circular isolation of the pulmonary veins: lessons from double Lasso technique. *Circulation* 2005;**111**:127–35.
26. Tamborero D, Mont L, Berruezo A, Guasch E, Rios J, Nadal M *et al*. Circumferential pulmonary vein ablation: does use of a circular mapping catheter improve results? A prospective randomized study. *Heart Rhythm* 2010;**7**:612–8.
27. Chierchia GB, Namdar M, Sarkozy A, Sorgente A, de Asmundis C, Casado-Arroyo R *et al*. Verification of pulmonary vein isolation during single transseptal cryoballoon ablation: a comparison between the classical circular mapping catheter and the inner lumen mapping catheter. *Europace* 2012;**14**:1708–14.
28. Shah D. Electrophysiological evaluation of pulmonary vein isolation. *Europace* 2009;**11**:1423–33.
29. Miyazaki S, Kajiyama T, Watanabe T, Taniguchi H, Nakamura H, Hamaya R *et al*. Validation of electrical ostial pulmonary vein isolation verified with a spiral inner lumen mapping catheter during second-generation cryoballoon ablation. *J Cardiovasc Electrophysiol* 2017;**28**:870–5.
30. Kühne M, Knecht S, Altmann D, Ammann P, Schaer B, Osswald S *et al*. Validation of a novel spiral mapping catheter for real-time recordings from the pulmonary veins during cryoballoon ablation of atrial fibrillation. *Heart Rhythm* 2013;**10**: 241–6.
31. Meissner A, Maagh P, Christoph A, Oernek A, Plehn G. Pulmonary vein potential mapping in atrial fibrillation with high density and standard spiral (lasso) catheters: a comparative study. *J Arrhythm* 2017;**33**:192–200.
32. Anter E, Tschabrunn CM, Contreras-Valdes FM, Li J, Josephson ME. Pulmonary vein isolation using the Rhythmia mapping system: verification of intracardiac signals using the Orion mini-basket catheter. *Heart Rhythm* 2015;**12**:1927–34.
33. Ballesteros G, Ramos P, Neglia R, Menéndez D, García-Bolao I. Atrial fibrillation ablation guided by a novel nonfluoroscopic navigation system. *Rev Esp Cardiol (Engl Ed)* 2017;**70**:706–12.
34. Kosiuk J, Hilbert S, John S, Bertagnolli L, Hindricks G, Bollmann A. Preliminary experience with high-density electroanatomical mapping for ablation of atrial fibrillation—comparison of mini-basket and novel open irrigated magnetic ablation catheter in consecutive patients. *Int J Cardiol* 2017;**228**:401–5.
35. Rottner L, Metzner A, Ouyang F, Heeger C, Hayashi K, Fink T *et al*. Direct comparison of point-by-point and rapid ultra-high-resolution electroanatomical mapping in patients scheduled for ablation of atrial fibrillation. *J Cardiovasc Electrophysiol* 2017;**28**:289–97.
36. Garcia-Bolao I, Ballesteros G, Ramos P, Menéndez D, Erkiaga A, Neglia R *et al*. Identification of pulmonary vein reconnection gaps with high-density mapping in redo atrial fibrillation ablation procedures. *Europace* 2018;**20**:f351–8.
37. Segerson NM, Lynch B, Mozes J, Marks MM, Noonan DK, Gordon D *et al*. High density mapping and ablation of concealed low voltage activity within pulmonary vein antra results in improved freedom from atrial fibrillation compared to pulmonary vein isolation alone. *Heart Rhythm* 2018; doi: 10.1016/j.hrthm.2018.04.035 [Epub ahead of print].

ESC European Society of Cardiology
Europace (2019) **21**, i12–i20
doi:10.1093/europace/euy289

REVIEW

Pulmonary vein reconnections or substrate in the left atrium: what is the reason for atrial fibrillation recurrences? A dialogue on a pressing clinical situation

Clemens Jilek[1] and Waqas Ullah[2]*

[1]Internistisches Klinikum München Süd, Peter-Osypka-Heart Centre, Munich, Germany; and [2]Cardiology Department, University Hospital Southampton, National Health Service Foundation Trust, Southampton, UK

Received 13 April 2018; editorial decision 10 November 2018; accepted 5 January 2019

Pulmonary vein isolation (PVI) has long been held as the cornerstone for atrial fibrillation (AF) ablation. There are patients who do not have successful AF ablations though, especially among those with persistent AF. At the same time, the evidence suggests that ablating beyond the pulmonary veins does not improve success rates. Two possibilities for the incomplete success rates from the procedure are discussed: that more attention needs to be paid to PVI, optimizing delivery of durable, transmural lesions; or alternatively, shifting the focus away from just PVI and addressing the left atrial substrate itself. These two approaches are likely complementary though, and high-density mapping may offer us the ability to undertake them more effectively. The conclusion from this dialogue is that AF is a heterogenous disease and key is to recognize this heterogeneity and respond to it, rather than have a standardized, dogmatic approach. Durable PVI is clearly an important determinant of success but concurrently, we would suggest we need to go beyond this where appropriate to maximize success rates. Clearly the challenge is defining which patients this is appropriate for and how best to do this. Consequently, rather than being 'the' cornerstone of AF ablation, it is more appropriate to consider PVI as 'a' cornerstone of the procedure going forwards and high-density mapping may be the key to optimizing both aspect of the procedure and in so doing improve long term success rates.

Keywords Atrial fibrillation • Pulmonary vein isolation • High-density mapping • LA substrate • Ablation • Efficacy

Introduction

Atrial fibrillation (AF) is associated with significantly increased mortality[1] and stroke risk[2] and is a cause of increasing health care expenditure.[3] Catheter ablation of AF is highly effective and supported as a treatment by international guidelines.[4] The success rates from the procedure are limited though: recent multicentre studies for patients with paroxysmal AF (PAF) have reported single procedure 1 year success rates, off antiarrhythmic drugs of 50–65%,[5,6] with lower success rates for persistent atrial fibrillation (PeAF), 36.4%.[7] Similar results have been reported from a large, 1300 patient, European registry: 40.7% in PAF, 30.2% in PeAF, and 36.7% for long-standing PeAF.[8]

In this article, two views are presented regarding where we should focus our efforts in AF ablation to improve our success rates: assessing and preventing pulmonary vein (PV) reconnections or left atrial scar-guided substrate ablation, and the potential role for high-density mapping to improve these approaches is considered.

Pulmonary vein isolation as cornerstone—Dr Clemens Jilek

Pulmonary vein isolation (PVI) is the cornerstone of the interventional treatment of AF.[9] Despite improvements in catheter and mapping technologies, the recurrence rate of AF remains between 30% and 60% in the first year after ablation depending on the type of underlying AF.

One factor favouring arrhythmia free survival among patients with PAF is the complete isolation of all PVs with circumferential PV

* Corresponding author. Tel: +442381204036; fax: +442381208693. *E-mail address*: waqas@doctors.org.uk

isolation. Circumferential PV isolation allows both isolation of focal PV triggers and ablation/isolation of antral myocardium that plays a role in maintaining AF by its fibre architecture.[10] Patients with incomplete isolation show an increased recurrence rate of 79.2% compared with patients with complete isolation, with a recurrence rate of 62.2% 3 months after ablation procedure.[11] About 90% of patients with incomplete PVI and about 70% of patients with acute complete PVI revealed a PV reconnection in a redo procedure 3 months after the index ablation procedure.[11] The PRESSURE trial[12] confirmed again the key role of reconnection of PVs triggering recurrence of PAF: patients randomized for a second PVI procedure 2 months after index PVI irrespective of symptoms or AF recurrence showed a significantly higher arrhythmia free survival and lower AF burden compared with patients with index PVI alone.

Among patients with PeAF, additional substrate modification had no benefit in the STAR AF II trial compared with PVI alone,[7] and a stepwise approach did not provide additional benefit over PVI alone[13] and even sinus rhythm as the endpoint of the ablation procedure did not perform better than PVI only.[14] As PVI is not thought to increase AF burden one may conclude that substrate modification performed in the actual manner does not influence the arrhythmia free survival rate among all comer patients with PeAF scheduled for ablation. The role of substrate modification will be addressed in the other section of the dialogue.

In the following section, we will discuss two possible factors why catheter driven ablation of AF has low success rates:

(1) Shortcomings in the achievement of transmural, durable ablation lesions
(2) The reliability of conventional mapping catheters in resolving gaps in PVI circles

Pulmonary vein isolation—achieving transmural and durable ablation lesions

Different energy forms are used for PVI including different catheter designs: balloon-based catheters such as cryoballoon or laserballoon maintain circumferential contact with the PV antrum, whereas tip catheters with radiofrequency energy encircle the PVs point by point. Midterm success rates for balloon based vs. catheter tip based PVI are equal,[6,15–17] but there are studies suggesting an advantage of higher success with balloon based PVI. In the randomized 'Cryo vs. RF Trial', the success rate after cryoballoon was higher with 67% compared with radiofrequency with 47% 1 year after procedure.[18] In the FIRE AND ICE trial, subgroup analysis hints in the same direction: despite being not powered for this analysis, the second generation cryoballoon ablation showed a numerically higher success compared with radiofrequency ablation.[6]

A new ablation approach is a high-power short-duration ablation using 90 W of irrigated radiofrequency energy for 4 s. In an animal model, the safety profile was comparable to conventional energy settings but resulted in higher chronic line integrity and lesion transmurality.[19] The impact in humans has yet to be evaluated in randomized trials.

A big effort is currently being made focusing on surrogate parameters to predict a transmural and durable ablation lesion. Parameters are calculated from data derived from impedance, contact force, time, and catheter-tip temperature. Until now there is still a debate about the parameters that have to be taken into consideration and the absolute values or changes that predict a transmural, durable lesion.[20] Up to now, it is too early to give a final conclusion about the impact of these parameters. One may state that, overall, contact force driven PVI has not yet demonstrated any significant advantage compared with non-contact force driven PVI in randomized trials, whereas in observational studies, adequate contact force predicts a higher success rate without influencing complication rate.[21] A new method that is now available is local impedance measurement that reflects catheter-tissue contact and lesion formation in an animal model.[22] A first in man cohort study showed that local impedance gives reproducible values reflecting scar levels and drop of local impedance gives information about tissue contact and lesion formation.[23] Further studies are needed to evaluate if this new technology may predict durable and transmural ablation lesions.

Beyond the attempt to make ablation more efficient and predictable, a different focus lies on identifying dormant conduction after PVI. The hypothesis here being that the presence of dormant conduction may predict long-term PVI failure. Dormant conduction may be unmasked by adenosine testing. In a meta-analysis, including five randomized controlled trials with 2839 patients, no benefit with regard to success rate could be demonstrated by additional adenosine testing.[24]

Does complete pulmonary vein isolation result in a real disconnection or do we miss pulmonary vein potentials with conventional mapping catheters?

Pulmonary vein isolation is confirmed by using circular multipolar mapping catheters. Concerns have been raised about the sensitivity of conventional mapping catheters as the surface size and the electrode spacing is large and small PV potentials may be missed. This means that PV may be interpreted as disconnected when they are actually not.

High-density mapping may give a different view on PV isolation. A new basket-like, 64-pole catheter, ORION (Boston Scientific, Marlborough, MA, USA) with an electrode surface area of 0.4 mm^2, a

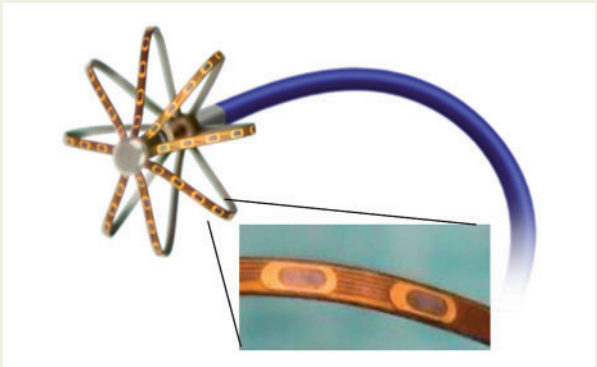

Figure 1 The ORION basket catheter with 64 electrodes with a surface area of 0.4 mm^2 (Boston Scientific, Marlborough, MA, USA).

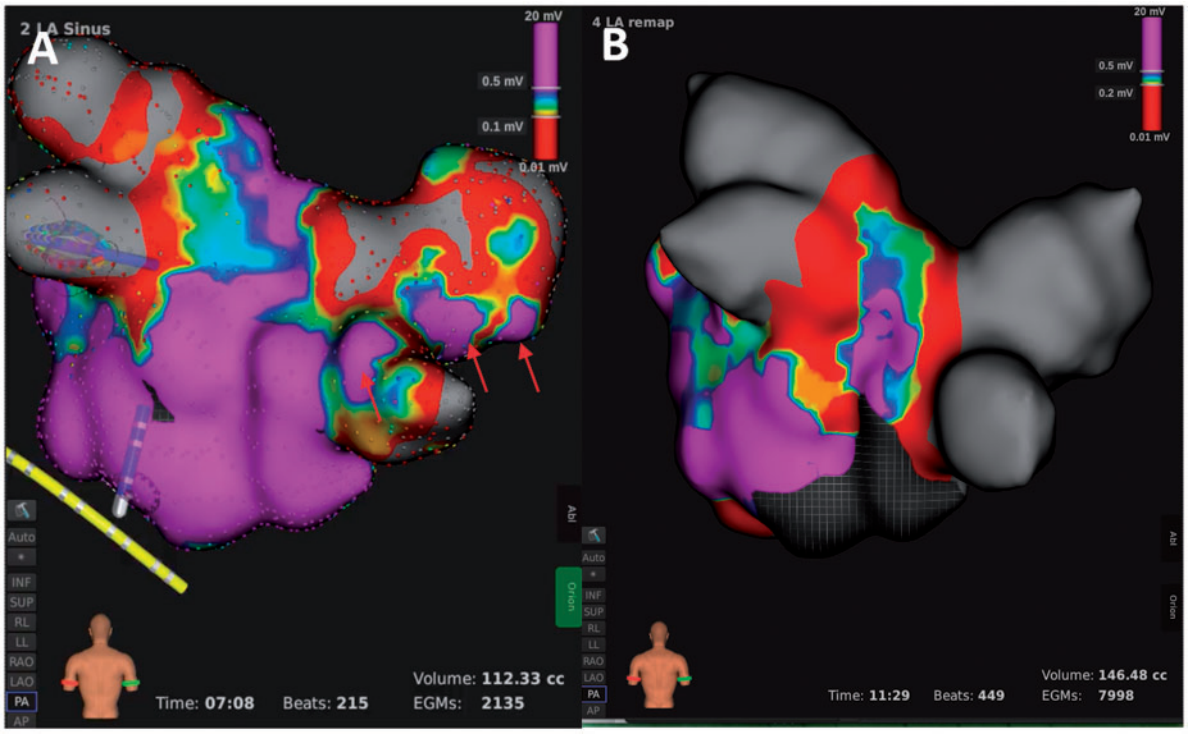

Figure 2 High-density voltage map (left side *A*) with confirmation of a reconnection of the right pulmonary veins (purple area in the veins marked with red arrows) and confirmation of disconnection after ablation (right side *B*).

non-ring electrode design and a small inter-electrode spacing gives the possibility to create high-density maps of the left atrium and the PV ostia (*Figure 1*).[25] The local resolution is higher with the ORION catheter compared with a conventional catheter. This leads to a higher detection rate of PV potentials with the ORION catheters prior to ablation.[26] After PVI, high-density voltage maps can identify gaps non-detected by conventional circular mapping catheters (*Figure 2*). In a pilot study by Anter *et al.*,[27] 22% of PV judged as isolated by a conventional circular mapping catheter could be shown to be non-isolated with the ORION catheter (*Figure 3*). In redo procedures, the findings of Anter could be confirmed: high-density catheters could significantly identify more PV gaps compared with conventional mapping catheters.[28] Due to the higher resolution of the ORION catheter, smaller signals may be displayed in a more detailed way allowing the identification of low voltage signals as correlates of electrical conduction (*Figure 4*). Due to its basket design, the ORION catheter may over detect potentials in the PV arising from neighbouring structures as the left atrial appendage which have to be distinguished from true PV-potential by e.g. pacing manoeuvres.[23]

Considering that there are only data available from a pilot study, there is a hint that the resolution of conventional circular mapping catheters may be too low to identify small gaps in the line encircling the PV ostia. Randomized studies are needed to evaluate the impact of high-density mapping on arrhythmia free survival.

Section conclusion

Pulmonary vein reconnection is a common clinical challenge after PVI. New techniques such as high-density mapping catheters may act as an eye opener for an important reason as to why reconnection of PVs occurs so frequently: namely that gaps in the isolation lines may be missed by conventional circular mapping catheters due to insufficient resolution.

The case for substrate-guided ablation—Dr Waqas Ullah

Since the seminal demonstration of PV firing initiating AF[29] the cornerstone of AF ablation has been PVI.[4] Indeed, based on current AF ablation guidelines, ablation beyond PVI has only a Class IIb recommendation.[4] Technology has consequently focused on attempting to improve our ability to isolate the PVs.[5,6,30,31]

Re-evaluating the importance of durable pulmonary vein isolation

While based on established convention alone it is difficult to dispute the importance of the PVs to AF, it would be expected that there should be a strong relationship between chronic PV isolation and success rates. In a 172 patient study, late-gadolinium enhancement MRI (LGE-MRI) was used to assess left atria 3 months after ablation,

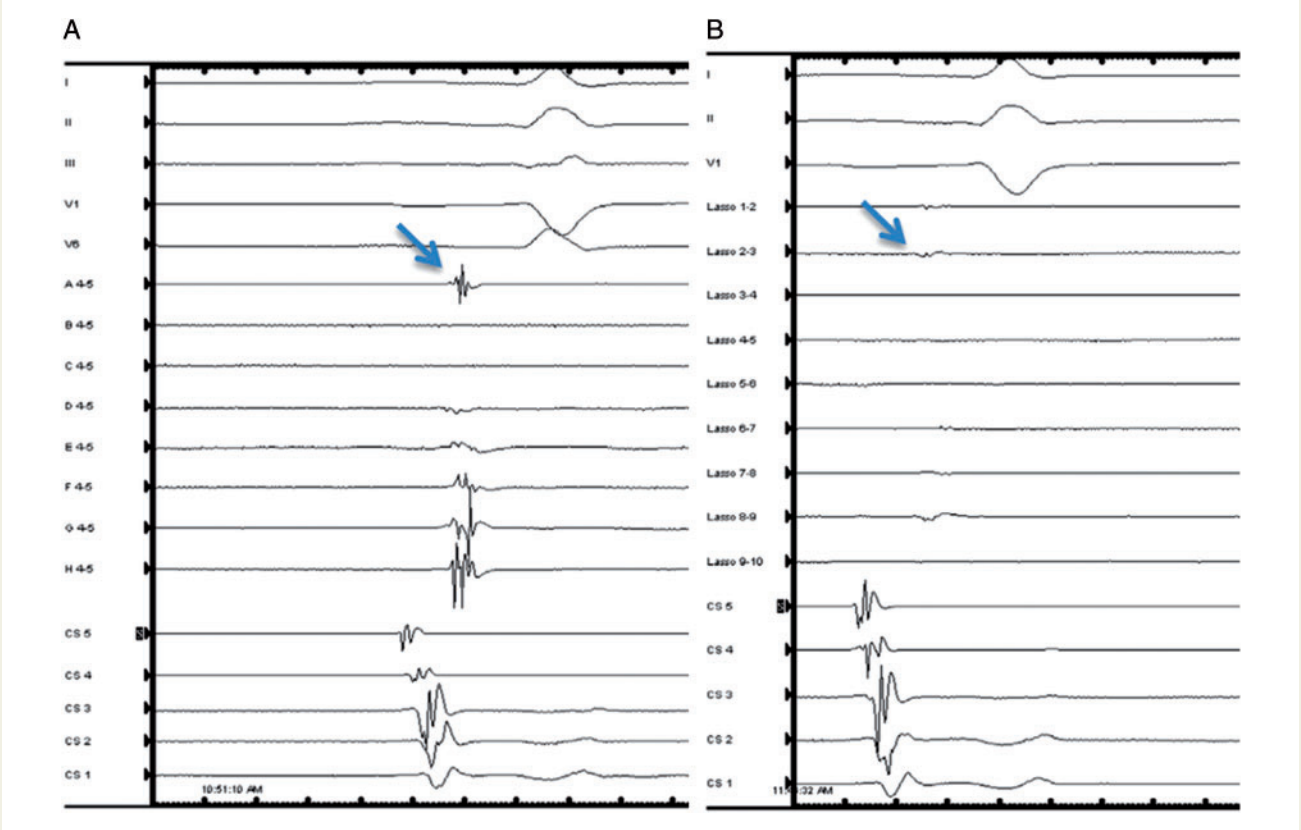

Figure 3 Comparison between mapping with a high-density basket catheter (left side *A*) and a conventional circular mapping catheter. Signals can be displayed with the basket catheter but not with the conventional catheter (Copyright from Anter *et al.*[27]).

specifically assessing for the presence of contiguous scar in the PVI lines.[32] In this study, there was contiguous encirclement of all veins in only 15/172 patients (8.7%). At the same time, the 1 year success rate was much higher than this at 65.1%. This implies that in a high proportion of patients in this study the procedure had been successful without the veins having chronically intact lines of scar. One could argue of course that the latter is not the same as the veins maintaining electrical isolation. In another study, patients without AF recurrence at 1 year were invasively restudied and recovery of PV conduction was observed in 29/32 (90.6%) of patients.[33] This latter approach using interval electrical assessment of PV reconnection has been subjected to meta-analysis, with the conclusion that there was a relationship between durable PVI and reduced AF recurrence, but this was surprisingly modest (RR 0.57, 95% confidence interval 0.37–0.86; $P = 0.008$); also of interest was the finding that in 178/304 (58.6%) patients who were free of AF, there was reconnection of at least one PV.[34] These data could be interpreted to suggest that the benefit of a PVI procedure may not simply relate to the isolation of the veins but in fact to fortuitously incidental modification non-PV of substrate in the process: whether this is ganglionated plexi, rotors, or focal sources,[35] is open to speculation. One could also look at this the other way by assessing the recurrence rate in PAF patients who have proven PV isolation. In a trial of 56 patients with PAF, 52 had a protocol driven restudy at around 3 months and all veins were confirmed isolated in 32 patients. At 1 year, 28.1% of these patients had recurrent AF, despite confirmed PVI at 3 months.[36]

Therefore, patients with clinical success from their ablation procedures can have this without durable PVI and those with durable PVI may not necessarily have clinical success.

The success rates for PeAF are generally worse than PAF,[8] with the assumption being that the substrate beyond the PVs is playing a greater role in maintaining the arrhythmia in PeAF. It is based on this assumption, rather than an alternative explanation that durable PVI is more challenging to achieve in these patients, that clinicians have sought to ablate beyond PVI in PeAF cases. As mentioned in the previous section of the dialogue, the STARAF II trial showed in a multicentre, randomized setting that there was no benefit in adding ablation of complex fractionated electrograms or linear ablation to PVI at 18 months' follow-up.[7] Therefore, these results could be taken to mean that the optimal approach for ablation in PeAF patients is PVI alone: on the other hand, the overall success rate for these patients at 18 months was only 36.4%.

Clearly patients with AF need a more effective ablation strategy, and even more so in the case of PeAF. It would also seem that a more individualized approach, beyond the standard PVI may be warranted in some patients. Determining who these patients are is a challenge and is clearly not contingent on our arbitrary definitions of cases as PAF or PeAF—as a proportion of the former have AF recurrences despite confirmed durable PVI,[36] and a proportion of PeAF

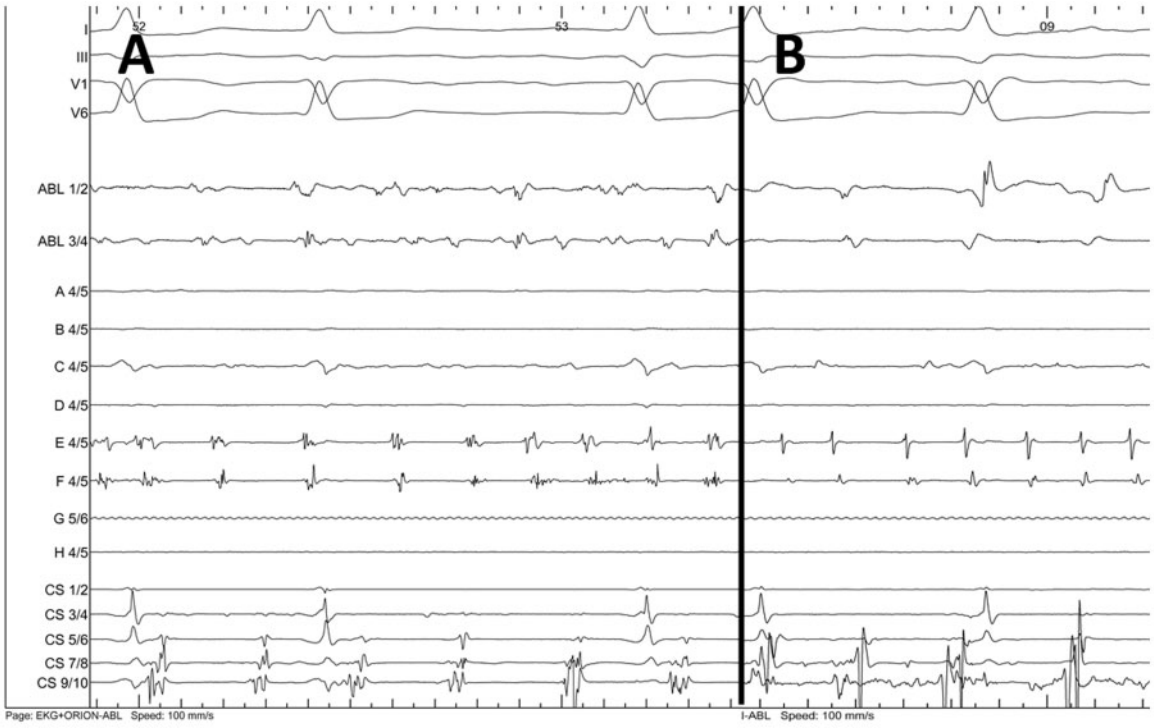

Figure 4 Comparison between high-density basket catheter ORION (left side *A*) and a conventional circular mapping catheter (right side *B*) mapping the same location of an atrial tachycardia. The signals of the high-density catheters are sharper and rich in detail compared with the signals of the conventional circular mapping catheter.

patients have successful procedures despite only PVI being delivered.[7]

Beyond pulmonary vein isolation—triggers, focal sources, and rotors

There has been interest in non-PV trigger ablation for PAF. Empirically isolating the superior vena cava did improve outcomes in one study for PAF patients (but not non-PAF patients),[37] but not in another.[38] Another interesting study in PAF patients found that in those patients with non-PV triggers identified, not ablating these was associated with far worse outcomes compared with patients with such triggers ablated: ablating such triggers led to an equalization of outcomes between patients with non-PV triggers identified and those without.[39] In a persistent AF ablation study, ablation of non-PV triggers was associated with better outcomes than fractionated electrogram ablation.[40] With respect to non-PV triggers, another study found that in a mixed AF subtype patient population undergoing redo procedures, isolating the left atrial appendage, where firing from this was observed, was associated with better outcomes.[41] The difficulty with these more tailored invasive approaches for identifying non-PV triggers is that the protocols involved with attempting to stimulate such triggers are arduous, requiring multiple biatrial catheters, high levels of clinician skill to interpret multiple signals, and there is the possibility that in a given procedure a relevant source may not be triggered and so missed.

An alternative approach which is actively being investigated for PeAF involves panoramic mapping of AF, whether non-invasively[42] or invasively.[43,44] These approaches have the advantage of incorporating automated data processing to highlight focal sources and rotors putatively driving the arrhythmia. While an impressive proportion of procedural AF termination has been observed with this approach, 72–86%,[43,45] multicentre randomized control data looking at outcomes is lacking. Non-randomized multicentre observational data for the invasive Focal Impulse and Rotor Modulation approach, demonstrated disappointing results, with a 1 year off anti-arrhyhtmic drug single procedure success (freedom from atrial arrhythmia) rate of 21%[46]; and for a non-invasive mapping approach a success rate of 44.2%.[45] These results are very much in line with preceding conventional ablation studies.[7,8]

A possible reason for a lack of benefit from an AF panoramic-mapping guided ablation approach could be that this approach targets achieving AF termination through ablation. As highlighted in the previous section of this dialogue, this does not translate into increased long-term success rates. A randomized trial comparing a strategy of attaining AF termination through ablation vs. a standardized lesion set in PeAF patients found no significant difference in outcomes at 1 year.[47] This is in keeping with registry data,[48] including a registry studying patients ablated with a panoramic mapping strategy[49] and a sub-study of the STARAF II trial.[14]

The issue with pursuing rotors and focal sources is that it is possible that not all such sources are present simultaneously. Just because

one is able to terminate AF at one point in time, this does not mean there are not other potential AF sources which happen to be inactive at that moment capable of initiating or maintaining AF. One could attempt to combine the panoramic mapping procedures with the non-PV trigger stimulation protocols to see if this yields better results, though this would not work for a non-invasive mapping approach and would require simultaneous biatrial mapping for an invasive panoramic mapping approach. The success of such an approach would depend on how effectively one is able to stimulate all relevant triggers.

The optimal approach for ablation is clearly one able to target all potential contributors to AF at one procedure. Approaches targeting left atrial scar, which is a fixed target may allow this to be achieved.

Left atrial scar—measurement

Structural remodelling at the tissue level occurs in patients with AF: thick layers of fibrosis between myocytes forming collagenous septa have been observed in the atria[50] and significantly more collagen Type I is seen in the atria of these patients compared with patients without AF.[51,52] An important question is how this scar is clinically measured. MRI-based scar imaging is an attractive prospect as this could be performed pre-ablation to help plan procedures, but there are technical challenges to such imaging. These have been discussed previously,[34] and include the thinness of the left atrial wall, the difficulties with gating and segmenting imaging and most importantly, lack of standardization in distinguishing fibrotic from normal myocardium. Indeed, in the landmark multicentre DECCAF study, 17.3% of the enrolled patients were excluded from the analysis due to poor quality MRI scans.[53]

Voltage mapping is an alternative means of assessing left atrial scar, with a good correlation between voltage maps and MRI scar maps.[54] There are procedural challenges in collecting voltage maps though. The contact force between the mapping catheter and the myocardium is known to affect the measured voltage.[55] The nature of the electrode collecting the data also affect the maps produced, with small electrodes producing a significantly smaller area of scar and able to more accurately pick up lower voltage signals.[56,57] In published studies, where stated, the number of points collected to generate left atrial scar maps is relatively low: 100–120[58] in one study, 54–158 (mean 115)[59] in another, and 164 ± 68[60] in another. Such maps have previously been collected manually. Automated point collection leads to more rapid scar map acquisition: in a study comparing the two approaches more points were collected using automated point collection (923 ± 382.6) points compared with point by point (228.5 ± 95.6 points).[61] These findings as a whole are of great relevance as high-density mapping technologies such as the Rhythmia mapping system with the Orion catheter (Boston Scientific) have now become available, which are able to collect a large number of points by automated collection using mapping catheters with dense, small electrodes, generating maps typically containing thousands of points (*Figure 5*). This produces left atrial voltage maps, which are far more detailed, with less interpolation, than those previously

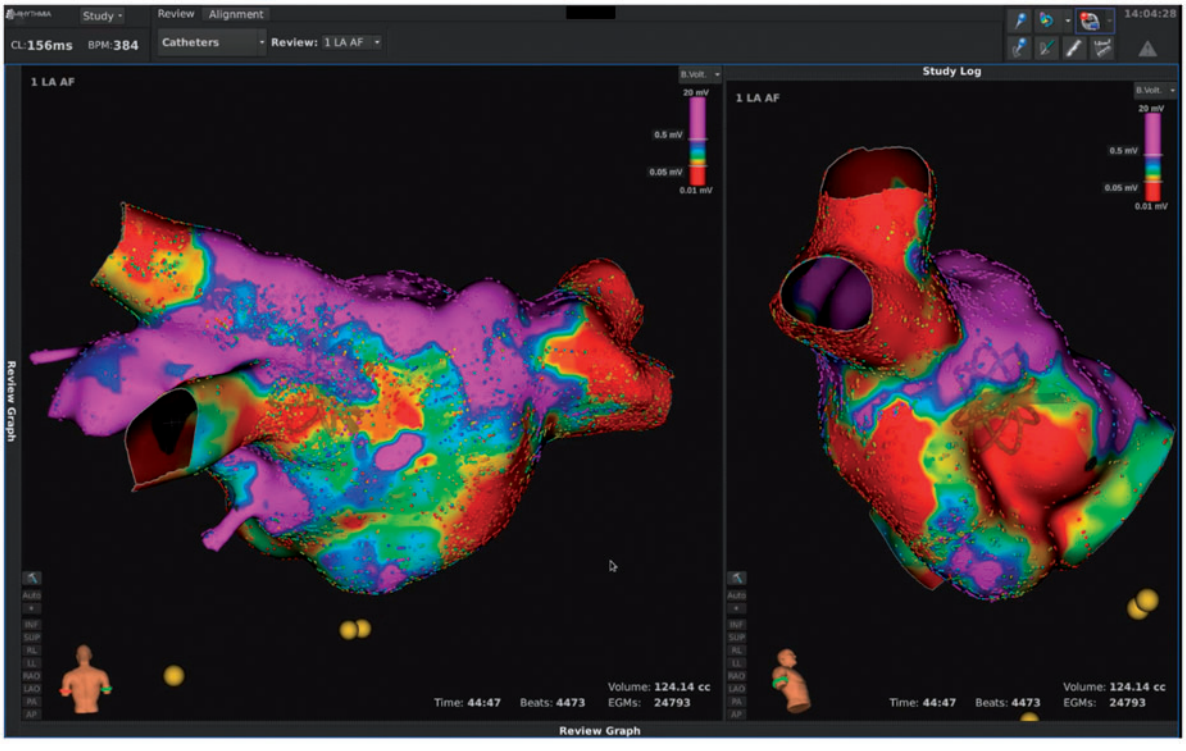

Figure 5 Left atrial voltage map collected using a 64 pole mini basket catheter (Orion) and the Rhythmia mapping system. The map contains 24 793 mapping points. Posterior view on left and off-axis right lateral view on right. Purple areas are healthy myocardium (voltage >0.5 mv). Non-purple areas represent varying degrees of scar, with red areas having a voltage of <0.05 mV.

produced. Whether this level of detail provides an incremental benefit for strategies involving scar ablation is an area of future investigation—one would hypothesize that having a more accurate scar map would mean that more scar regions would be identified, and the extent of these delineated more accurately, to better guide ablation.

One limitation to the current approaches for atrial scar delineation is that they focus on endocardial scar. Recent work has reported asynchrony between the endocardium and epicardium in man with a suggestion made that this could be a driver for persistent AF.[62] Such three-dimensional re-entry would not be appreciated by our current mapping approaches. In this respect, the growing understanding of the three-dimensional nature of scar may be of great importance. Scar has been described as compact, diffuse, patchy and interstitial, and these different patterns of scar are postulated to contribute differently to the maintenance of AF.[63] In a fascinating study of *ex vivo* human right atrial tissue, endocardial/epicardial optical mapping was combined with extremely high resolution three-dimensional gadolinium-enhanced MRI.[64] This study demonstrated that transmural activation delay at increasing pacing rates was influenced by intramural fibrosis, and such fibrosis also provided a substrate for intramural micro re-entry, with ablation here terminating pharmacologically induced AF.[64] It may be in the future that an even more detailed understanding and delineation of scar allows us to identify accurately which sub-regions in a patch of scar are sustaining AF, by anatomical-arrhythmic correlation, and so target them.

Left atrial scar—clinical relevance

The current literature examining the relevance of left atrial scar clinically is based on MRI data and in the case of invasively determined electrical scar, predates the use of high-density mapping and has focused on endocardial scar exclusively. While the electrical scar mapping approach therefore has theoretical limitations, the results as discussed below are intriguing.

Patients with a high burden of left atrial scar as determined by contact mapping have an increased likelihood of AF recurrence after ablation.[60] A similar finding has been found using cardiac MRI and in this case, on multivariable analysis, MRI-determined left atrial fibrosis is significantly predictive of recurrence, while other factors included in the model such as AF subtype and left atrial size are not, suggesting fibrosis is a greater determinant of success.[53] In a further MRI study, a multivariable model was constructed including the degree of left atrial fibrosis pre-ablation and the number of PVs with contiguous scar encirclement at 3 months on MRI, and the only predictive factor for success at 1 year was left atrial fibrosis, suggesting the latter is more important than durable PVI.[32]

Groups have compared atrial scar with AF sources as determined by panoramic mapping. A higher MRI-detected left atrial scar burden correlates with a greater number of non-invasively detected AF drivers, with areas of scar having a high sensitivity (82%) but a lower specificity (65%) for harbouring sources detected on a pre-procedural non-invasive mapping study.[49] One could suggest that the latter may be contributed to by the transience of driver sources. Similarly, in an invasive panoramic mapping study, 85.7% of observed drivers occurred in areas of scar.[44] These data lend a mechanistic explanation for the importance of left atrial scar to perpetuating AF clinically, complementing *ex vivo* work,[64] and giving credence to the idea that addressing scar by ablation will significantly improve success rates for the procedure and would have an advantage over strategies looking for drivers as the former is fixed and the latter are less temporally stable.

While the discussion has focused on ablation, there is also a vital role for upstream treatment to improve AF risk factors. For instance, treating sleep apnoea with CPAP in patients with sleep apnoea improves ablation outcomes,[65] aerobic interval training reduces time in AF,[66] and ablation outcomes as a whole have been found to be better for patients who undergo aggressive risk factor management (including smoking cessation, blood pressure management, and weight loss).[67] These upstream factors likely have an effect on ablation outcomes through their effect on left atrial substrate: there is more evidence of atrial remodelling and lower voltages have been observed in the context of obesity[68] and sleep apnoea[69] than controls. This feeds into the argument that left atrial substrate is a unifying predictor of procedural success, and presents risk factor control, rather than just ablation, as another way of treating this. Such risk factor control would also be of continuing importance after ablation to maintain success by preventing further substrate development post-ablation. Consequently, management of AF in the future may be a multidisciplinary approach, focusing not just on the ablation procedure, but the expertise of several specialists to address upstream factors both pre and post ablation.

While left atrial scar burden is predictive of ablation success, the question is whether strategies to ablate AF which target atrial scar directly may be beneficial. Ablation of these regions has been studied in non-randomized studies, using electrical scar to guide ablation.[58,59,70,71] On retrospective comparison, in one study, the success rate in patients with low voltage zones improved from 27% to 70% with a scar-guided ablation strategy,[59] with a similar magnitude of improvement in another study (38% vs. 72%).[71] Ablation approaches for scar-guided ablation have varied in their approach, for example, using the presence of low voltage areas to determine if a box lesion should be applied—in this case if the scar is >0.5*0.5 cm[70]; box isolation of fibrotic areas[58]; scar homogenization,[71] and a mixture of homogenization and lines.[59] Importantly, these approaches lead to an equalization of outcomes between patients with left atrial scar to those without—the outcomes for the former are worse if scar is not treated.

These non-randomized trials are encouraging, but the real test will be when a substrate-based ablation approach is subject to prospective randomized trials. There are two such trials underway and their results are therefore eagerly awaited. One is a prospective left atrial voltage-determined scar ablation multicentre randomized control trial, ERASE-AF (NCT02732626), which aims to randomize 320 PeAF patients. The other trial will be using MRI-based scar to guide AF ablation, is currently also being investigated in the DECAAFII trial (NCT02529319), a randomized trial, aiming for 888 PeAF patients.

Future work should focus on the impact of left atrial scar maps determined by high-density mapping and the role of epicardial scar. One would predict that high-density scar maps, by more accurately delineating scar, will allow us to be more targeted with our ablation allowing maximization of safety and efficacy.

Section conclusion

There is a body of evidence suggesting PVI alone may be insufficient as a strategy for ablation in all patients. To truly improve on our

results, we need to more effectively tailor our procedures to the individual patient. One exciting approach to this may be atrial scar-guided ablation. Such a strategy could identify patients needing more extensive ablation prior to the procedure using MRI, or during the procedure based on voltage mapping, irrespective of the PAF or PeAF label they have been given. In the future, a greater appreciation of the three-dimensional nature of scar, incorporating the endocardium, epicardium and intramural portion of the atrium, may further refine this approach. Randomized trials are underway to determine the efficacy of a scar-guided ablation approach and future work will explore the best approach to obtain scar data, specifically whether the level of detail provided by high-density voltage mapping is of clinical relevance.

Conclusions

The above discussions have proposed two different approaches for the ablation of AF. For the purposes of the dialogue they have been posed as opposing, but this division is clearly an artificial one. AF is a heterogenous disease and the key thing is to recognize this heterogeneity and respond to it rather than have a standardized, dogmatic approach. Durable PVI is clearly an important determinant of success rates for the procedure, and our ability to achieve and assess this is paramount. At the same time though, there is a clear need to address other elements of the atrium to significantly increment our success rates. The fact that ablation additional to PVI has not been shown in randomized trials to improve success rates to date suggest that the generic atrial defragmentation approaches studied in those trials are incorrect. Scar-guided ablation, which is an individualized rather than generic approach, is a potentially exciting in this respect but requires randomized trials to confirm its utility, and requires refinement with regard to how scar data is collected. High-density mapping technologies may help us improve both PVI and scar appraisal and consequently help optimize ablation procedures and deliver the best outcomes for our patients.

We would predict that in the future, rather than durable PVI being 'the' cornerstone for AF ablation, it may be relegated to simply 'a' cornerstone of the procedure, with the appraisal and treatment of atrial substrate constituting the other cornerstone of a successful procedure.

Conflict of interest: W.U. has received Speaker and Travel fees from Biosense Webster Inc and Boston Scientific, as well as Proctorship fees from Boston Scientific. C.J. has conflicts of interest with Abbott, Biotronik, Boston Scientific and Medtronic.

References

1. Benjamin EJ, Wolf PA, D'Agostino RB, Silbershatz H, Kannel WB, Levy D. Impact of atrial fibrillation on the risk of death: the Framingham Heart Study. *Circulation* 1998;**98**:946–52.
2. Wolf PA, Abbott RD, Kannel WB. Atrial fibrillation as an independent risk factor for stroke: the Framingham Study. *Stroke* 1991;**22**:983–8.
3. Stewart S, Murphy NF, Murphy N, Walker A, McGuire A, McMurray JJV. Cost of an emerging epidemic: an economic analysis of atrial fibrillation in the UK. *Heart Br Card Soc* 2004;**90**:286–92.
4. Calkins H, Hindricks G, Cappato R, Kim Y-H, Saad EB, Aguinaga L *et al.* 2017 HRS/EHRA/ECAS/APHRS/SOLAECE expert consensus statement on catheter and surgical ablation of atrial fibrillation. *Europace* 2018;**20**:e1–160.
5. Ullah W, McLean A, Tayebjee MH, Gupta D, Ginks MR, Haywood GA *et al.* Randomized trial comparing pulmonary vein isolation using the SmartTouch catheter with or without real-time contact force data. *Heart Rhythm* 2016;**13**:1761–7.
6. Kuck K-H, Brugada J, Fürnkranz A, Metzner A, Ouyang F, Chun KRJ *et al.* Cryoballoon or radiofrequency ablation for paroxysmal atrial fibrillation. *N Engl J Med* 2016;**374**:2235–45.
7. Verma A, Jiang C, Betts TR, Chen J, Deisenhofer I, Mantovan R *et al.* Approaches to catheter ablation for persistent atrial fibrillation. *N Engl J Med* 2015;**372**:1812–22.
8. Arbelo E, Brugada J, Hindricks G, Maggioni AP, Tavazzi L, Vardas P *et al.* The atrial fibrillation ablation pilot study: an European Survey on Methodology and results of catheter ablation for atrial fibrillation: conducted by the European Heart Rhythm Association. *Eur Heart J* 2014;**35**:1466–78.
9. Kirchhof P, Benussi S, Kotecha D, Ahlsson A, Atar D, Casadei B *et al.* 2016 ESC Guidelines for the management of atrial fibrillation developed in collaboration with EACTS. *Europace* 2016;**18**:1609–78.
10. Hamabe A, Okuyama Y, Miyauchi Y, Zhou S, Pak H-N, Karagueuzian HS *et al.* Correlation between anatomy and electrical activation in canine pulmonary veins. *Circulation* 2003;**107**:1550–5.
11. Kuck K-H, Hoffmann BA, Ernst S, Wegscheider K, Treszl A, Metzner A *et al.* Impact of complete versus incomplete circumferential lines around the pulmonary veins during catheter ablation of paroxysmal atrial fibrillation: results from the Gap-Atrial Fibrillation-German Atrial Fibrillation Competence Network 1 Trial. *Circ Arrhythm Electrophysiol* 2016;**9**:e003337.
12. Das M, Wynn GJ, Saeed Y, Gomes S, Morgan M, Ronayne C *et al.* Pulmonary vein re-isolation as a routine strategy regardless of symptoms: the PRESSURE randomized controlled trial. *JACC Clin Electrophysiol* 2017;**3**:602–11.
13. Vogler J, Willems S, Sultan A, Schreiber D, Lüker J, Servatius H *et al.* Pulmonary vein isolation versus defragmentation: the CHASE-AF clinical trial. *J Am Coll Cardiol* 2015;**66**:2743–52.
14. Kochhäuser S, Jiang C-Y, Betts TR, Chen J, Deisenhofer I, Mantovan R *et al.* Impact of acute atrial fibrillation termination and prolongation of atrial fibrillation cycle length on the outcome of ablation of persistent atrial fibrillation: a substudy of the STAR AF II trial. *Heart Rhythm* 2017;**14**:476–83.
15. Schmidt B, Neuzil P, Luik A, Osca Asensi J, Schrickel JW, Deneke T *et al.* Laser balloon or wide-area circumferential irrigated radiofrequency ablation for persistent atrial fibrillation: a multicenter prospective randomized study. *Circ Arrhythm Electrophysiol* 2017;**10**. doi:10.1161/CIRCEP.117.005767.
16. Murray M-I, Arnold A, Younis M, Varghese S, Zeiher AM. Cryoballoon versus radiofrequency ablation for paroxysmal atrial fibrillation: a meta-analysis of randomized controlled trials. *Clin Res Cardiol* 2018;**107**:658–69.
17. Buiatti A, Olshausen G, von Barthel P, Schneider S, Luik A, Kaess B *et al.* Cryoballoon vs. radiofrequency ablation for paroxysmal atrial fibrillation: an updated meta-analysis of randomized and observational studies. *Europace* 2017;**19**:378–84.
18. Hunter RJ, Baker V, Finlay MC, Duncan ER, Lovell MJ, Tayebjee MH *et al.* Point-by-point radiofrequency ablation versus the cryoballoon or a novel combined approach: a randomized trial comparing 3 methods of pulmonary vein isolation for paroxysmal atrial fibrillation (The Cryo Versus RF Trial). *J Cardiovasc Electrophysiol* 2015;**26**:1307–14.
19. Barkagan M, Contreras-Valdes FM, Leshem E, Buxton AE, Nakagawa H, Anter E. High-power and short-duration ablation for pulmonary vein isolation: safety, efficacy, and long-term durability. *J Cardiovasc Electrophysiol* 2018;**29**:1287–96.
20. Das M, Loveday JJ, Wynn GJ, Gomes S, Saeed Y, Bonnett LJ *et al.* Ablation index, a novel marker of ablation lesion quality: prediction of pulmonary vein reconnection at repeat electrophysiology study and regional differences in target values. *Europace* 2016;**19**:775–83.
21. Lin H, Chen Y-H, Hou J-W, Lu Z-Y, Xiang Y, Li Y-G. Role of contact force-guided radiofrequency catheter ablation for treatment of atrial fibrillation: a systematic review and meta-analysis. *J Cardiovasc Electrophysiol* 2017;**28**:994–1005.
22. Sulkin MS, Laughner JI, Hilbert S, Kapa S, Kosiuk J, Younan P *et al.* Novel measure of local impedance predicts catheter—tissue contact and lesion formation. *Circ Arrhythm Electrophysiol* 2018;**11**:e005831.
23. Martin CA, Martin R, Gajendragadkar PR, Maury P, Takigawa M, Cheniti G *et al.* First clinical use of novel ablation catheter incorporating local impedance data. *J Cardiovasc Electrophysiol* 2018;**29**:1197–206.
24. Afzal MR, Kahaly O, Weiss R, Houmsse M, Daoud EG, Hummel JD. Adenosine triphosphate/adenosine guided pulmonary vein isolation does not improve the outcomes of ablation: a meta-analysis of randomized controlled trials. *Expert Rev Cardiovasc Ther* 2018;**16**:313–8.
25. Sohns C, Saguner AM, Lemes C, Santoro F, Mathew S, Heeger C *et al.* First clinical experience using a novel high-resolution electroanatomical mapping system for left atrial ablation procedures. *Clin Res Cardiol* 2016;**105**:992–1002.
26. Meissner A, Maagh P, Christoph A, Oernek A, Plehn G. Pulmonary vein potential mapping in atrial fibrillation with high density and standard spiral (lasso) catheters: a comparative study. *J Arrhythm* 2017;**33**:192–200.

27. Anter E, Tschabrunn CM, Contreras-Valdes FM, Li J, Josephson ME. Pulmonary vein isolation using the Rhythmia mapping system: verification of intracardiac signals using the Orion mini-basket catheter. *Heart Rhythm* 2015;**12**:1927–34.
28. Lin C-Y, Te ALD, Lin Y-J, Chang S-L, Lo L-W, Hu Y-F *et al.* High-resolution mapping of pulmonary vein potentials improved the successful pulmonary vein isolation using small electrodes and inter-electrode spacing catheter. *Int J Cardiol* 2018;**272**:90–6.
29. Haissaguerre M, Jais P, Shah DC, Takahashi A, Hocini M, Quiniou G *et al.* Spontaneous initiation of atrial fibrillation by ectopic beats originating in the pulmonary veins. *N Engl J Med* 1998;**339**:659.
30. Hussein A, Das M, Chaturvedi V, Asfour IK, Daryanani N, Morgan M *et al.* Prospective use of Ablation Index targets improves clinical outcomes following ablation for atrial fibrillation. *J Cardiovasc Electrophysiol* 2017;**28**:1037–47.
31. Ullah W, Hunter RJ, Finlay MC, McLean A, Dhinoja MB, Sporton S *et al.* Ablation index and surround flow catheter irrigation: impedance-based appraisal in clinical ablation. *JACC Clin Electrophysiol* 2017;**3**:1080–8.
32. Akoum N, Morris A, Perry D, Cates J, Burgon N, Kholmovski E *et al.* Substrate modification is a better predictor of catheter ablation success in atrial fibrillation than pulmonary vein isolation: an LGE-MRI study. *Clin Med Insights Cardiol* 2015;**9**: 25–31.
33. Jiang R-H, Po SS, Tung R, Liu Q, Sheng X, Zhang Z-W *et al.* Incidence of pulmonary vein conduction recovery in patients without clinical recurrence after ablation of paroxysmal atrial fibrillation: mechanistic implications. *Heart Rhythm* 2014; **11**:969–76.
34. Nery PB, Belliveau D, Nair GM, Bernick J, Redpath CJ, Szczotka A *et al.* Relationship between pulmonary vein reconnection and atrial fibrillation recurrence: a systematic review and meta-analysis. *JACC Clin Electrophysiol* 2016;**2**:474–83.
35. Narayan SM, Krummen DE, Clopton P, Shivkumar K, Miller JM. Direct or coincidental elimination of stable rotors or focal sources may explain successful atrial fibrillation ablation: on-treatment analysis of the CONFIRM (CONventional ablation for AF with or without Focal Impulse and Rotor Modulation) trial. *J Am Coll Cardiol* 2013;**62**:138–47.
36. Dukkipati SR, Neuzil P, Kautzner J, Petru J, Wichterle D, Skoda J *et al.* The durability of pulmonary vein isolation using the visually guided laser balloon catheter: multicenter results of pulmonary vein remapping studies. *Heart Rhythm* 2012;**9**: 919–25.
37. Corrado A, Bonso A, Madalosso M, Rossillo A, Themistoclakis S, Di Biase L *et al.* Impact of systematic isolation of superior vena cava in addition to pulmonary vein antrum isolation on the outcome of paroxysmal, persistent, and permanent atrial fibrillation ablation: results from a randomized study. *J Cardiovasc Electrophysiol* 2010;**21**:1–5.
38. Wang X-H, Liu X, Sun Y-M, Shi H-F, Zhou L, Gu J-N. Pulmonary vein isolation combined with superior vena cava isolation for atrial fibrillation ablation: a prospective randomized study. *Europace* 2008;**10**:600–5.
39. Elayi CS, Biase LD, Bai R, Burkhardt JD, Mohanty P, Santangeli P *et al.* Administration of isoproterenol and adenosine to guide supplemental ablation after pulmonary vein antrum isolation. *J Cardiovasc Electrophysiol* 2013;**24**: 1199–206.
40. Dixit S, Marchlinski FE, Lin D, Callans DJ, Bala R, Riley MP *et al.* Randomized ablation strategies for the treatment of persistent atrial fibrillation: RASTA study. *Circ Arrhythm Electrophysiol* 2012;**5**:287–94.
41. Biase LD, Burkhardt JD, Mohanty P, Sanchez J, Mohanty S, Horton R *et al.* Left atrial appendage an underrecognized trigger site of atrial fibrillation. *Circulation* 2010;**122**:109–18.
42. Haissaguerre M, Hocini M, Shah AJ, Derval N, Sacher F, Jais P *et al.* Noninvasive panoramic mapping of human atrial fibrillation mechanisms: a feasibility report. *J Cardiovasc Electrophysiol* 2013;**24**:711–7.
43. Narayan SM, Krummen DE, Shivkumar K, Clopton P, Rappel W-J, Miller JM. Treatment of atrial fibrillation by the ablation of localized sources. *J Am Coll Cardiol* 2012;**60**:628–36.
44. Honarbakhsh S, Schilling RJ, Dhillon G, Ullah W, Keating E, Providencia R *et al.* A novel mapping system for panoramic mapping of the left atrium: application to detect and characterize localized sources maintaining atrial fibrillation. *JACC Clin Electrophysiol* 2018;**4**:124–34.
45. Knecht S, Sohal M, Deisenhofer I, Albenque J-P, Arentz T, Neumann T *et al.* Multicentre evaluation of non-invasive biatrial mapping for persistent atrial fibrillation ablation: the AFACART study. *Europace* 2017;**19**:1302–9.
46. Buch E, Share M, Tung R, Benharash P, Sharma P, Koneru J *et al.* Long-term clinical outcomes of focal impulse and rotor modulation for treatment of atrial fibrillation: a multicenter experience. *Heart Rhythm* 2016;**13**:636–41.
47. Yuan-Long W, Xu L, Yu Z, Wei-Feng J, Li Z, Mu Q *et al.* Optimal endpoint for catheter ablation of longstanding persistent atrial fibrillation: a randomized clinical trial. *Pacing Clin Electrophysiol* 2018;**41**:172–8.
48. Elayi CS, Di Biase L, Barrett C, Ching CK, Al AM, Lucciola M *et al.* Atrial fibrillation termination as a procedural endpoint during ablation in long-standing persistent atrial fibrillation. *Heart Rhythm* 2010;**7**:1216–23.
49. Cochet H, Dubois R, Yamashita S, Al Jefairi N, Berte B, Sellal J-M *et al.* Relationship between fibrosis detected on late gadolinium-enhanced cardiac magnetic resonance and re-entrant activity assessed with electrocardiographic imaging in human persistent atrial fibrillation. *JACC Clin Electrophysiol* 2018;**4**: 17–29.
50. Rücker-Martin C, Pecker F, Godreau D, Hatem SN. Dedifferentiation of atrial myocytes during atrial fibrillation: role of fibroblast proliferation *in vitro*. *Cardiovasc Res* 2002;**55**:38–52.
51. Xu J, Cui G, Esmailian F, Plunkett M, Marelli D, Ardehali A *et al.* Atrial extracellular matrix remodeling and the maintenance of atrial fibrillation. *Circulation* 2004; **109**:363–8.
52. Kostin S, Klein G, Szalay Z, Hein S, Bauer EP, Schaper J. Structural correlate of atrial fibrillation in human patients. *Cardiovasc Res* 2002;**54**:361–79.
53. Marrouche NF, Wilber D, Hindricks G, Jais P, Akoum N, Marchlinski F *et al.* Association of atrial tissue fibrosis identified by delayed enhancement MRI and atrial fibrillation catheter ablation: the DECAAF study. *JAMA* 2014;**311**:498.
54. Zghaib T, Keramati A, Chrispin J, Huang D, Balouch MA, Ciuffo L *et al.* Multimodal examination of atrial fibrillation substrate: correlation of left atrial bipolar voltage using multi-electrode fast automated mapping, point-by-point mapping, and magnetic resonance image intensity ratio. *JACC Clin Electrophysiol* 2018;**4**:59–68.
55. Ullah W, Hunter RJ, Baker V, Ling L-H, Dhinoja MB, Sporton S *et al.* The impact of catheter contact force on human left atrial electrogram characteristics in sinus rhythm and atrial fibrillation. *Circ Arrhythm Electrophysiol* 2015;**8**:1030–9.
56. Anter E, Tschabrunn CM, Josephson ME. High-resolution mapping of scar-related atrial arrhythmias using smaller electrodes with closer interelectrode spacing. *Circ Arrhythm Electrophysiol* 2015;**8**:537–45.
57. Huemer M, Qaiyumi D, Attanasio P, Parwani A, Pieske B, Blaschke F *et al.* Does the extent of left atrial arrhythmogenic substrate depend on the electroanatomical mapping technique: impact of pulmonary vein mapping catheter vs. ablation catheter. *Europace* 2017;**19**:1293–301.
58. Kottkamp H, Berg J, Bender R, Rieger A, Schreiber D. Box Isolation of Fibrotic Areas (BIFA): a patient-tailored substrate modification approach for ablation of atrial fibrillation. *J Cardiovasc Electrophysiol* 2016;**27**:22–30.
59. Rolf S, Kircher S, Arya A, Eitel C, Sommer P, Richter S *et al.* Tailored atrial substrate modification based on low-voltage areas in catheter ablation of atrial fibrillation. *Circ Arrhythm Electrophysiol* 2014;**7**:825–33.
60. Verma A, Wazni OM, Marrouche NF, Martin DO, Kilicaslan F, Minor S *et al.* Pre-existent left atrial scarring in patients undergoing pulmonary vein antrum isolationAn independent predictor of procedural failure. *J Am Coll Cardiol* 2005; **45**:285–92.
61. Liang JJ, Elafros MA, Muser D, Pathak RK, Santangeli P, Supple GE *et al.* Comparison of left atrial bipolar voltage and scar using multielectrode fast automated mapping versus point-by-point contact electroanatomic mapping in patients with atrial fibrillation undergoing repeat ablation. *J Cardiovasc Electrophysiol* 2017;**28**:280–8.
62. de GN, van der DL, Yaksh A, Lanters E, Teuwen C, Knops P *et al.* Direct proof of endo-epicardial asynchrony of the atrial wall during atrial fibrillation in humans. *Circ Arrhythm Electrophysiol* 2016;**9**:e003648.
63. Hansen BJ, Zhao J, Fedorov VV. Fibrosis and atrial fibrillation: computerized and optical mapping: a view into the human atria at submillimeter resolution. *JACC Clin Electrophysiol* 2017;**3**:531–46.
64. Hansen BJ, Zhao J, Csepe TA, Moore BT, Li N, Jayne LA *et al.* Atrial fibrillation driven by micro-anatomic intramural re-entry revealed by simultaneous sub-epicardial and sub-endocardial optical mapping in explanted human hearts. *Eur Heart J* 2015;**36**:2390–401.
65. Fein AS, Shvilkin A, Shah D, Haffajee CI, Das S, Kumar K *et al.* Treatment of obstructive sleep apnea reduces the risk of atrial fibrillation recurrence after catheter ablation. *J Am Coll Cardiol* 2013;**62**:300–5.
66. Malmo V, Nes BM, Amundsen BH, Tjonna A-E, Stoylen A, Rossvoll O *et al.* Aerobic interval training reduces the burden of atrial fibrillation in the short term: a randomized trial. *Circulation* 2016;**133**:466–73.
67. Pathak RK, Middeldorp ME, Lau DH, Mehta AB, Mahajan R, Twomey D *et al.* Aggressive risk factor reduction study for atrial fibrillation and implications for the outcome of ablation: the ARREST-AF cohort study. *J Am Coll Cardiol* 2014; **64**:2222–31.
68. Mahajan R, Lau DH, Brooks AG, Shipp NJ, Manavis J, Wood JPM *et al.* Electrophysiological, electroanatomical, and structural remodeling of the atria as consequences of sustained obesity. *J Am Coll Cardiol* 2015;**66**:1–11.
69. Dimitri H, Ng M, Brooks AG, Kuklik P, Stiles MK, Lau DH *et al.* Atrial remodeling in obstructive sleep apnea: implications for atrial fibrillation. *Heart Rhythm* 2012; **9**:321–7.
70. Cutler MJ, Johnson J, Abozguia K, Rowan S, Lewis W, Costantini O *et al.* Impact of voltage mapping to guide whether to perform ablation of the posterior wall in patients with persistent atrial fibrillation. *J Cardiovasc Electrophysiol* 2016;**27**:13–21.
71. Yamaguchi T, Tsuchiya T, Nakahara S, Fukui A, Nagamoto Y, Murotani K *et al.* Efficacy of left atrial voltage-based catheter ablation of persistent atrial fibrillation. *J Cardiovasc Electrophysiol* 2016;**27**:1055–63.

ESC European Society of Cardiology
Europace (2019) **21**, i21–i26
doi:10.1093/europace/euy182

REVIEW

Scar identification, quantification, and characterization in complex atrial tachycardia: a path to targeted ablation?

Decebal Gabriel Laţcu[1]*, Sok-Sithikun Bun[1], Ruben Casado Arroyo[2], Ahmed Moustfa Wedn[1], Fatima Azzahrae Benaich[1], Karim Hasni[1], Bogdan Enache[1], and Nadir Saoudi[1]

[1]Service de Cardiologie, Centre Hospitalier Princesse Grace, Avenue Pasteur 98000, Monaco; and [2]Department of Cardiology, Erasme University Hospital, Université Libre de Bruxelles, Brussels, Belgium

Received 2 April 2018; editorial decision 21 July 2018; accepted 23 July 2018

Successful catheter ablation of scar-related atrial tachycardia depends on correct identification of the critical isthmus. Often, this is a represented by a small bundle of viable conducting tissue within a low-voltage area. It's identification depends on the magnitude of the signal/noise ratio. Ultra-high density mapping, multipolar catheters with small (eventually unidirectional) and closely-spaced electrodes improves low-voltage electrogram detection. Background noise limitation is also of major importance for improving the signal/noise ratio. Electrophysiological properties of the critical isthmus and the characteristics of the local bipolar electrograms have been recently demonstrated as hallmarks of successful ablation sites in the setting of scar-related atrial tachycardia.

Keywords Scar • Fibrosis • Atrial tachycardia • Electroanatomical mapping

Introduction

Complex atrial tachycardia (AT) are frequently scar-related, either after atrial fibrillation (AF) ablation or incisional. The success of catheter ablation depends on the precise diagnosis of the AT mechanism, which is sometimes very challenging[1] despite reliable electrocardiogram (ECG)-based algorithms that have been proposed and are used in everyday practice.[2–5] Recent advances in mapping resolution and precise automatic annotation of intracardiac electrograms (EGM) are major steps in the evolution of electro-anatomical mapping systems.[6] Entrainment mapping remains very useful to select the chamber to be mapped, to diagnose/confirm the AT mechanism and to rule out passive loops.[7]

On top of these techniques precise knowledge of previously created lesions (ablation reports, previous maps with ablation tags, and surgical reports) along with substrate imaging contribute to scar identification. This step plays a key role since critical areas of arrhythmogenesis occur often in diseased tissue where voltage is attenuated. In this article, we will review the particularities of scar identification at the atrial level and of the detection of viable tissue within scars by improving the signal/noise ratio.

Pathophysiology of atrial scar

Electrical[8] and structural[9] remodelling are, in many cases, the substrate of atrial tachyarrhythmias. Fibrosis is the hallmark of structural remodelling[10]; replacement fibrosis (e.g. post-myocardial infarction) and interstitial fibrosis (reactive—due to ageing, hypertension, obstructive sleep apnoea, or infiltrative—such as in amyloidosis) are commonly described, with both types coexisting in many late-stage conditions.[11] They all have in common an increase of the extracellular matrix at the expense of cardiomyocytes. Myofibroblats of various origins synthetize collagen, which is deposited in the extracellular space.[12] Various factors such as pressure and volume overload induce an imbalance between matrix metalloproteinase[13] and tissue inhibitor of metalloproteinases, leading to an insufficient degradation of the extracellular matrix, and finally myocardial fibrosis.[14]

* Corresponding author. Tel: +377 97 98 97 71; fax: +377 97 98 97 32. *E-mail address:* dglatcu@yahoo.com

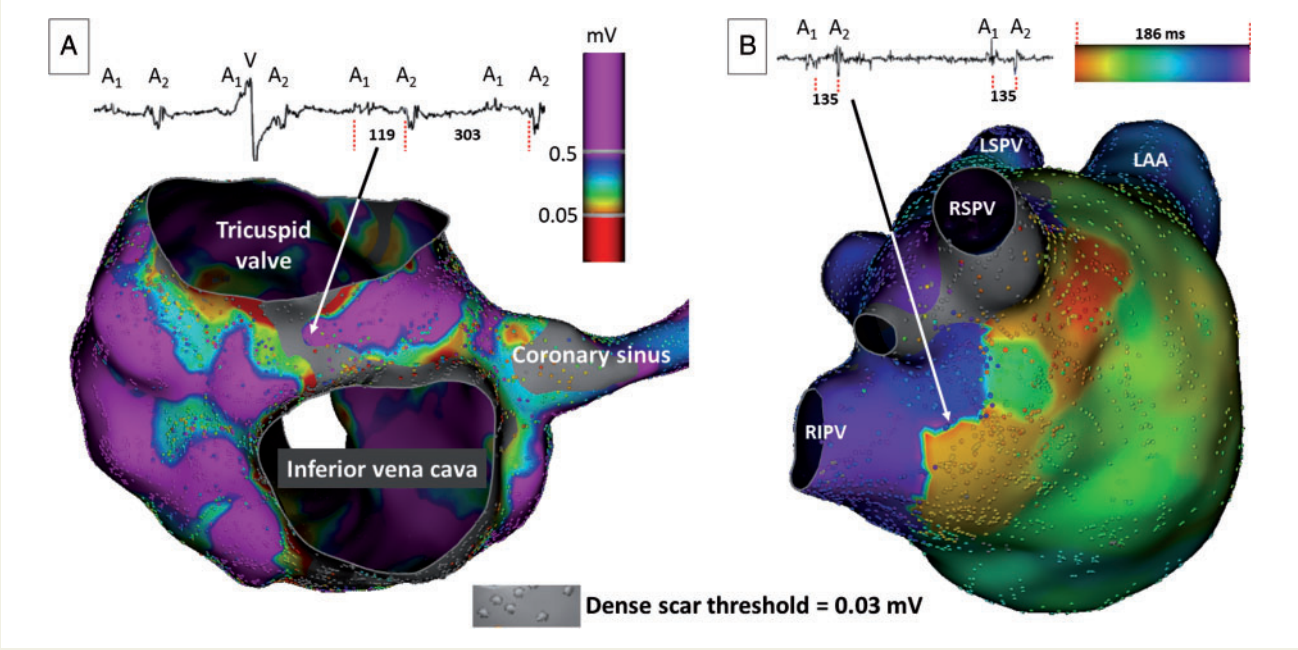

Figure 1 (*A*) Voltage mapping of the right atrium (inferior view) for recurring right AT in a patient with a previous cavo-tricuspid isthmus (CTI) linear RF ablation. Complete endocardial block at the CTI is suggested by the local low voltage and widely separated double potentials (bipolar EGM) along the line. (*B*) Activation mapping of the left atrium (LA) in sinus rhythm (right lateral view) in a patient with an ancient mitral valve repair. The surgical report indicated a direct incision of the LA posterior to the septum, in front of the right pulmonary veins, in the Sondergaard groove. The local block line indicated by the activation mapping (with double potentials) helps localizing the surgical scar. AT, atrial tachycardia; A/V, atrial/ventricular EGM; EGM, electrograms; LAA, left atrial appendage; LSPV, left superior pulmonary vein; RIPV, right inferior pulmonary vein; RSPV, right superior pulmonary vein.

Iatrogenic scar may be created in the atria by previous ablation (with radiofrequency or other energy sources) or surgical incisions (*Figure 1*). *Radiofrequency* catheter ablation induces acute (coagulation necrosis[15]), mid-term (fatty infiltration surrounded by chronic inflammation[16]), and long-term (fibrotic scar with uniform linear scars after linear ablation[17]) pathological modifications. The uniformity of these chronic lesions explain the lack of proarrhythmic effect in the absence of ablation gaps. *Cryotherapy*, through ice crystals formation and thawing yields cellular destruction in the acute phase.[18] Ischaemic necrosis follows (through haemorrhage, inflammation, and cell-membrane disruptions) and finally, replacement fibrosis give rise to the mature cryolesion within weeks.[19]

Data about healing of post-operative cardiac wounds is scarce in the literature.[20] Proliferation of collagen epicardially, weakness due to lack of adhesion between sutured edges, and slow development of a neointima have been reported for atrial wall incisions.[21]

Clinical diagnostic methods of cardiac fibrosis include serum markers,[10] various imaging modalities,[22] and histology of endomyocardial biopsy. When assessing a proarrhythmic substrate, localization is capital and is only provided by imaging techniques. Of these, late-gadolinium enhancement (LGE) in cardiac magnetic resonance (CMR) imaging[23] detects patchy and focal areas of fibrosis while measurement of the extra-cellular volume fraction by T_1 mapping detects diffuse and microscopic cardiac fibrosis.[24]

Analysis of atrial-wave amplitude on standard 12-lead surface ECG also informs on the extent of atrial fibrosis.[25–27] Shrinking of the F-wave amplitude on the surface ECG is related to the magnitude of the underlying atrial voltage, which is also related to the amount of viable atrial muscle.[25,26] It has been associated with AF duration and patient's age, both in V_1 and II, with lower values (<0.12 mV in V_1) linked to AF recurrence after catheter ablation.[25] Our group[27] proposed a fibrillatory wave computation in multiple leads that improved the non-invasive prediction of ablation outcome in persistent AF.

Preprocedural imaging

While ventricular fibrosis assessment has achieved excellent results with LGE-CMR,[28,29] imaging of atrial fibrosis remains delicate.[30] Several publications with a strong scientific impact proposed LGE-CMR for detection of both pre-existing and post-ablation induced atrial fibrosis. The extent of baseline LGE has been shown to predict AF recurrence after ablation[31] and may improve patient selection[32] for ablation procedures. LGE-CMR may also provide information about gaps in previous ablation lines[33–35]; integration of these images in 3D mapping systems may facilitate ablation procedures by targeting the breaks visualized in the previous lesion sets.

Nevertheless, LGE-CMR for detection of atrial scar has not been wildly adopted in clinical practice, mainly because of insufficient reproducibility.[36,37] Late-gadolinium enhancement sites on CMR were

lacking in 20% of ablation lesion sets in an AF ablation patient population, which could be due to a limitation of MRI but also to tissue recovery in incomplete, non-transmural reasons.[38] Late-gadolinium enhancement also correlated poorly with low-voltage areas in another post-AF ablation patient series.[39]

Detection of atrial scar in the electrophysiology lab: how to choose the right catheter in order to maximize the electrical signals

While mapping a scar-related AT, viable tissue within scars should be detected as it may represent the critical isthmus (CI) of a re-entrant circuit.[40] Detection of low-amplitude signals is thus mandatory for successful diagnosis. The lower threshold of recordable physiological electric signals will be represented by the amplitude of electronic noise, which should be minimized in order to improve the signal/noise ratio.

The morphology and amplitude of the recorded EGM depends on myocardial properties, wavefront direction, conducting medium, catheter-tissue contact and orientation, catheter electrodes size, composition, shape and inter-electrode spacing. The fundamentals of unipolar and bipolar EGM recording are beyond the scope of this overview article. Nevertheless data exists proving that mapping with small closely spaced electrodes can improve mapping resolution, which is of capital importance within areas of low voltage.[41]

Until a very recent past (e.g. 5 years) the standard catheter for mapping was (and still is in a number of centres and/or clinical situations) a linear catheter with a 3.5 mm tip electrode separated by 2 mm for a proximal 2 mm electrode (i.e. Navistar/ThermoCool/SmartTouch, Biosense-Webster; BW). This results in an interelectrode distance (centre-to-centre) of 4.75 mm. More recently, multielectrode mapping using 1 mm electrode catheters with a 2 mm interelectrode spacing (3 mm centre-to-centre; PentaRay, BW) have been introduced and widely used along with the advent of automatic annotation of EGM. A comparative study in normal atria with simultaneous mapping by both catheters found a very similar normal cut-off for bipolar voltage for both catheters (0.48 vs. 0.52 mV, $P = 0.65$ in the right atrium and 0.50 vs. 0.52 mV, $P = 0.80$ in the left atrium[41]), suggestive that the inferior limit of the bipolar voltage EGM is independent of the mapping electrode dipole size and spacing (within these above-mentioned ranges).

If a higher mapping density was expected with the multipolar catheter,[42] several other results[41] emphasize the importance of smaller size—closely-spaced electrodes when mapping scar-related AT. In these conditions, EGM duration is shorter (by eliminating far-fields and minimizing the mapped area by each point), delineation of low-voltage areas is improved (abnormal, low-voltage, as well as dense-scar areas are smaller), late potentials and EGM fractionation are more frequently recorded. The authors[41] elegantly demonstrated that not the mapping density, but the smaller electrode size and inter-electrode spacing were responsible for the resolution improvement, especially within scarred tissue. Another important finding was that mapping with a linear ablation catheter (3.5-2-2 mm dipole) demonstrated lower mean voltage of the fractionated EGM, limiting accurate activation time annotation. Overall, in severely scarred atria, 54.4% of all data points recorded with 2-2-2 mm dipoles had distinct EGM that allowed annotation vs. 21.4% of all low-voltage points recorded with linear catheters ($P = 0.02$).[41] A lower atrial pacing threshold was also demonstrated with this type of catheter.

The more recent 64-pole basket mapping catheter (IntellaMap Orion™, Boston Scientific; BS) further improved these aspects (*Figure 2*). It incorporates very small, flat (0.4 mm^2; 2.5 mm spacing), unidirectional electrodes.[43,44] Owing to their exclusive location on the external side of the splines, they are structurally less influenced by noise and far-field signals. Maps produced experimentally with the Rhythmia mapping system (BS) using this catheter had an unprecedented EGM resolution (2.6 mm), the noise was very low (<0.01 mV) and were highly accurate, without need for manual reannotation. EGM along the lines of conduction block demonstrated double potentials while EGM recorded at the level of gaps exhibited fusion of double potentials. The initial experimental results have been validated clinically in a prospective setting,[1] with a mapping resolution of 209 ± 128 points/cm^2. By recording higher bipolar voltage EGM, it has also been reported that, compared with Lasso (BW), the minibasket catheter has improved sensitivity in detecting PV potentials after RF ablation.[45]

Background noise limitation

Electrical noise is the other aspect of the signal/noise ratio; artefacts may have various origins and may bias EGM interpretation. Electromagnetic fields and intermittent connections are the main causes of noise interference in the electrophysiology lab. If poor cable connections, surface ECG leads and catheter handles can be easily managed, electromagnetic noise sources are more difficult to suppress. A set of measures contribute to noise reduction before the signal amplification process: correct routing of the intracardiac, radiofrequency and ECG cables without floor contact, isolation of power cables away from signal cables, and careful skin preparation. Intracardiac noise may also be reduced by using an indifferent unipolar electrode inside the inferior vena cava, deep sedation, or general anaesthesia.

Despite all these measures, in many laboratories background noise (BGN) still persists at levels that might be comparable to the magnitude of the smallest electrical signals from viable tissue within the scar (*Figures 2 and 3*). Noise levels have rarely been the subject of published research. In a recent study from our group,[1] we measured the electronic noise on the Rhythmia system using the voltage callipers with adequate amplification and speed. From the bipolar EGM acquired during scar-related AT with the Orion catheter, BGN was assessed at six pre-specified sites for the left atrium (mid-roof, mid-posterior wall, posterior mitral annulus, inter-atrial septum, mid-anterior wall, and appendage) and four pre-specified sites for the RA (cavo-tricuspid isthmus, septum, appendage, and crista terminalis). The BGN was also assessed on the bipolar EGM recorded with a standard decapolar catheter (2 mm ring electrodes and spacing) and on the surface ECG.

Background noise ranged from 10 to 12 μV (0.011 ± 0.004 mV) for the basket catheter EGM, without significant differences between sites (*Figure 2*). It is worth noting that this value is much lower than

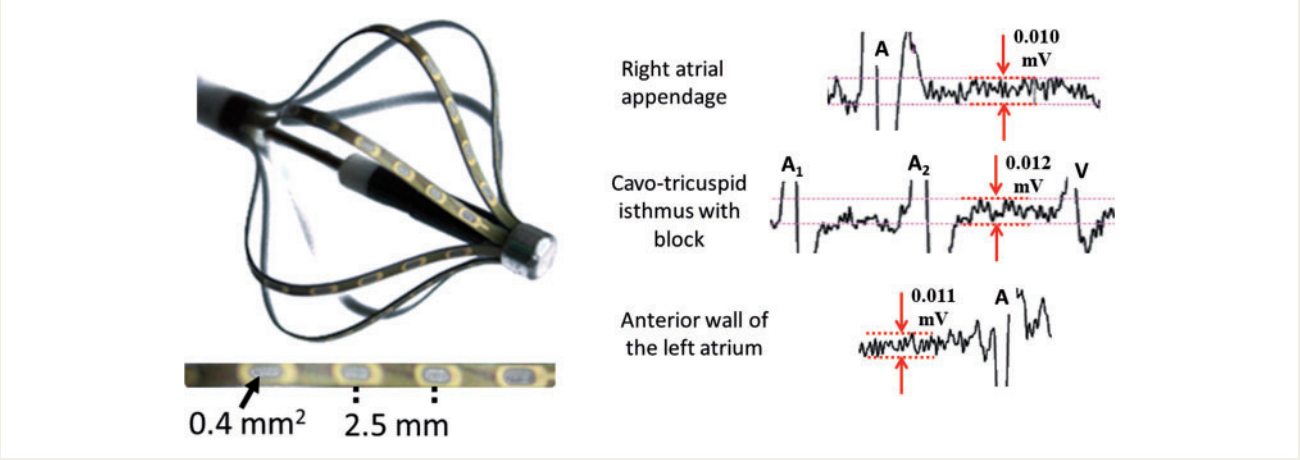

Figure 2 The fully deployed 64-pole basket mapping catheter (IntellaMap Orion™, Boston Scientific; BS) and size/spacing of the unidirectional electrodes. Examples of intracardiac EGM and bipolar noise level at various atrial sites. A/V, atrial/ventricular EGM.

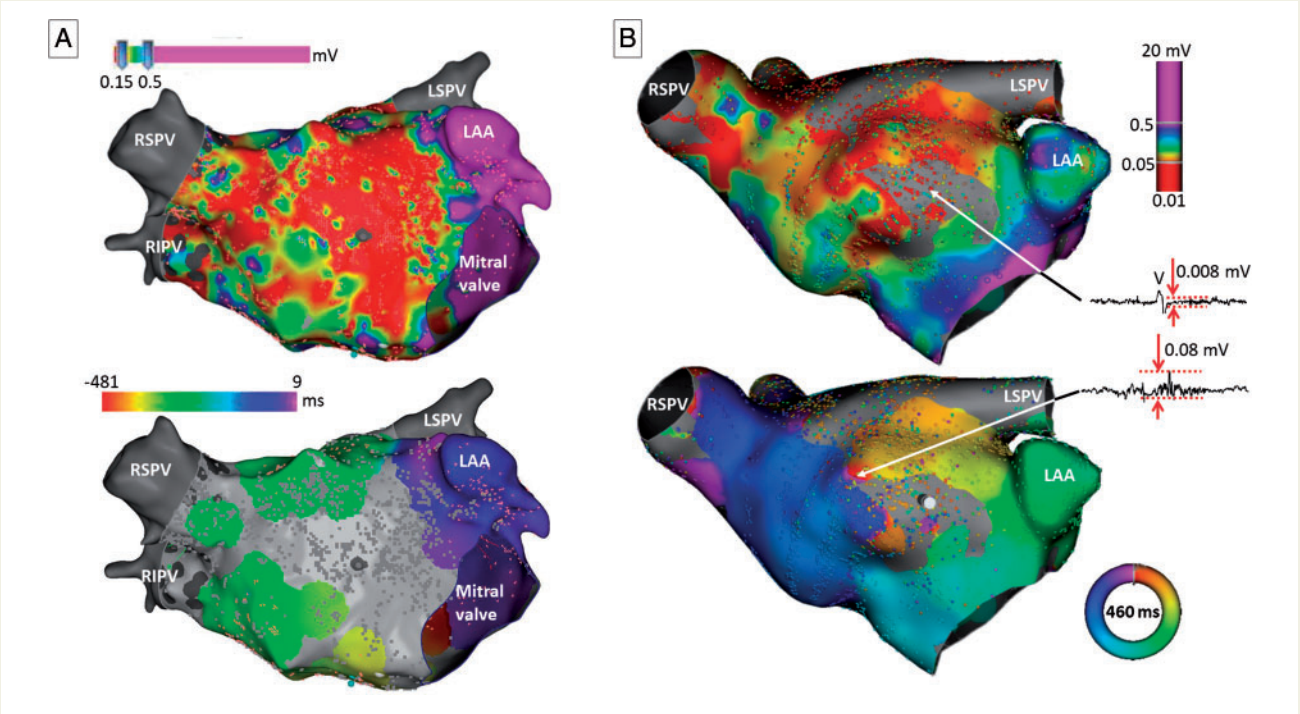

Figure 3 (*A*) Anterior view of left atrial (LA) voltage (upper image) and activation mapping (lower image) during clockwise perimitral flutter (cycle length 490 ms) in a patient with previous pulmonary vein isolation and severe dilation of the LA. The map was acquired with the PentaRay catheter and the Confidense module of Carto 3 (Biosense-Webster). The dense scar threshold was lowered to 0.01 mV. A wide scar area is visualized at the level of the anterior wall, without distinguishable endocardial gap at this level. Entrainment confirmed that both septal and lateral aspects of the mitral valve were in the circuit and endo-epi ablation at the mitral isthmus was successful. (*B*) Antero-superior view of left atrial (LA) voltage (upper image) and activation mapping (lower image) during anterior wall clockwise macro-re-entrant AT (cycle length 460 ms). The map was acquired with the Orion catheter and the Rhythmia system (Boston-Scientific). The dense scar threshold was also set to 0.01 mV. There is a large scar on the anterior wall of the LA extending to the roof with a low-voltage gap in its superior part (despite very low bipolar EGM amplitude of 0.08 mV at this level, the signal/noise ratio = 10). Ablation at this level successfully terminated the tachycardia. LAA, left atrial appendage; LSPV, left superior pulmonary vein; RIPV, right inferior pulmonary vein; RSPV, right superior pulmonary vein.

nominal setting of 'dense scar' in the mapping systems (generally 0.03–0.05 mV). The small, flat (unidirectional) and closely spaced electrodes of the Orion had less noise than that of the standard decapolar catheter (0.016 ± 0.019 mV) and the surface ECG leads (0.02 ± 0.01 mV) acquired on the Rhythmia system ($P = 0.00009$).[1]

This unprecedented low level of BGN opens new possibilities for efficient mapping of viable tissue within scar, by appropriated thresholding of 'dense scar' to lower levels, closer to BGN.

Scar detection by bipolar voltage mapping and scar thresholding

Ventricular cut-offs for scar detection by endocardial bipolar voltage mapping were proposed by Marchlinski *et al.*,[46] but limited data exists for the atria. A recent study[47] reported values for delineating inexcitable dense scars in patients undergoing AF ablation ranging from 0.15 mV to 0.45 mV using the Carto system (BW). Ultra-high density mapping data for scar detection has even less been reported. In a ventricular scar animal model, scar detected by the Rhythmia system using the basket for mapping correlated best with the magnetic resonance imaging.[48] A small series[49] found an excellent correlation between scar-distribution on CMR and high-density voltage mapping using the Rhythmia system during AT, with a bipolar cut-off of 0.5 mV.

In the previously mentioned scar-related AT series,[1] using a bipolar cut-off of 0.5 mV the extent of low-voltage areas was very important [58 ± 25% of the left atrial (LA) surface]. A commonly used dense-scar thresholding approach (e.g. with a cut-off of 0.05 mV) yielded a result of the 'dense-scar' extent of 22 ± 16% of the LA surface. We proposed a patient-specific scar-thresholding process. Thus, after map completion, dense scar thresholding was performed in each case wherever necessary (*Figure 3B*). The 'confidence mask' parameter was than fine-tuned and lowered as much as needed (but above the BGN) to visualize the entire circuit for each AT. Dense scar threshold ('confidence mask') was established at 0.016 ± 0.009 mV (median 0.015 mV). Only 12 ± 8% of the LA surface remained inferior to the patient-specific dense scar threshold; a supplemental 10% of the LA surface became thus accessible to analysis and activation interpretation compared with the standard 0.05 mV threshold.

A recently developed technology may bring new insights into scar detection through electrical coupling analysis.[50] The measure of the local (bipolar) impedance provides information about the catheter-tissue contact and its decrease is experimentally correlated with the lesion size.[50] The ongoing LOCALIZE study (ClinicalTrials.gov Identifier: NCT03232645) will correlate these innovative parameters with gap localization after PV ablation in paroxysmal AF patients. Above these features, local impedance values have informative potential about the stiffness of the tissue and may indirectly assess the extent of fibrosis.

Detection of critical isthmus of atrial tachycardia allows targeted ablation

Critical isthmus of macro-re-entrant AT is a region of significant narrowing and/or slowing of the wavefront. The hallmark characteristics of the CI are lower voltage and slower conduction.[40,51,52] Ultra-high density mapping brought new insights into these characteristics. We demonstrated that bipolar EGM at the CI systematically show low voltage (0.08 ± 0.11 mV), prolonged duration with multicomponent signals (100 ± 63 ms, covering 35 ± 18% of the cycle length), and significantly lower conduction velocity than the adjacent segments of the circuit: 0.27 ± 0.19 m/s, lower than orthodromically before (1 ± 0.49 m/s, $P < 0001$) or after the CI (1 ± 0.73 m/s, $P < 0001$).[1] Interestingly, in our series, 50% of the AT had bipolar EGM amplitude within the CI of less than 0.05 mV, and in 27% of less than 0.03 mV; activation mapping would not have been diagnostic in these cases with the higher bipolar dense scar threshold (such as 0.03 mV or 0.05 mV, which are generally used).

A recent very elegant study[53] based on ultra-high density activation mapping of AT demonstrated that the association of low voltage (0.07 ± 0.05 mV) and long duration (121 ± 11 ms) of bipolar EGM is specific for slow conduction areas (0.08 ± 0.02 m/s) and help discriminate fractionated potential due to slow conduction from wavefront collision/friction and pivot sites (e.g. at the extremity of a block line).

Ablation at the CI is highly successful.[1,54] On top of entrainment mapping techniques, identification of CI within scars by activation mapping and EGM characteristics may be particularly helpful.

Conclusion

Scar characterization in complex AT aims to detect viable conducting tissue in a low-voltage area. All the technical measures improving the signal/noise ratio address this objective. Critical area of arrhythmogenesis are often located in theses area, and their ablation, after confirmation of their critical role in scar-related AT, is highly successful.

Conflict of interest: D.G.L. and S.-S.B.: consulting fees for Boston Scientific.

References

1. Lațcu DG, Bun SS, Viera F, Delassi T, El Jamili M, Al Amoura A. Selection of critical isthmus in scar-related atrial tachycardia using a new automated ultrahigh resolution mapping system. *Circ Arrhythm Electrophysiol* 2017;**10**:e004510.
2. Medi C, Kalman JM. Prediction of the atrial flutter circuit location from the surface electrocardiogram. *Europace* 2008;**10**:786–96.
3. Gerstenfeld EP, Dixit S, Bala R, Callans DJ, Lin D, Sauer W *et al.* Surface electrocardiogram characteristics of atrial tachycardias occurring after pulmonary vein isolation. *Heart Rhythm* 2007;**4**:1136–43.
4. Bun SS, Latcu DG, Marchlinski F, Saoudi N. Atrial flutter: more than just one of a kind. *Eur Heart J* 2015;**36**:2356–63.
5. Casado Arroyo R, Lațcu DG, Maeda S, Kubala M, Santangeli P, Garcia FC *et al.* Coronary sinus activation and ECG characteristics of roof-dependent left atrial flutter after pulmonary vein isolation. *Circ Arrhythm Electrophysiol* 2018;**11**:e005948.
6. Bun SS, Latcu DG, Delassi T, Jamili ME, Amoura AA, Saoudi N. Ultra-high-definition mapping of atrial arrhythmias. *Circ J* 2016;**80**:579–86.
7. Pathik B, Lee G, Nalliah C, Joseph S, Morton JB, Sparks PB *et al.* Entrainment and high-density three-dimensional mapping in right atrial macroreentry provide critical complementary information: entrainment may unmask "visual reentry" as passive. *Heart Rhythm* 2017;**14**:1541–9.
8. Wijffels MC, Kirchhof CJ, Dorland R, Allessie MA. Atrial fibrillation begets atrial fibrillation. A study in awake chronically instrumented goats. *Circulation* 1995;**92**:1954–68.
9. Goette A, Kalman JM, Aguinaga L, Akar J, Cabrera JA, Chen SA *et al.* EHRA/HRS/APHRS/SOLAECE expert consensus on atrial cardiomyopathies: definition, characterization, and clinical implication. *Europace* 2016;**18**:1455–90.
10. Liu T, Song D, Dong J, Zhu P, Liu J, Liu W *et al.* Current understanding of the pathophysiology of myocardial fibrosis and its quantitative assessment in heart failure. *Front Physiol* 2017;**8**:238.

11. Hashimura H, Kimura F, Ishibashi-Ueda H, Morita Y, Higashi M, Nakano S *et al.* Radiologic-pathologic correlation of primary and secondary cardiomyopathies: MR imaging and histopathologic findings in hearts from autopsy and transplantation. *Radiographics* 2017;**37**:719–36.
12. Kong P, Christia P, Frangogiannis NG. The pathogenesis of cardiac fibrosis. *Cell Mol Life Sci* 2014;**71**:549–74.
13. Spinale FG, Janicki JS, Zile MR. Membrane-associated matrix proteolysis and heart failure. *Circ Res* 2013;**112**:195–208.
14. Bonnans C, Chou J, Werb Z. Remodelling the extracellular matrix in development and disease. *Nat Rev Mol Cell Biol* 2014;**15**:786–801.
15. Huang SK, Bharati S, Graham AR, Lev M, Marcus FI, Odell RC. Closed chest catheter desiccation of the atrioventricular junction using radiofrequency energy—a new method of catheter ablation. *J Am Coll Cardiol* 1987;**9**:349–58.
16. Huang SK, Bharati S, Lev M, Marcus FI. Electrophysiologic and histologic observations of chronic atrioventricular block induced by closed-chest catheter desiccation with radiofrequency energy. *Pacing Clin Electrophysiol* 1987;**10**:805–16.
17. Avitall B, Urbonas A, Urboniene D, Millard S, Helms R. Time course of left atrial mechanical recovery after linear lesions: normal sinus rhythm versus a chronic atrial fibrillation dog model. *J Cardiovasc Electrophysiol* 2000;**11**:1397–406.
18. Markovitz LJ, Frame LH, Josephson ME, Hargrove WC. Cardiac cryolesions: factors affecting their size and a means of monitoring their formation. *Ann Thorac Surg* 1988;**46**:531–5.
19. Dubuc M, Roy D, Thibault B, Ducharme A, Tardif JC, Villemaire C *et al.* Transvenous catheter ice mapping and cryoablation of the atrioventricular node in dogs. *Pacing Clin Electrophysiol* 1999;**22**:1488–98.
20. Elsberg CA. An experimental investigation of the treatment of wounds of the heart by means of suture of the heart muscle. *J Exp Med* 1899;**4**:479–520.
21. Tamura K, Koizumi K, Yamate N, Shoji T, Sugisaki Y, Yamanaka N *et al.* Healing of operative cardiac wounds. *Nihon Geka Gakkai Zasshi* 1985;**86**:482–8.
22. Baues M, Dasgupta A, Ehling J, Prakash J, Boor P, Tacke F *et al.* Fibrosis imaging: current concepts and future directions. *Adv Drug Deliv Rev* 2017;**121**:9–26.
23. Karamitsos TD, Francis JM, Myerson S, Selvanayagam JB, Neubauer S. The role of cardiovascular magnetic resonance imaging in heart failure. *J Am Coll Cardiol* 2009;**54**:1407–24.
24. Barison A, Del Torto A, Chiappino S, Aquaro GD, Todiere G, Vergaro G *et al.* Prognostic significance of myocardial extracellular volume fraction in nonischaemic dilated cardiomyopathy. *J Cardiovasc Med* 2015;**16**:681–7.
25. Nault I, Lellouche N, Matsuo S, Knecht S, Wright M, Lim KT *et al.* Clinical value of fibrillatory wave amplitude on surface ECG in patients with persistent atrial fibrillation. *J Interv Card Electrophysiol* 2009;**26**:11–9.
26. Cheng Z, Deng H, Cheng K, Chen T, Gao P, Yu M *et al.* The amplitude of fibrillatory waves on leads AVF and V1 predicting the recurrence of persistent atrial fibrillation patients who underwent catheter ablation. *Ann Noninvasive Electrocardiol* 2013;**18**:352–8.
27. Zarzoso V, Latcu DG, Hidalgo-Munoz AR, Meo M, Meste O, Popescu I *et al.* Non-invasive prediction of catheter ablation outcome in persistent atrial fibrillation by fibrillatory wave amplitude computation in multiple electrocardiogram leads. *Arch Cardiovasc Dis* 2016;**109**:679–88.
28. Lima JA, Judd RM, Bazille A, Schulman SP, Atalar E, Zerhouni EA. Regional heterogeneity of human myocardial infarcts demonstrated by contrast-enhanced MRI. Potential mechanisms. *Circulation* 1995;**92**:1117–25.
29. Kim RJ, Fieno DS, Parrish TB, Harris K, Chen EL, Simonetti O *et al.* Relationship of MRI delayed contrast enhancement to irreversible injury, infarct age, and contractile function. *Circulation* 1999;**100**:1992–2002.
30. Pontecorboli G, Figueras IVRM, Carlosena A, Benito E, Prat-Gonzales S, Padeletti L *et al.* Use of delayed-enhancement magnetic resonance imaging for fibrosis detection in the atria: a review. *Europace* 2017;**19**:180–9.
31. Oakes RS, Badger TJ, Kholmovski EG, Akoum N, Burgon NS, Fish EN *et al.* Detection and quantification of left atrial structural remodeling with delayed-enhancement magnetic resonance imaging in patients with atrial fibrillation. *Circulation* 2009;**119**:1758–67.
32. Akoum N, Daccarett M, McGann C, Segerson N, Vergara G, Kuppahally S *et al.* Atrial fibrosis helps select the appropriate patient and strategy in catheter ablation of atrial fibrillation: a DE-MRI guided approach. *J Cardiovasc Electrophysiol* 2011;**22**:16–22.
33. Peters DC, Wylie JV, Hauser TH, Kissinger KV, Botnar RM, Essebag V *et al.* Detection of pulmonary vein and left atrial scar after catheter ablation with three-dimensional navigator-gated delayed enhancement mr imaging: initial experience. *Radiology* 2007;**243**:690–5.
34. Badger TJ, Daccarett M, Akoum NW, Adjei-Poku YA, Burgon NS, Haslam TS *et al.* Evaluation of left atrial lesions after initial and repeat atrial fibrillation ablation: lessons learned from delayed-enhancement mri in repeat ablation procedures. *Circ Arrhythm Electrophysiol* 2010;**3**:249–59.
35. Halbfass PM, Mitlacher M, Turschner O, Brachmann J, Mahnkopf C. Lesion formation after pulmonary vein isolation using the advance cryoballoon and the standard cryoballoon: lessons learned from late gadolinium enhancement magnetic resonance imaging. *Europace* 2015;**17**:566–73.
36. Hunter RJ, Jones DA, Boubertakh R, Malcolme-Lawes LC, Kanagaratnam P, Juli CF *et al.* Diagnostic accuracy of cardiac magnetic resonance imaging in the detection and characterization of left atrial catheter ablation lesions: a multicenter experience. *J Cardiovasc Electrophysiol* 2013;**24**:396–403.
37. Sramko M, Peichl P, Wichterle D, Tintera J, Weichet J, Maxian R *et al.* Clinical value of assessment of left atrial late gadolinium enhancement in patients undergoing ablation of atrial fibrillation. *Int J Cardiol* 2015;**179**:351–7.
38. Taclas JE, Nezafat R, Wylie JV, Josephson ME, Hsing J, Manning WJ *et al.* Relationship between intended sites of RF ablation and post-procedural scar in AF patients, using late gadolinium enhancement cardiovascular magnetic resonance. *Heart Rhythm* 2010;**7**:489–96.
39. Harrison JL, Sohns C, Linton NW, Karim R, Williams SE, Rhode KS *et al.* Repeat left atrial catheter ablation: cardiac magnetic resonance prediction of endocardial voltage and gaps in ablation lesion sets. *Circ Arrhythm Electrophysiol* 2015;**8**:270–8.
40. Nakagawa H, Shah N, Matsudaira K, Overholt E, Chandrasekaran K, Beckman KJ *et al.* Characterization of reentrant circuit in macroreentrant right atrial tachycardia after surgical repair of congenital heart disease: isolated channels between scars allow "focal" ablation. *Circulation* 2001;**103**:699–709.
41. Anter E, Tschabrunn CM, Josephson ME. High-resolution mapping of scar-related atrial arrhythmias using smaller electrodes with closer interelectrode spacing. *Circ Arrhythm Electrophysiol* 2015;**8**:537–45.
42. Bun SS, Delassi T, Latcu DG, El Jamili M, Ayari A, Errahmouni A *et al.* A comparison between multipolar mapping and conventional mapping of atrial tachycardias in the context of atrial fibrillation ablation. *Arch Cardiovasc Dis* 2018;**111**:33–40.
43. Nakagawa H, Ikeda A, Sharma T, Lazzara R, Jackman WM. Rapid high resolution electroanatomical mapping: evaluation of a new system in a canine atrial linear lesion model. *Circ Arrhythm Electrophysiol* 2012;**5**:417–24.
44. Anter E, McElderry TH, Contreras-Valdes FM, Li J, Tung P, Leshem E *et al.* Evaluation of a novel high-resolution mapping technology for ablation of recurrent scar-related atrial tachycardias. *Heart Rhythm* 2016;**13**:2048–55.
45. Anter E, Tschabrunn CM, Contreras-Valdes FM, Li J, Josephson ME. Pulmonary vein isolation using the rhythmia mapping system: verification of intracardiac signals using the Orion mini-basket catheter. *Heart Rhythm* 2015;**12**:1927–34.
46. Marchlinski FE, Callans DJ, Gottlieb CD, Zado E. Linear ablation lesions for control of unmappable ventricular tachycardia in patients with ischemic and nonischemic cardiomyopathy. *Circulation* 2000;**101**:1288–96.
47. Squara F, Frankel DS, Schaller R, Kapa S, Chik WW, Callans DJ *et al.* Voltage mapping for delineating inexcitable dense scar in patients undergoing atrial fibrillation ablation: a new end point for enhancing pulmonary vein isolation. *Heart Rhythm* 2014;**11**:1904–11.
48. Thajudeen A, Jackman WM, Stewart B, Cokic I, Nakagawa H, Shehata M *et al.* Correlation of scar in cardiac MRI and high-resolution contact mapping of left ventricle in a chronic infarct model. *Pacing Clin Electrophysiol* 2015;**38**:663–74.
49. Frontera A, Takigawa M, Kitamura T, Martin R, Vlachos K, Cheniti G *et al.* P386: relationship between scar and atrial tachycardia mechanisms: insight from registered magnetic resonance and ultra-high density activation mapping using the rhythmia system. *Europace* 2017;**19**:iii75–6.
50. Sulkin MS, Laughner JI, Hilbert S, Kapa S, Kosiuk J, Younan P *et al.* Novel measure of local impedance predicts catheter-tissue contact and lesion formation. *Circ Arrhythm Electrophysiol* 2018;**11**:e005831.
51. Kalman JM, VanHare GF, Olgin JE, Saxon LA, Stark SI, Lesh MD. Ablation of 'incisional' reentrant atrial tachycardia complicating surgery for congenital heart disease. Use of entrainment to define a critical isthmus of conduction. *Circulation* 1996;**93**:502–12.
52. Jais P, Shah DC, Haissaguerre M, Hocini M, Peng JT, Takahashi A *et al.* Mapping and ablation of left atrial flutters. *Circulation* 2000;**101**:2928–34.
53. Frontera A, Takigawa M, Martin R, Thompson N, Cheniti G, Massoullie G *et al.* Electrogram signature of specific activation patterns: analysis of atrial tachycardias at high-density endocardial mapping. *Heart Rhythm* 2018;**15**:28–37.
54. Schaeffer B, Hoffmann BA, Meyer C, Akbulak RO, Moser J, Jularic M *et al.* Characterization, mapping, and ablation of complex atrial tachycardia: initial experience with a novel method of ultra high-density 3D mapping. *J Cardiovasc Electrophysiol* 2016;**27**:1139–50.

ESC European Society of Cardiology

Europace (2019) **21**, i27–i33
doi:10.1093/europace/euy173

REVIEW

Is it feasible to offer 'targeted ablation' of ventricular tachycardia circuits with better understanding of isthmus anatomy and conduction characteristics?

Felix Bourier[1,2], Ruairidh Martin[1,2], Claire A. Martin[1,2], Masateru Takigawa[1,2], Takeshi Kitamura[1,2], Antonio Frontera[1,2], Ghassen Cheniti[1,2], Anna Lam[1,2], Konstantinos Vlachos[1,2], Josselin Duchateau[1,2,3,4], Thomas Pambrun[1,2,3,4], Nicolas Derval[1,2,3,4], Arnaud Denis[1,2,3,4], Nicolas Klotz[1,2,3,4], Mélèze Hocini[1,2,3,4], Michel Haïssaguerre[1,2,3,4], Pierre Jaïs[1,2,3,4], Hubert Cochet[1,2,3,4], and Frédéric Sacher[1,2,3,4]*

[1]IHU Liryc, Electrophysiology and Heart Modeling Institute, fondation Bordeaux Université, F-33600 Pessac- Bordeaux, France; [2]Bordeaux University Hospital (CHU), Electrophysiology and Ablation Unit, F-33600 Pessac, France; [3]University Bordeaux, Centre de recherche Cardio-Thoracique de Bordeaux, U1045, F-33000 Bordeaux, France; and [4]INSERM, Centre de recherche Cardio-Thoracique de Bordeaux, U1045, F-33000 Bordeaux, France

Received 4 April 2018; editorial decision 27 June 2018; accepted 13 August 2018

Successful mapping and ablation of ventricular tachycardias remains a challenging clinical task. Whereas conventional entrainment and activation mapping was for many years the gold standard to identify reentrant circuits in ischaemic ventricular tachycardia ablation procedures, substrate mapping has become the cornerstone of ventricular tachycardia ablation. In the last decade, technology has dramatically improved. In parallel to high-density automated mapping, cardiac imaging and image integration tools are increasingly used to assess the structural ventricular tachycardia substrate. The aim of this review is to describe the technologies underlying these new mapping systems and to discuss their possible role in providing new insights into identification and visualization of reentrant tachycardia mechanisms.

Keywords Ventricular tachycardia • Ablation • Automatic mapping • Image integration

Introduction

Mapping and ablation of reentrant ventricular tachycardia remains a challenging task and may be difficult to achieve, particularly as it requires full comprehension of underlying mechanisms which maintain the tachycardia circuit, as well as suitable ablation strategies. For many years, conventional electrophysiology manoeuvers such as entrainment mapping and stimulation manoeuvers were the gold standard for identification of relevant reentrant circuits.[1,2] Over the years there have been many advances in mapping and imaging technologies, which have allowed improvements in the efficacy of ventricular tachycardia ablation procedures. The first electroanatomic mapping systems were able to provide basic information about electrical conduction, voltage, and anatomy.[3,4] More recently, high-density multielectrode mapping catheters have been increasingly used in clinical electrophysiology practice. As several thousand electrograms can be recorded within short time, multi-electrode catheters are frequently used in combination with mapping algorithms that automatically annotate recorded electrograms and promise to create fast, precise maps with less interpolation. As a result, high-density ventricular maps, consisting of several thousand annotated electrograms, can be generated, allowing unique insights and visualization of ventricular tachycardia mechanisms.

* Corresponding author. Tel: +33 55 765 6471; fax: ++33 55 765 6509. *E-mail address*: Frederic.Sacher@chu-bordeaux.fr

Clinical challenge and necessary developments

Entrainment and activation mapping can model a ventricular tachycardia circuit including its critical isthmus, bystanders, entrance, and exit sites. These conventional strategies were the gold standard in ventricular tachycardia ablation procedures for many years. However, they were limited by the inducibility of clinical arrhythmias, and are only possible for haemodynamically tolerated tachycardias. As a result of this clinical challenge, substrate based mapping, and ablation concepts [local abnormal ventricular activation (LAVA) ablation; late, split, or fractionated potentials; ablation in low-voltage areas; core isolation or channel based on imaging] have been developed in order to overcome these limitations.[5–7] These substrate mapping-based approaches have become the new cornerstone of current ventricular tachycardia ablation procedures.[8]

Although these substrate-based approaches have been proven to be effective in ischaemic ventricular tachycardia patients, recurrence of arrhythmia is still common.[9,10] One limitation of substrate-based approaches is that radiofrequency ablation may be unnecessarily delivered in areas that are not related to current or future clinical tachycardias. Furthermore, lines of block, which define the protected isthmus of a reentrant tachycardia, may not be anatomically fixed but rather be partially functional, and thus not identifiable when performing substrate mapping in sinus rhythm. Even anatomically fixed isthmi may be masked within global ventricular activation depending on activation wavefront propagation.[11,12] Thus, activation mapping remains a complementary strategy, which can allow a more refined substrate based ablation or for identification of the specific substrate sustaining the clinical ventricular tachycardia.

As a result, there is an increasing need to develop new technologies which allow rapid and precise identification of arrhythmia substrate, as well as more detailed activation mapping of arrhythmias. These developments include hardware (multi-electrode mapping catheters with sufficiently small electrodes and close interelectrode spacing), and software components (automatic electrogram detection and annotation algorithms). The combined application of these hardware and software components is claimed to provide automated fast electrogram collection, annotation, and visualization.

In parallel with advances in intraprocedural mapping technology, cardiac imaging plays a crucial role for the assessment of structural ventricular tachycardia substrate. Current electroanatomic mapping systems provide real-time integration of electroanatomic data and precise preprocedural imaging of cardiac anatomy. Assessments of the relative merits of these technologies for specific clinical situations are critical. Where mapping technologies are used for ischaemic ventricular tachycardia ablation procedures, we know that identification and ablation of reentrant tachycardia entrance, isthmus, and exit sites is independently associated with prevention of recurrence of the initial clinical ventricular tachycardia.[13] This makes identification and targeted elimination of ventricular tachycardia isthmus sites the minimal procedural endpoint of ablation procedures. Isthmi are often located in so-called scar and low-voltage areas. Adequate sensing of low-voltage potentials, with fractionation and amplitudes which can be less than 0.1 mV, has required new catheter designs. The development of smaller electrodes and shorter interelectrode distances has improved nearfield electrogram detection and reduced the sensitivity to far field signals, as depicted in *Figure 1*.[14]

High-density automatic mapping technologies for isthmus visualization

The large number of recorded electrograms acquired by multi-electrode mapping catheters makes automated analysis and annotation a necessity. Consequently, new computer-assisted mapping algorithms, which detect and annotate electrograms automatically, have been developed and integrated into current 3D navigation systems. Ultimately it is the combined use of both a modern multi-electrode mapping catheter and an automatic annotation algorithm in the associated 3D navigation system, which facilitates the generation of high-density ventricular maps.

Currently, there are three clinically available combinations of multi-electrode catheters and 3D mapping systems featuring high-density mapping capabilities: IntellaMap Orion + Rhythmia HDx (Boston Scientific, Cambridge, MA, USA), PentaRay + CARTO3v6 (Biosense Webster, Diamond Barr, CA, USA), and HD Grid + EnSite Precision (Abbott, Chicago, IL, USA).

Recent studies have described the use of Rhythmia and CARTO3 (in combination with Ripple Mapping) to guide ventricular tachycardia ablation.

Both systems allow electrogram collection using multi-electrode mapping catheters and contain new electrogram detection and annotation algorithms that overcome the limitations of conventional activation mapping as described above. Electrogram detection can be adjusted patient by patient, using filter settings based on electrogram morphology, cycle length duration, or stability criteria.

CARTO3 Ripple Mapping visualizes electrical activation as 'bars' that are projected onto the acquired anatomy. The height of each bar is displayed proportionally to bipolar voltage at each location over time, rather than depicting each electrogram as a single onset time and voltage. When multiple electrograms are collected in a dense and even spread across the map, a visual effect of passing wavefronts is created while the movement of bars traverses from one area to the next ('Ripples'). In contrast to activation mapping, where electrical activation is visually represented as a colour-gradient relative to a chosen window-of-interest, which is linked to fixed temporal references, ripple bars are analysed in relation to each other. Ripple mapping therefore claims to be the only mapping algorithm that simultaneously visualizes both voltage and electrical activation, while the sequence of bar movements defines local activation direction across all areas. Thus, Ripple mapping may show multiple small, slowly oscillating ripples indicating fractionated signals (such as in a ventricular tachycardia isthmus), or single tall 'up and down' bars indicating noncomplex signals in ventricular tissue with normal electrical conduction properties.[15–17]

Rhythmia HDx mapping technology is based on a similar principle to Ripple mapping. Each location of an annotated electrogram is displayed accordingly to a colour-gradient over time, which allows visualization of advancing wavefront directions and conduction velocity in these directions. Rhythmia activation mapping is usually performed

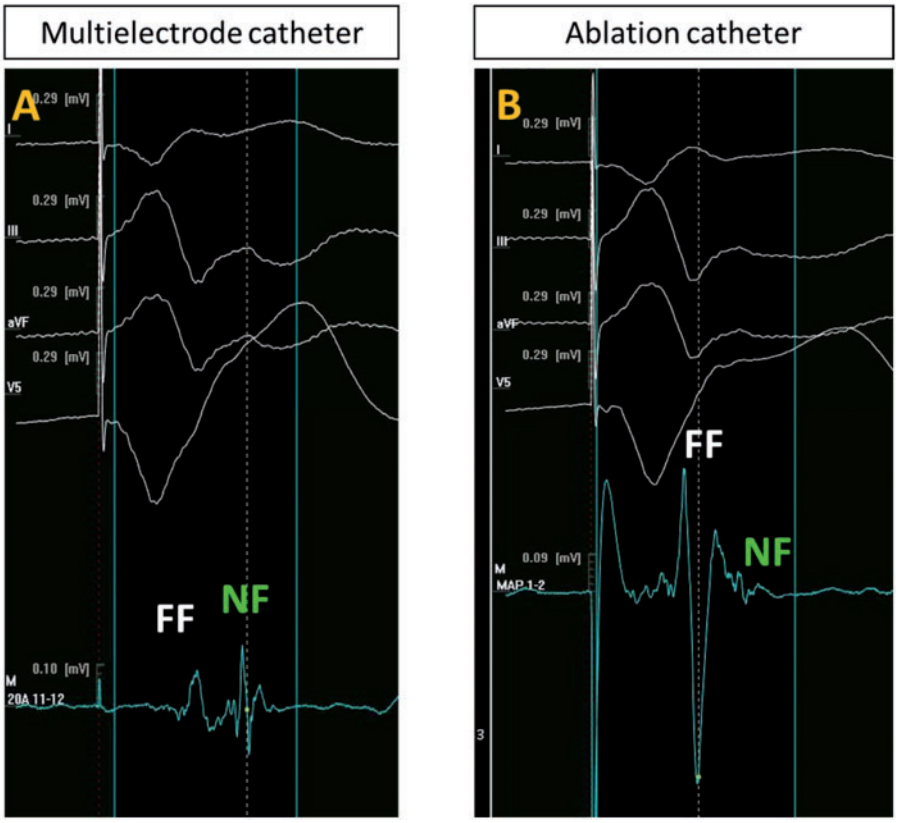

Figure 1 Nearfield and farfield components of an electrogram recorded at the same site in a low voltage are using a multi-electrode mapping catheter (*A*, 'IntellaMap Orion', Boston Scientific) or a standard ablation catheter (*B*, 'Thermocool', Biosense Webster). FF, farfield; NF, nearfield.

using the proprietary 64 mini-electrode basket catheter (IntellaMap Orion, Boston Scientific, MA, USA), consisting of eight splines, each containing eight miniaturized electrodes (interelectrode spacing = 2.5 mm, electrode surface area = 0.4 mm^2). Local electrogram activation is determined based on a combination of the bipolar and unipolar electrograms and timed at the maximum negative *dV/dt* of the local unipolar electrogram. At sites with multi-component or fractionated bipolar potentials, the activation time is determined by the maximum negative *dV/dt* of the corresponding unipolar electrogram and the system can consider the timing of electrograms in the adjacent area. The low-noise level of the Rhythmia HDx system (<0.01 mV) allows the recording of very low amplitude electrograms. This may prove especially effective in activation mapping of the scarred ventricular myocardium of post-infarct patients.[18,19]

Although the utilization of the EnSite Precision system was not specifically reported for ventricular tachycardia isthmus visualization by now, published studies confirm that its implemented automatic mapping technology ('AutoMap') facilitates a similar multi-fold increase in the number of collected mapping points and a decrease of procedure time. When compared to other mapping systems, the catheter compatibility of the EnSite Precision system is more diverse. As the catheter localization technology of the EnSite Precision system is based on electrical impedance measurements, the system and its automatic mapping algorithm is technically compatible with almost all types of catheters. The localization technology of the other mapping systems is based on electromagnetic localization, which is mainly compatible with purpose-built catheters only. However, electromagnetic tracking results in better technical accuracies and impedance based tracking may be more sensitive to patient movements, volume shifts, and respiration.[20,21]

An example of high-density mapping of reentrant ventricular tachycardia, including visualization of the protected isthmus, is depicted in *Figure 2*.

Experience from *in vivo* studies using high-resolution mapping systems

Recently, Anter *et al.*[19] used the Rhythmia HDx mapping technology to characterize the electrophysiological properties of post-infarction reentrant ventricular tachycardia circuits in a porcine model. The authors report that activation mapping of scar related ventricular tachycardias was feasible using the high-resolution technology, resulting in very detailed visualization of the reentrant circuits. The system allowed the visualization of distinct electrophysiological elements of the mapped reentrant circuits, including the entrance site of the wavefront, the protected isthmus surrounded by mostly functional lines of block, as well as the exit site and outer loops.

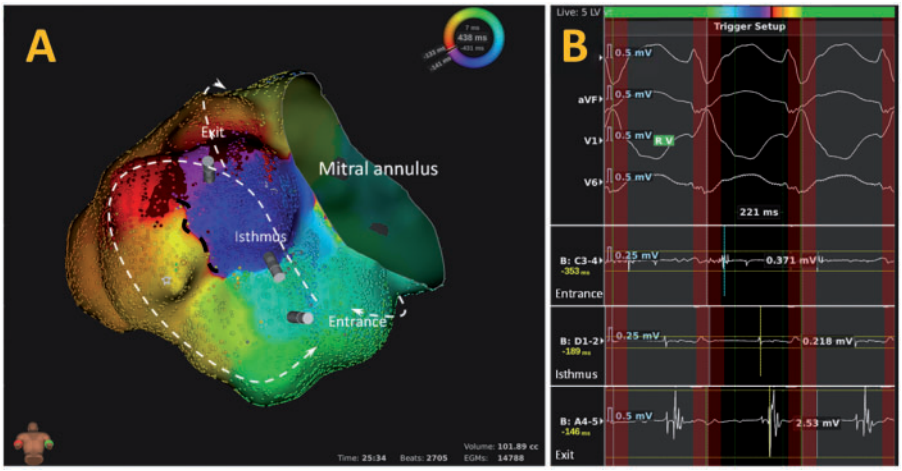

Figure 2 (*A*) A high-density Rhythmia activation map of perimitral reentrant ventricular tachycardia is shown. The dashed white line demonstrates the reentrant circuit as assessed by activation mapping. The dashed black line represents a functional line of block. (*B*) Recorded electrograms during activation mapping are shown. The color-coded reentrant cycle of *A* is shown as a scale on top of *B*. Electrograms recorded at entrance, isthmus, and exit sites with corresponding early, mid-diastolic, and late timing of local electrograms.

Entrance sites had the slowest conduction velocities within the reentrant circuit. The common channel was surrounded by lines of functional block and had an almost normal conduction velocity. Conduction velocities within the circuit were found to be dynamic and not geometrically fixed. When comparing high-density activation mapping to classical entrainment mapping of the circuit, the authors observed an overestimation of isthmus dimension with entrainment mapping. Specifically, the exit sites were localized further from the isthmus of the circuit during entrainment mapping when compared with activation mapping using the Rhythmia mapping system. Deceleration conduction zones are generally attractive sites for targeted ablation, so high-resolution mapping and visualization of these areas may be a promising strategy to guide ablation.[22]

Martin *et al.*[22] firstly used the Rhythmia HDx technology for a detailed description of human ventricular tachycardia isthmus morphology in post-infarct patients. Their in-human Rhythmia activation maps showed wavefronts entering and exiting the protected isthmus at multiple points. In concordance with the data from Anter *et al.*,[19] a pattern of activation wavefront slowing at isthmus entrance and exit sites, with relative preservation of conduction velocity in the protected isthmus, was observed. Reentry exit sites were activated at 77% diastolic interval, and activation of isthmi occurred largely in diastole. Activation of entrance sites was more variable, and frequently overlapped with the preceding QRS complex. Almost one-third of isthmi showed a tortuous course (defined as >90° change in activation direction within the isthmus) and two-third of mapped isthmi had one or more dead ends of activation, indicating that protected isthmus topography is more complex than previously described.[23,24]

The first detailed in-human experience with high-density mapping of post-infarct reentrant circuits with CARTO3 Ripple mapping was recently described by Luther *et al.*[24] Applying this mapping technology in clinical electrophysiology (EP) procedures allowed identification of channels and protected isthmi. In concordance with the findings of Martin *et al.* and Anter *et al.*, mapping identified functional lines of block harbouring the protected isthmus.[25]

Recent studies also implemented extra-stimuli protocols in the use of 3D mapping systems in order to identify functional conduction block and unmask ventricular tachycardia substrate in ischaemic and non-ischaemic ventricular tachycardia patients. Ablation of these identified areas resulted in a significant reduction of ventricular tachycardia burden.[26–28] Especially in non-ischaemic cardiomyopathy patients, ventricular tachycardia circuits may involve endocardial but also epicardial substrate. Data presented by Hutchinson *et al.*[29] demonstrate that epicardial substrate can be identified using the larger electrical field of view of endocardial unipolar voltage mapping, also in areas of normal bipolar endocardial voltage amplitude. However, electroanatomic mapping systems are still limited in their ability to detect intramural and non-transmural scars.

Image integration for ventricular tachycardia isthmus visualization

For many years the function of cardiac imaging was mainly limited to determining the underlying aetiology and prognosis of patients presenting with ventricular tachycardia arrhythmias. Currently, in parallel with advances in electroanatomic mapping technologies, the role of cardiac imaging is expanding from a tool for diagnosis of left ventricular dysfunction and scar burden to one providing specific anatomical guidance for ventricular tachycardia ablation procedures.[30]

Image integration techniques, which combine different imaging modalities [computed tomography (CT), magnetic resonance imaging (MRI), electroanatomic mapping, fluoroscopy], have been proven to provide added value and information to EP ablation procedures.[31] Information on vascular access, cardiac anatomy including myocardial scar and electrophysiological ventricular tachycardia isthmi can be

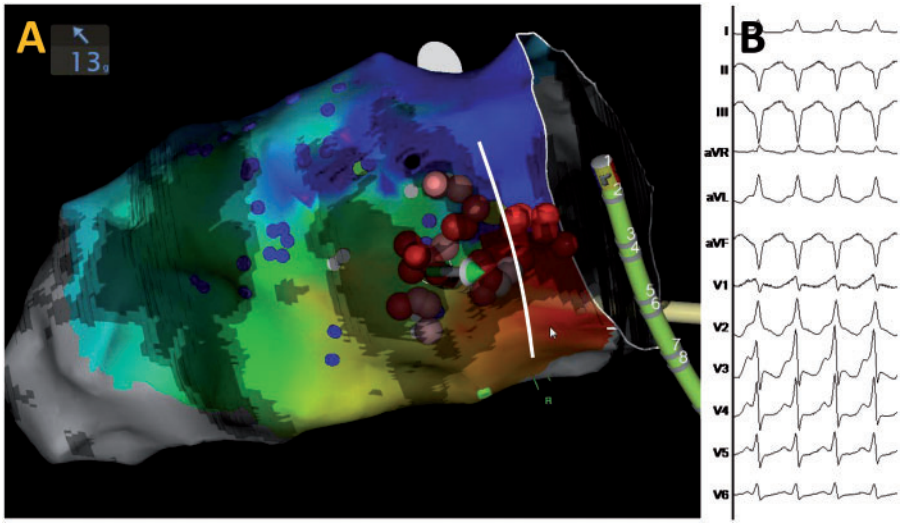

Figure 3 (*A*) Wall-thinning mapping (3 mm and 4 mm thickness, dark areas) is integrated into CARTO3 navigation, posterior-inferior view. The location of the predefined isthmus (white line) was confirmed by high-density activation mapping. Targeted isthmus ablation using a contact force sensing catheter. The blue markers depict sites in which LAVA electrograms were identified in SR. (*B*) The clinical VT morphology during activation mapping is shown. LAVA, local abnormal ventricular activation; SR, sinus rhythm; VT, ventricular tachycardia.

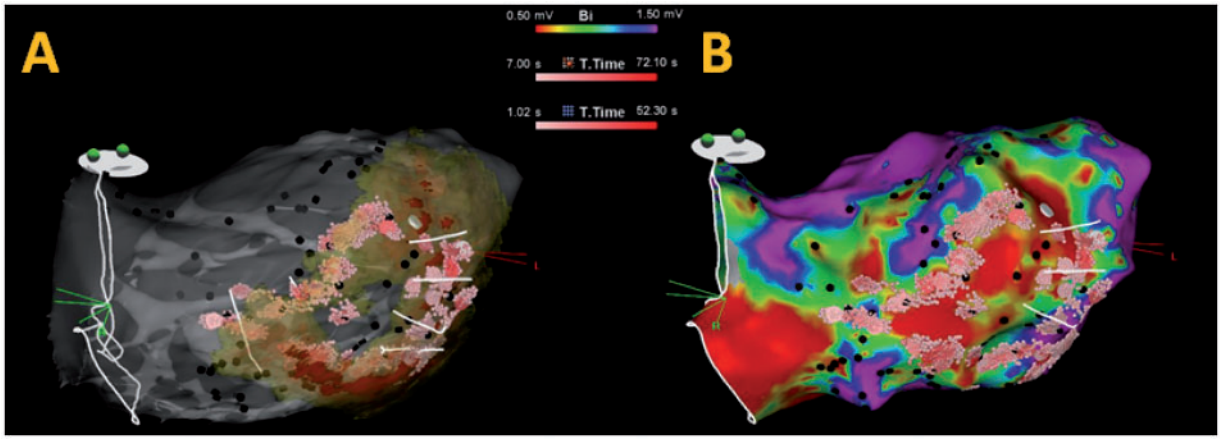

Figure 4 (*A*) An anterior-inferior image integration view of a preprocedurally acquired CT dataset during an ischaemic ventricular tachycardia ablation procedure in a patient with left-inferior myocardial infarction is shown. The ECG-gated contrast-enhanced CT delineates myocardial scar (identified as areas of wall thinning <5 mm). Wall thickness mapping shows six anatomic isthmi (white lines) of relatively preserved thickness between areas of severe thinning. The wall thickness map, derived from the CT dataset, is merged with an anatomical map of the patient's left ventricle is shown. (*B*) The corresponding LV voltage map is shown. CT, computed tomography; LV, left ventricle.

acquired using preprocedural imaging.[30–35] Recent work by Yamashita *et al.* investigated the usefulness of image integration during ventricular tachycardia ablation procedures. The systematic application of MRI and CT image integration was found to be feasible in a large series of patients. Integrated imaging provided information on substrate in ischaemic and non-ischaemic cardiomyopathy (NICM) patients, and impacted procedural management particularly in NICM procedures.[30,31]

Furthermore, integrating information on substrate, derived from late gadolinium enhancement cardiac MRI, to guide ventricular tachycardia ablation in electroanatomic mapping systems, has been shown to significantly improve rates of non-inducibility and arrhythmia-free survival.[7,33]

Myocardial wall thinning ≤5 mm, as assessed by CT cardiac imaging, is associated with scar and LAVA in ischaemic cardiomyopathy patients.[34] Ghannam *et al.* correlated electroanatomic mapping data, obtained during ventricular tachycardia ablation procedures, with wall thinning as determined by cardiac computed tomography. In 84% of ventricular tachycardias, ablation targets were found on isthmi as identified in the processed wall thinning CT dataset. Ablation of these targeted locations resulted in a post-ablation non-inducibility in 73% of patients. The authors conclude from this data that ridges of myocardial tissue, as assessed by CT imaging, are often part of critical reentrant circuits in post-infarction ventricular tachycardia patients.[35] CT image processing was performed, as previously described, using a proprietary software (MUSIC software, IHU LIRYC Bordeaux and Inria Sophia Antipolis, France).[36]

Image integration of the structural ventricular tachycardia substrate, as defined by non-invasive preprocedural CT imaging, with intraprocedural invasive electroanatomic mapping, may identify targets of ablation therapy preprocedurally, thereby has the potential to enhance safety and efficacy of ablation procedures. *Figures 3* and *4* illustrate the clinical use of this technology.

Limitations of advanced mapping technologies

Although high-density visualization resulting from automatic mapping may intuitively promise effective and precise ablation strategies, this is not yet proven by long-term outcome data. In clinical practice it is important to recognize that mapping is still dependent on underlying technologies. For example, the automatic annotation of low-amplitude fragmented signals as well as the discrimination between nearfield and farfield electrograms may sometimes fail particularly in borderzone area. A suboptimal catheter contact or catheter designs, which are not precisely adapted to delicate anatomical structures, may result in falsely low-amplitude measurements and incorrect scar detection. This is why signal characteristics are more important that voltage alone. Thus, a careful review of automatically acquired maps still remains mandatory.

Discussion

When utilizing advanced mapping technologies in clinical practice, it is important to recognize that their visualization and evidence is still dependent on the quality of the underlying technologies and data processed in the applied algorithms. This underlines the general need for high-density mapping and effective data processing algorithms to incorporate the acquired electrograms into consistent maps. In the interim, a careful review of acquired maps remains mandatory in clinical practice. Nevertheless, new high-density mapping technologies have overcome the main limitations of conventional activation mapping in reentrant tachycardias, as they operate independently from temporal references and have a visualization approach which appears to be intuitive and close to reality (*Figure 2*).[17,19]

In addition, each imaging and mapping modality is also affected by the underlying physics, resulting in specific effects on data acquisition and visualization. The use of image integration techniques in ventricular tachycardia ablation procedures may combine their specific advantages and create an added value to the procedure (*Figures 3* and *4*). Recently published studies have demonstrated that high-density mapping and image integration techniques facilitate reentrant tachycardia mapping and isthmus detection. Use of CT-based image integration techniques and high-density mapping of ventricular scar, followed by complete LAVA elimination have been proven to be independent predictors of ventricular tachycardia-free survival after catheter ablation for post-myocardial infarction ventricular tachycardia.[36] However, further prospective studies will be required to validate the impact of these new, technology-based workflows of targeted catheter ablation on patients' long-term outcome.

Conclusions

Mapping and ablation of ventricular tachycardias still remains a challenging clinical task. Advances in cardiac imaging, mapping technologies, and image integration techniques improved the understanding and visualization of mechanisms, anatomy, and conduction characteristics of ventricular tachycardia isthmi, which offers a more precisely targeted ablation of underlying reentrant circuits. However, its impact on patients' long-term outcome still needs to be assessed, therefore further prospective studies are required.

Funding

This work was supported by IHU LIRYC [ANR-10-IAHU-04 grant]. F.B. was supported by a grant from the German Heart Foundation.

Conflict of interest: P.J. and F.S. received consulting fees and speaker honorarium from Boston scientific, Biosense Webster, and Abbott. M.H., M.H. and N.D. received speaker honorarium from Biosense Webster; P.J., N.D., and M.H. received consulting fees from Biosense Webster. All other authors declare to have no conflict of interest.

References

1. de Groot NM, Schalij MJ, Zeppenfeld K, Blom NA, Van der Velde ET, Van der Wall EE. Voltage and activation mapping: how the recording technique affects the outcome of catheter ablation procedures in patients with congenital heart disease. *Circulation* 2003;**108**:2099–106.
2. Stevenson WG, Khan H, Sager P, Saxon LA, Middlekauff HR, Natterson PD *et al.* Identification of reentry circuit sites during catheter mapping and radiofrequency ablation of ventricular tachycardia late after myocardial infarction. *Circulation* 1993;**88**:1647–70.
3. Stevenson WG, Wilber DJ, Natale A, Jackman WM, Marchlinski FE, Talbert T *et al.* Irrigated radiofrequency catheter ablation guided by electroanatomic mapping for recurrent ventricular tachycardia after myocardial infarction: the multicenter thermocool ventricular tachycardia ablation trial. *Circulation* 2008;**118**:2773–82.
4. Sacher F, Tedrow UB, Field ME, Raymond JM, Koplan BA, Epstein LM *et al.* Ventricular tachycardia ablation: evolution of patients and procedures over 8 years. *Circ Arrhythm Electrophysiol* 2008;**1**:153–61.
5. Wolf M, Sacher F, Cochet H, Kitamura T, Takigawa M, Yamashita S *et al.* Long-term outcome of substrate modification in ablation of post-myocardial infarction ventricular tachycardia. *Circ Arrhythm Electrophysiol* 2018;**11**:e005635.
6. Sacher F, Lim HS, Derval N, Denis A, Berte B, Yamashita S *et al.* Substrate mapping and ablation for ventricular tachycardia: the LAVA approach. *J Cardiovasc Electrophysiol* 2015;**26**:464–71.
7. Berruezo A, Fernández-Armenta J, Andreu D, Penela D, Herczku C, Evertz R *et al.* Scar dechanneling: new method for scar-related left ventricular tachycardia substrate ablation. *Circ Arrhythm Electrophysiol* 2015;**8**:326–36.
8. Di Biase L, Burkhardt JD, Lakkireddy D, Carbucicchio C, Mohanty S, Mohanty P *et al.* Ablation of stable VTs versus substrate ablation in ischemic cardiomyopathy: the VISTA Randomized Multicenter Trial. *J Am Coll Cardiol* 2015;**66**:2872–82.

9. Sapp JL, Wells GA, Parkash R, Stevenson WG, Blier L, Sarrazin JF *et al*. Ventricular tachycardia ablation versus escalation of antiarrhythmic drugs. *N Engl J Med* 2016;**375**:111–21.
10. Tung R, Vaseghi M, Frankel DS, Vergara P, Di Biase L, Nagashima K *et al*. Freedom from recurrent ventricular tachycardia after catheter ablation is associated with improved survival in patients with structural heart disease: an International VT Ablation Center Collaborative Group study. *Heart Rhythm* 2015;**12**:1997–2007.
11. Josephson ME, Anter E. Substrate mapping for ventricular tachycardia. *JACC Clin Electrophysiol* 2015;**1**:341–52.
12. Irie T, Yu R, Bradfield JS, Vaseghi M, Buch EF, Ajijola O *et al*. Relationship between sinus rhythm late activation zones and critical sites for scar-related ventricular tachycardia: systematic analysis of isochronal late activation mapping. *Circ Arrhythm Electrophysiol* 2015;**8**:390–9.
13. Tokuda M, Kojodjojo P, Tung S, Inada K, Matsuo S, Yamane T *et al*. Characteristics of clinical and induced ventricular tachycardia throughout multiple ablation procedures. *J Cardiovasc Electrophysiol* 2016;**27**:88–94.
14. Berte B, Relan J, Sacher F, Pillois X, Appetiti A, Yamashita S *et al*. Impact of electrode type on mapping of scar-related VT. *J Cardiovasc Electrophysiol* 2015; doi: 10.1111/jce.12761.
14. Jamil-Copley S, Linton N, Koa-Wing M, Kojodjojo P, Lim PB, Malcolme-Lawes L *et al*. Application of ripple mapping with an electroanatomic mapping system for diagnosis of atrial tachycardias. *J Cardiovasc Electrophysiol* 2013;**24**:1361–9.
15. Linton NW, Koa-Wing M, Francis DP, Kojodjojo P, Lim PB, Salukhe TV *et al*. Cardiac ripple mapping: a novel three-dimensional visualization method for use with electroanatomic mapping of cardiac arrhythmias. *Heart Rhythm* 2009;**6**: 1754–62.
16. Luther V, Cortez-Dias N, Carpinteiro L, de Sousa J, Balasubramaniam RN, Agarwal SC *et al*. Ripple mapping: initial multicenter experience of an intuitive approach to overcoming the limitations of 3d activation mapping. *J Cardiovasc Electrophysiol* 2017;**28**:1285–94.
17. Viswanathan K, Mantziari L, Butcher C, Hodkinson E, Lim E, Khan H *et al*. Evaluation of a novel high-resolution mapping system for catheter ablation of ventricular arrhythmias. *Heart Rhythm* 2017;**14**:176–83.
18. Anter E, Tschabrunn CM, Contreras-Valdes FM, Li J, Josephson ME. Pulmonary vein isolation using the Rhythmia mapping system: verification of intracardiac signals using the Orion mini-basket catheter. *Heart Rhythm* 2015;**12**:1927–34.
19. Anter E, Tschabrunn CM, Buxton AE, Josephson ME. High-resolution mapping of postinfarction reentrant ventricular tachycardia: electrophysiological characterization of the circuit. *Circulation* 2016;**134**:314–27.
20. Ptaszek LM, Moon B, Rozen G, Mahapatra S, Mansour M. Novel automated point collection software facilitates rapid, high-density electroanatomical mapping with multiple catheter types. *J Cardiovasc Electrophysiol* 2018;**29**:186
21. Bourier F, Fahrig R, Wang P, Santangeli P, Kurzidim K, Strobel N *et al*. Accuracy assessment of catheter guidance technology in electrophysiology procedures: a comparison of a new 3D-based fluoroscopy navigation system to current electroanatomic mapping systems. *J Cardiovasc Electrophysiol* 2014;**25**:74–83.
22. Martin R, Maury JP, Wong T, Dallet C, Frontera A, Takigawa M *et al*. High density mapping of conduction barriers in ventricular tachycardia. *Heart Rhythm* 2018;**14**:S543.
23. Martin CA, Martin R, Wong T, Maury P, Dallet C, Takigawa M *et al*. Effect of activation wavefront on electrogram characteristics during ventricular tachycardia ablation. *Europace* 2017;**19**:i16.
24. Luther V, Linton NW, Jamil-Copley S, Koa-Wing M, Lim PB, Qureshi N *et al*. A prospective study of ripple mapping the post-infarct ventricular scar to guide substrate ablation for ventricular tachycardia. *Circ Arrhythm Electrophysiol* 2016;**9**: e004072.
25. Mahida S, Sacher F, Dubois R, Sermesant M, Bogun F, Haïssaguerre M *et al*. Cardiac imaging in patients with ventricular tachycardia. *Circulation* 2017;**136**: 2491–507.
26. Sacher F, Lim HS, Derval N, Denis A, Berte B, Yamashita S *et al*. Substrate mapping and ablation for ventricular tachycardia: the LAVA approach. *J Cardiovasc Electrophysiol* 2015;**2**:464–71.
27. de Riva M, Naruse Y, Ebert M, Androulakis AF, Tao Q, Watanabe M *et al*. Targeting the hidden substrate unmasked by right ventricular extrastimulation improves ventricular tachycardia ablation outcome after myocardial infarction. *JACC Clin Electrophysiol* 2018; doi:10.1016/j.jacep.2018.01.013.
28. Porta-Sánchez A, Jackson N, Lukac P, Kristiansen SB, Nielsen JM, Gizurarson S *et al*. Multicenter study of ischemic ventricular tachycardia ablation with decrement evoked potential (DEEP) mapping with extra stimulus. *JACC Clin Electrophysiol* 2018; doi:10.1016/j.jacep.2017.12.005.
29. Hutchinson MD, Gerstenfeld EP, Desjardins B, Bala R, Riley MP, Garcia FC *et al*. Endocardial unipolar voltage mapping to detect epicardial VT substrate in patients with nonischemic left ventricular cardiomyopathy. *Circ Arrhythm Electrophysiol* 2011;**4**:49–55.
30. Yamashita S, Sacher F, Mahida S, Berte B, Lim HS, Komatsu Y *et al*. Image integration to guide catheter ablation in scar-related ventricular tachycardia. *J Cardiovasc Electrophysiol* 2016;**27**:699–708.
31. Zghaib T, Ipek EG, Hansford R, Ashikaga H, Berger RD, Marine JE *et al*. Standard ablation versus magnetic resonance imaging-guided ablation in the treatment of ventricular tachycardia. *Circ Arrhythm Electrophysiol* 2018;**11**:e006413.
32. Andreu D, Penela D, Acosta J, Fernández-Armenta J, Perea RJ, Soto-Iglesias D *et al*. Cardiac magnetic resonance-aided scar dechanneling: influence on acute and long-term outcomes. *Heart Rhythm* 2017;**14**:1121–8.
33. Yamashita S, Sacher F, Hooks DA, Berte B, Sellal JM, Frontera A *et al*. Myocardial wall thinning predicts transmural substrate in patients with scar-related ventricular tachycardia. *Heart Rhythm* 2017;**14**:155–63.
34. Ghannam M, Cochet H, Jais P, Sermesant M, Patel S, Siontis KC *et al*. Correlation between computer tomography-derived scar topography and critical ablation sites in postinfarction ventricular tachycardia. *J Cardiovasc Electrophysiol* 2018;**29**:438
35. Komatsu Y, Cochet H, Jadidi A, Sacher F, Shah A, Derval N *et al*. Regional myocardial wall thinning at multidetector computed tomography correlates to arrhythmogenic substrate in postinfarction ventricular tachycardia: assessment of structural and electrical substrate. *Circ Arrhythm Electrophysiol* 2013;**6**:342–50.
36. Yamashita S, Cochet H, Sacher F, Mahida S, Berte B, Hooks D *et al*. Impact of new technologies and approaches for post-myocardial infarction ventricular tachycardia ablation during long-term follow-up. *Circ Arrhythm Electrophysiol* 2016; **9**:e003901.

ESC European Society of Cardiology
Europace (2019) **21**, i34–i42
doi:10.1093/europace/euy273

CLINICAL RESEARCH

A novel assessment of local impedance during catheter ablation: initial experience in humans comparing local and generator measurements

Melanie Gunawardene[1]*, Paula Münkler[1,2], Christian Eickholt[1], Ruken Ö. Akbulak[1], Mario Jularic[1], Niklas Klatt[1], Jens Hartmann[1], Leon Dinshaw[1], Christiane Jungen[1,2], Julia M. Moser[1], Lydia Merbold[3], Stephan Willems[1,2], and Christian Meyer[1,2]*

[1]Department of Cardiac Electrophysiology, University Heart Center, University Hospital Hamburg Eppendorf, Martinistrasse 52, 20246 Hamburg, Germany; [2]DZHK (German Center for Cardiovascular Research), Partner Site Hamburg/Kiel/Luebeck, Berlin, Germany; and [3]Boston Scientific, Marlborough, MA, USA

Received 19 April 2018; editorial decision 18 October 2018; accepted 10 November 2018

Aims A novel measure of local impedance (LI) has been found to predict lesion formation during radiofrequency current (RFC) catheter ablation. The aim of this study was to investigate the utility of this novel approach, while comparing LI to the well-established generator impedance (GI).

Methods and results In 25 consecutive patients with a history of atrial fibrillation, catheter ablation was guided by a 3D-mapping system measuring LI in addition to GI via an ablation catheter tip with three incorporated mini-electrodes. Local impedance and GI before and during RFC applications were studied. In total, 381 RFC applications were analysed. The baseline LI was higher in high-voltage areas (>0.5 mV; LI: 110.5 ± 13.7 Ω) when compared with intermediate-voltage sites (0.1–0.5 mV; 90.9 ± 10.1 Ω, $P < 0.001$), low-voltage areas (<0.1 mV; 91.9 ± 16.4 Ω, $P < 0.001$), and blood pool LI (91.9 ± 9.9 Ω, $P < 0.001$). During ablation, mean LI drop (△LI; 13.1 ± 9.1 Ω) was 2.15 times higher as mean GI drop (△GI) (6.1 ± 4.2 Ω, $P < 0.001$). Baseline LI correlated with △LI: a mean LI of 99.9 Ω predicted a △LI of 12.9 Ω [95% confidence interval (12.1–13.6), R^2 0.41; $P < 0.001$]. This relationship was weak for baseline GI predicting △GI (R^2 0.06, $P < 0.001$). Catheter movements were represented by rapid LI changes. The duration of an RFC application was not predictive for catheter–tissue coupling with no further change of △LI ($P = 0.247$) nor △GI ($P = 0.376$) during prolonged ablation.

Conclusion Local impedance can be monitored during ablation. Compared with the sole use of GI, baseline LI is a better predictor of impedance drops during ablation and may provide useful insights regarding lesion formation. However, further studies are needed to investigate if this novel approach is useful to guide catheter ablation.

Keywords Atrial fibrillation • Catheter ablation • Radiofrequency current • Impedance • Ultra high-density mapping

Introduction

Radiofrequency current (RFC) is the most widely used energy form to perform catheter ablation of cardiac arrhythmias.[1] Radiofrequency current energy creates myocardial lesions by resistive heating of the myocardial tissue, followed by heat conduction to the adjacent tissue.[1] To date, impedance places an important role in lesion formation during RFC ablation[2–4]: first of all, better contact with the tissue causes higher impedances.[5] Secondly, to create adequate, deep lesions by resistive heating, a sufficient resistive load (which is equivalent to a high impedance) is well known to be required at the catheter–tissue interface.[5,6] Thirdly, a drop of impedance during energy delivery is predictive for lesion formation as it implicates damage to the underlying tissue.[6,7] Therefore, changes of resistivity directly reveal information about electrical coupling between the catheter tip and underlying tissue.[6,7]

Several technologies have attempted to measure the resistive load at the catheter–tissue interface via impedance. Radiofrequency

* Corresponding author. Tel: +49 40 7410 54120; fax: +49 40 7410 54125. *E-mail address:* c.mey@web.de; m.gunawardene@uke.de

What's new?

- The drop in local impedance (LI) measured from an ablation catheter tip with three incorporated mini-electrodes during radiofrequency current (RFC) application is about twice as high as the generator impedance (GI) drop.
- Higher LI at the start of an application predicts larger impedance drops during ablation, rather than the RFC GI.
- Baseline LI in high-voltage areas is higher when compared with intermediate- and low-voltage ablation sites as well as compared with blood pool LI.
- Local impedance can be monitored during ablation and may provide useful insights regarding catheter stability, tissue characteristics, and lesion formation compared with the sole use of GI.

current generators measuring transthoracic impedance of the energy delivery pathway from an ablation catheter tip electrode to an indifferent electrode on the skin are well established.[6] While RFC generators measure a modest impedance difference between blood and tissue, significant variation in the bulk of transthoracic impedance (including muscle, lung, and bone impedance) limits the utility of transthoracic/generator impedance (GI) as a precise measure of the actual local catheter–tissue coupling.[6]

Piorkowski *et al.*[8] presented an approach to estimate local impedance (LI) from the ablation catheter tip with a three-terminal model and two body-surface electrodes and were able to distinguish between contact and non-contact to the tissue with this method. However, this approach was reported to be confounded by remote structures and drift.[8–10]

Recently, a novel measure of LI recorded from miniature-electrodes integrated in an ablation catheter tip has shown to be a sufficient measure of LI predicting catheter–tissue contact and lesion formation during RFC catheter ablation in an experimental setting.[6] Yet, how this measure of LI can guide catheter ablation in humans is not known. The aim of this study was to investigate the clinical utility of this approach using LI recorded from miniature-electrodes during catheter ablation in patients with a history of symptomatic, recurrent atrial fibrillation (AF).

Objective

To investigate the utility of a novel measure of LI from an ablation catheter tip with three incorporated mini-electrodes during catheter ablation procedures and how LI is related to the well-established GI.

Methods

Study design

This study was a single-centre, pilot study with an explorative design. To investigate how LI is related to GI and low-voltage areas, consecutive patients with recurrent AF or atrial tachycardia (AT), after prior ablation for paroxysmal or persistent AF from 11/2017 until 01/2018 were enrolled. Written informed consent was obtained from all patients. The study was conducted in accordance with the provisions of the Declaration of Helsinki and its amendments. The institutional review board of the University Heart Center Hamburg approved the study.

Catheter ablation procedure

Catheter ablation was performed under deep sedation using a continuous infusion of propofol (1 mg/mL, B. Braun, Melsungen, Germany) combined with boluses of fentanyl (0.1 mg/mL, Rotexmedica, Trittau, Germany), as previously described.[11]

Intravenous heparin (heparin sodium, 25 000 IU/5 mL, Rotexmedica) was administered during the procedure aiming at an activated clotting time of 300–350 s.

Via both femoral veins, one long (SL0™, 8 Fr, St Jude), one steerable sheath (ZURPAZ™ 8.5 Fr, Boston Scientific, Marlborough, MA, USA), and two short haemostatic sheaths (Fast-Cath™, 6 Fr and 8 Fr, Daig Inc., Minnetonka, MN, USA) were inserted, followed by positioning of a reference catheter into the coronary sinus.

To access the left atrium (LA), one transseptal puncture using a modified Brockenbrough technique was performed and both, the long sheath and the steerable sheath were navigated into the LA. A 64-pole mini-basket mapping catheter (Orion™, Boston Scientific) was introduced to the LA via the steerable sheath. After LA angiography was completed, the mini basket catheter was used in combination with an ultra high-density mapping system (Rhythmia™, Boston Scientific) to reconstruct the LA geometry and to create activation- and/or voltage maps. An open-irrigated ablation catheter with three miniature-electrodes incorporated within the distal tip electrode (IntellaNav MiFi™ OI, Boston Scientific) was used for additional mapping and ablation.

The ablation strategy depended on the underlying rhythm at the beginning of the procedure: in case of recurrent paroxysmal AF, sole re-pulmonary vein isolation (Re-PVI) was performed. In patients with persistent AF, we performed the previously described stepwise approach[12] consisting of Re-PVI and substrate modification, if necessary. If a patient presented in AT, the underlying mechanism was identified, followed by specific ablation, as previously described.[13] During ablation, RFC was applied in a temperature-controlled fashion with a flush rate of 20 mL/min, a maximum of 30 W and temperature limit of 45°C. In voltage maps, high-voltage areas were defined by a voltage of more than 0.5 mV[14,15] when compared with intermediate voltage of 0.1–0.5 mV and low-voltage areas of <0.1 mV.

Local impedance measurement

Local impedance was measured by an open-irrigated single-tip mapping and ablation catheter (IntellaNav MiFi™ OI, Boston Scientific, *Figure 1*). The features of this novel ablation catheter have been described before[6]: from the tip of the catheter, the centre of each miniature-electrode is 2.0 mm away. Each electrode has a diameter of 0.80 mm. Local impedance is measured by a four-electrode method with separate circuits for field creation and field measurements.[6] Between the tip electrode and the proximal ring of the ablation catheter a non-stimulatory alternating current (5.0 μA at 14.5 kHz) is operated. Simultaneously, voltage is assessed passively between the miniature-electrodes and distal ring of the catheter.[6] To convert into impedance, these measured voltage values are divided by the stimulatory current. The maximum LI from the three miniature-electrodes was then displayed on the graphical user interface-screen of the ultra high-density mapping system and used for all analysis. The user interface displays the maximum LI value of all of the three miniature-electrode LI measurements. These maximum values were used for analysis in this study.

In each patient, after the electro-anatomical map of the LA was completed, blood pool impedance (as a non-contact reference) was

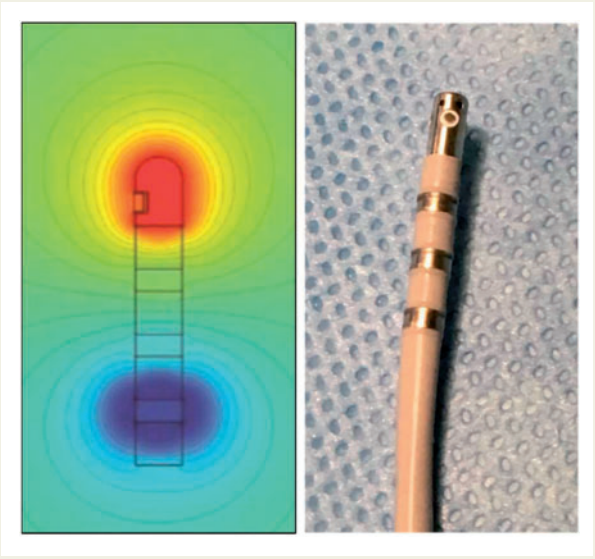

Figure 1 Field creation and ablation catheter for local impedance measurement. (Left panel) Simulation of the potential field created by injecting non-stimulatory current between the distal electrode and the proximal ring. A single miniature-electrode is shown in the distal tip. (Right panel) Photography of the open-irrigated ablation catheter with three miniature-electrodes (one is shown in the figure) at the distal tip electrode (IntellaNav MiFi^{TM} OI, Boston Scientific). Adapted with permission from Sulkin/Laughner *et al.*[6]

measured via the ablation catheter in the LA chamber, as indicated by the absence of electrograms on the conventional and mini-electrodes.

At the start of the RFC application the LI of the ablation site was recorded (so called 'baseline LI' in the following). In case of a dragged ablation lesion, LI measurements were only analysed until the first movement of the catheter. For each stable location of the catheter, which was verified by the electro-anatomical map, fluoroscopy, tactile feedback from the catheter and local electrograms,[8] the maximum LI drop (△LI) was analysed additionally.

The videos of the ablation procedures were exported from the mapping system (Rhythmia^{TM}, Boston Scientific) and displayed the procedure in real-time. Radiofrequency current applications were then retrospectively analysed. We excluded all lesions with instability of the catheter (not meeting the abovementioned criteria), interference with the mini-basket-catheter and applications with a duration of less than 10 s.

Generator impedance

Correspondingly to LI measurements, a RFC generator (EP Shuttle^{TM}, Stockert, Biosense Webster Inc., Diamond Bar, CA, USA) was used to record GI. The generator measured the system impedance by using a two-electrode method that included the same circuit for both field creation and field measurements.[6] Alternating current (500 kHz) was driven by the generator between the tip electrode of the ablation catheter to an indifferent electrode on the patient's skin.

Analogously to LI, GI was measured at the start of each ablation application (baseline GI) and the maximum GI drop (△GI) was additionally analysed for each lesion. Applications without GI information were excluded from analysis.

Table 1 Patients characteristics

	Patients (n = 25)
Male gender, *n* (%)	15 (60)
Age (years)	66.3 ± 12.8
Arterial hypertension, *n* (%)	15 (60)
Cardiomyopathy, *n* (%)	3 (12)
Coronary artery disease, *n* (%)	3 (12)
Diabetes, *n* (%)	1 (4)
Prior stroke/TIA, *n* (%)	5 (20)
BMI (kg/m^2)	27.0 ± 4.1
CHA_2DS_2-VASc score	2.6 ± 1.6
Indication for re-ablation, *n* (%)	
Recurrence of paroxysmal AF	4 (16)
Recurrence of persistent AF	11 (44)
Left/right atrial tachycardia	10 (40)
Number of prior ablations, *n*	2.4 ± 1.6

AF, atrial fibrillation; BMI, body mass index; CHA_2DS_2-VASc score is a clinical estimation of the risk of stroke in patients with atrial fibrillation; scores range from 0 to 9, with higher scores indicating a greater risk of stroke, Congestive heart failure, Hypertension, Age >75 years, Diabetes, previous Stroke, transient ischaemic attack, or thromboembolism, Vascular disease, Age 65–75 years, and Sex category; TIA, transient ischaemic attack.

Statistical analysis

Binary-coded and categorical data were described as counts and relative frequencies. Continuous data were expressed as mean ± standard deviation or by median and interquartile range. For group comparisons, Wilcoxon matched-pairs signed rank tests for paired values as well as a Mann–Whitney *U*-tests for unpaired values were performed. Additionally, a one-way analysis of variance (ANOVA) test was performed for analysis of the different anatomical locations. Further, linear regression analysis was calculated to determine relationships between LI and GI as well as △LI and △GI. A statistical significance was defined as a *P*-value <0.05. Statistics were calculated using 'R' [R Core Team (2017), A Language and Environment for Statistical Computing, R Core Team, R Foundation for Statistical Computing. Vienna, Austria, 2017] and GraphPad Prism 6.0 (GraphPad Software Inc., San Diego, CA, USA).

Results

Patients characteristics and procedural parameters

In 25 consecutive patients with a history of AF, catheter ablation, and analysis of LI were performed. An initial series of five patients (n = 5/30) was not included for analysis to avoid a learning-curve bias. Baseline characteristics are shown in *Table 1*. These 25 patients underwent 2.4 ± 1.6 prior catheter ablation procedures and returned for re-ablation due to recurrence of paroxysmal AF in four patients (16%, n = 4/25), persistent AF in 11 patients (44%, n = 11/25), and AT in 10 patients (40%, n = 10/25).

Procedural data are summarized in *Table 2*. The mean procedure duration and fluoroscopy times were 156.6 ± 53.1 min and 18.1 ± 10.3 min, respectively. A mean of 24.6 ± 16.5 RFC applications

Table 2 Procedural parameters

	Patients ($n = 25$)
Procedure duration (min)	156.6 ± 53.1
Fluoroscopy time (min)	18.1 ± 10.3
RFC applications (*n*)	24.6 ± 16.5
RFC duration (s)	1637.8 ± 1190.0
Cumulative energy (J)	44 605 ± 34 869
LA volume (mL)	96.6 ± 51.4
LA mapping time (min)	13.2 ± 10.3
LA mapping points (*n*)	9958.1 ± 8064.1
Ablation strategies, *n* (%)	
All PVs isolated	7 (28)
Re-PVI	18 (72)
Defragmentation	4 (16)
Ablation of LAT	9 (36)
Ablation of RAT	3 (12)
Re-CTI	8 (32)
Complications, *n* (%)	
Access site related	1 (4) minor groin haematoma
Pericardial tamponade	1 (4)
TIA/stroke	–
PV stenosis	–
Phrenic nerve palsy	–
Atrio-oesophageal fistula	–
Death	–

CTI, cavotricuspid isthmus ablation; LA, left atrium; LAT, left atrial tachycardia; PV, pulmonary vein; PVI, PV isolation; RAT, right atrial tachycardia; RFC, radiofrequency current; TIA, transient ischaemic attack.

were deployed per ablation procedure with a total count of 616 RFC applications without any steam popping.

Local and generator impedances

Of all 616 RFC applications counted by the generator, 381 (61.8%, $n = 381/616$) had a complete high quality data set with a RFC application >10 s and were included in the study analysis.

Overall, blood pool impedance levels tended to be lower when compared with baseline LI of myocardial tissue [99.9 ± 14.9 Ω, ($n = 447$)] vs. blood pool (91.9 ± 9.9 Ω, $P = 0.052$).

Baseline LI was lower when compared with baseline GI [LI: 99.9 ± 14.9 Ω ($n = 447$) vs. GI: 115.1 ± 11.7 Ω GI, $P < 0.001$], (*Figure 2A*). The mean impedance drop during RFC application was more than two times higher for △LI when compared with △GI [△LI: 13.1 ± 9.1 Ω ($n = 389$) vs. △GI: 6.1 ± 4.2 Ω ($n = 362$), $P < 0.001$], (*Figure 2B*).

The linear regression analysis revealed that a higher baseline LI in the LA predicted higher △LI during ablation [adjusted $R^2 = 0.41$, $P < 0.001$, slope = 0.39, 95% confidence interval (CI) (0.34–0.44), *Figure 2D*]. This means that a mean baseline LI of 99.9 Ω predicted a △LI of 12.9 Ω (95% CI (12.1–13.6)]. For the 1st quartile (q1), (90.0 Ω) and the 3rd quartile (q3), (109 Ω) of baseline LI, the predicted △LI was 8.9 Ω; [95% CI (8.0–9.9)] and 16.4 Ω [95% CI (15.5–17.2)], respectively.

The baseline GI was only a poor predictor of △GI [adjusted $R^2 = 0.06$; $P < 0.001$, slope = 0.09; 95% CI (0.05–0.14), *Figure 2C*]. A mean baseline GI (116.7 Ω) predicted a △GI of 6.0 Ω [95% CI (5.5–6.4)]. For the 1st quartile (109 Ω) and the 3rd quartile (175 Ω) of baseline GI, the predicted △GI was 5.1 Ω; [95% CI (4.6–5.8)] and 6.7 Ω [95% CI (6.2–7.3)], respectively.

The duration of an RFC application was not predictive for catheter–tissue coupling: once the maximum △LI or the maximum △GI were observed, prolongation of the RFC application did not further lower the LI nor GI, respectively (△LI: $P = 0.247$; △GI: $P = 0.376$).

Of 13 patients with right and/or left AT, specific termination into sinus rhythm was achieved in ten patients ($n = 10/13$, 76.9%) during ablation. The termination of AT was observed within a median of 7s (q1–q3: 5–13) of RFC delivery, with a mean △LI of 8.5 ± 4.6 Ω and a mean △GI of 4.2 ± 1.8 Ω at the time of termination. After a further median of 25 s (q1–q3: 15–32) of ablation, these RFC applications reached a maximum △LI of 14.8 ± 8.3 Ω and a maximum △GI of 8.8 ± 3.7 Ω. A power of 27.2 ± 2.4 W was applied in these termination lesions.

In a subset of 67 lesions (17.6%, $n = 67/381$, nine patients), the voltage values of different ablation sites were analysed: the mean baseline LI was higher in high-voltage areas of >0.5 mV (LI: 110.5 ± 13.7 Ω) when compared with ablations sites with intermediate voltage of 0.1–0.5 mV (LI: 90.9 ± 10.1 Ω, $P < 0.001$), low-voltage areas of <0.1 mV (LI 91.9 ± 16.4 Ω, $P < 0.001$) and compared with blood pool LI (LI: 91.9 ± 9.9 Ω, $P < 0.001$), (*Figure 3A*). The baseline LI at low- and intermediate voltage ablation sites was observed to be 4 Ω (q1–q3: 0, 25–9 Ω) higher (equals a 5% increase) than the individual patient's blood pool LI ($n = 8$ patients, $n = 46$ lesions). In 35 out of 46 lesions a numerical increase of baseline LI was found in low-voltage areas compared with the patients' blood pool impedance. Voltage maps were performed in sinus rhythm ($n = 4/9$ patients, 44.4%) or during AT ($n = 5/9$, 55.6%).

Baseline LI and baseline GI differed in areas of low ($P < 0.001$), intermediate ($P < 0.001$), and high voltage ($P = 0.001$) with wider ranges of LI standard deviations, (*Figure 3B*). A presentative example showing the LI in a LA low-voltage area in a patient with an AT is shown in the Supplementary material online, *Figure*.

Measurement of baseline LI among different anatomical localizations revealed a higher LI in the coronary sinus with 133.8 ± 21.7 Ω ($n = 5$), compared with left atrial LI: 99.6 ± 14.5 Ω ($n = 355$, $P = 0.001$), right atrial LI: 99.0 ± 14.3 Ω ($n = 73$, $P = 0.002$), and LI of the cavotricuspid isthmus region: 96.7 ± 10.3 Ω ($n = 43$, $P < 0.001$) as well as the blood pool LI: 91.9 ± 9.9 ($n = 5$; $P = 0.003$), (*Figure 4*).

Within the 90-days blanking period following the procedure, eight patients ($n = 7/25$, 28%) developed an AF/AT recurrence ($n = 5$ AF, $n = 2$ AT). During a median follow-up of 160 (q1–q3: 117–174) days, four patients ($n = 4/25$, 16%) developed an AF/AT recurrence after the blanking period ($n = 2$ AF, $n = 2$ AT; two of these patients already had an early AF recurrence within the blanking period).

Technical considerations and safety

Local impedance was successfully used during Re-PVI in 18 patients (18/25; 72%), substrate modification in four patients (4/25; 16%), cavotricuspid isthmus ablation in eight patients (8/25; 32%), and ablation of AT in 11 patients (11/25; 44%, *Table 2*) without the presence of any documented charring. *Figure 5* shows an example of real-time LI

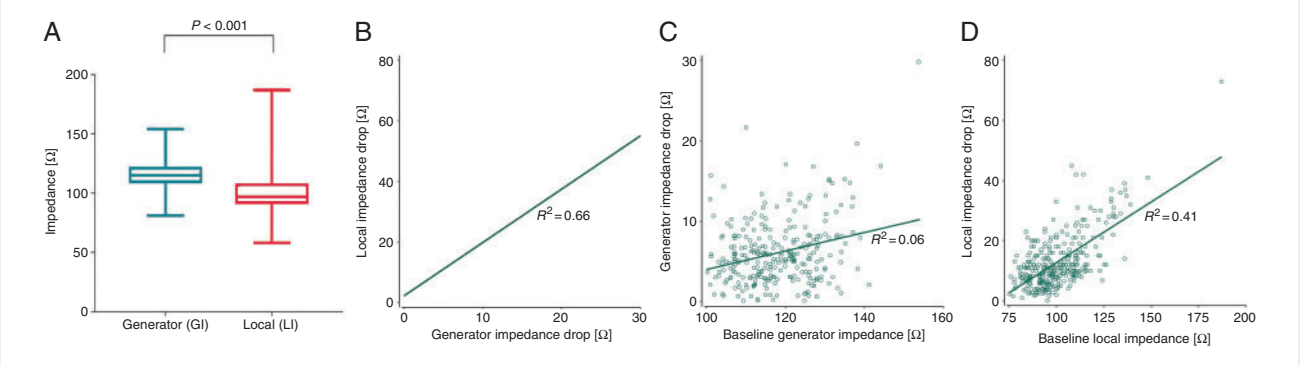

Figure 2 Relationship between LI and GI. (*A*) Discrimination between GI and LI.(*B*) Relationship between impedance drop of local impedance (△LI) compared with generator impedance (△GI): the local drop measured via the ablation catheter is more than two times higher when compared with the impedance drop of the generator.(*C*) Correlation between start impedances and generator impedance drops: the start impedance of the generator correlates poorly with the subsequent drop of impedance. (*D*) Correlation between local start impedances and local impedance drops: a higher local start impedances predicts higher △LI values. GI, generator impedance; LI, local impedance.

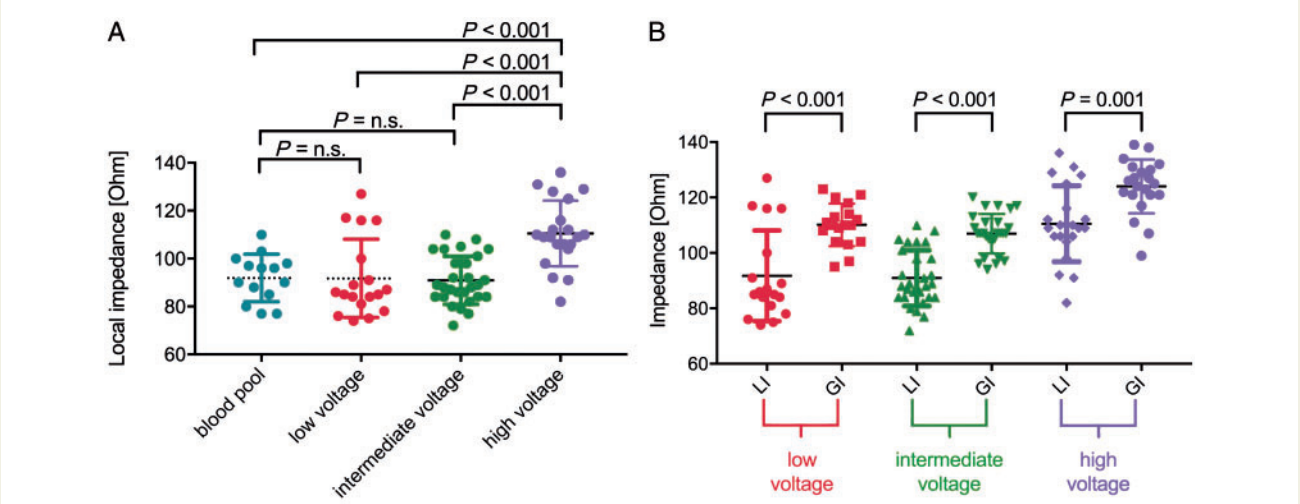

Figure 3 Relationship between impedance and voltage.(*A*) Local impedance values in low, intermediate and high-voltage areas of ablation, as well as the comparison towards blood pool impedance is shown. (*B*) The difference in local and generator impedance in low-, intermediate-, and high-voltage areas of ablation is shown. GI, generator impedance; LI, local impedance.

measurement during re-isolation of a left inferior pulmonary vein (PV). Here, an anterior gap of PV reconnection was detected by high-resolution activation mapping and confirmed by local mini-electrode signals (MIFI M3-M1) before RFC delivery. Acute pulmonary vein isolation occurred then within 4 s of ablation.

Twenty-three ablation procedures were performed successfully without any complications. In one patient a minor groin haematoma was documented and successfully treated conservatively. In another patient a pericardial tamponade manifested shortly after a RFC application with a rapid △LI of 45 Ω during an ongoing AT with a critical isthmus along the left atrial roof. Immediate, successful pericardiocentesis was performed, the AT was terminated by rapid atrial pacing and the patient was discharged 4 days later in a good medical condition.

In consequence, during the following ablation procedures ($n = 8$), RFC applications were stopped when a maximum cut-off △LI of <40 Ω was observed. After completion of this study, 97 additional atrial ablation procedures were performed in our department using this 40 Ω cut-off value without occurrence of a single pericardial tamponade. In this whole series, exceeding the here presented study population including 122 patients there was one transient dysarthria and two groin arteriovenous fistula with subsequent thrombin injection. No further complications occurred.

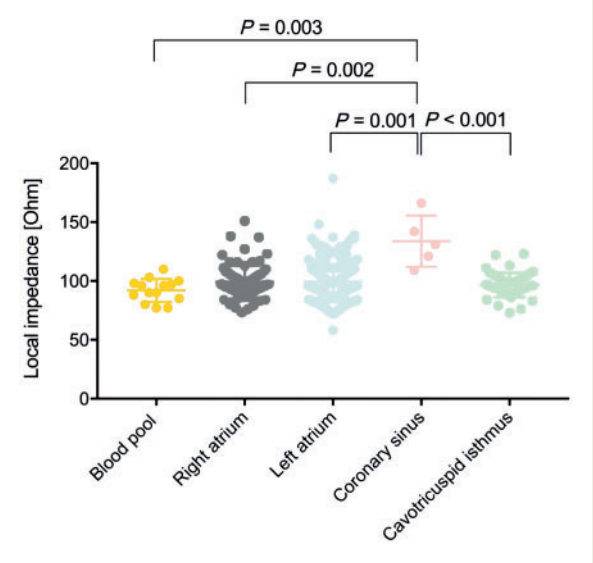

Figure 4 Local impedance among different anatomical localizations.

Further, during the ablation procedures, we observed different scenarios of how the real-time LI curves can present during RFC application, shown in *Figure 6*: (1) In this example, a very rapid and steep LI drop of 33 Ω within a few seconds was observed and energy delivery stopped. (2) Contact of the ablation catheter with the electrodes of the mini-basket catheter led to artefacts resulting in non-physiologic LI measurements of 316 Ω, in this example (△LI was 230 Ω during this interference). Therefore, LI cannot be determined during ablation when RF delivery is performed on the mini-basket catheter. (3) Instable catheter position resulted in systolic and diastolic movements of the catheter with rapid changes of the LI standard deviation. Image (4) shows an example of ablation in a low-voltage area: the baseline impedance (LI: 73 Ω) as well as △LI (−2.8 Ω) were comparably low. (5) When the ablation catheter was dragged during ablation, after an initial LI drop, LI raised again whenever the catheter was moved to a new position. (6) Lastly, respiration movements were reflected by fluctuating LI curves which could be observed in the changes of the real-time recordings during ablation.

Discussion

Major findings

The major findings of this study are as follows:

(1) Local impedance measurements from an ablation catheter tip with three incorporated mini-electrodes are related to the local tissue voltage. Baseline LI in high-voltage areas is higher when compared with intermediate- and low-voltage ablation sites as well as compared with blood pool LI.
(2) The drop in LI during RFC application was about twice as high as the GI drop.
(3) Higher LI at the start of an application predicted larger LI drops during ablation, while GI at baseline was not a good predictor for the GI drop during ablation.

Local and generator impedance measurements

Local impedance is a direct measure of the resistive load on the ablation catheter and provides a surrogate for the distal electrode surface area covered by myocardium.[6] It can distinguish between catheter–tissue contact from non-contact, as has been demonstrated by initial experimental findings and is supported by the here presented study.[6] Noteworthy and not surprisingly, observed LI was lower than GI measurements. In contrast, during ablation the △LI was greater than the △GI. This observation of larger LI drops were also in accordance with findings from prior experimental studies.[6] Therefore, the data of the present study indicate that LI makes it more likely the operator will achieve a target LI drop, as the baseline LI is more predictive than GI. It seems that △LI could be a more sensitive parameter for electrical coupling between catheter tip and tissue, when compared with the well-established △GI. The quality of LI data is not expected to be influenced by the generator. In experimental studies, △LI was a better predictor of lesion dimensions than △GI.[6]

So far, the optimal decrease of LI for lesion formation as well as the optimal modality over time during ablation cannot be defined. However, a surrogate parameter for acute efficacy in this study was provided by addressing the time course of LI and its decrease during RF delivery before AT termination into sinus rhythm. Additionally, when discussing the optimal decrease of LI, safety aspects need to be considered. In this study, a rapid decrease of the LI was seen in the patient with the cardiac tamponade. Nguyen *et al.*[16] support this finding and showed an association between the occurrence of steam pops and more rapid initial GI reduction during catheter ablation (1.40 Ω/s with vs. 0.38 Ω/s without steam pops). However, additional studies are warranted and underway to evaluate the safety of the here presented approach. No general safety recommendation can be made at this time.

Furthermore, our finding that higher start LI values were associated with larger △LI, is in line with the fact that higher initial impedance values are associated with better contact to the tissue.[5] RFC energy appears to be better transferred to the underlying tissue if high LI is measured due to better contact.[5,6] However, our study does not provide any information on the quality of the tissue contact, since so far, no contact force measurements are available for the presented approach. As information on the quality of tissue contact is missing, LI might not be able to detect excessive contact, a very important element to avoid complications. This needs further studies in the future.

Potential benefit of local impedance measurement

More than two decades ago, Josephson *et al.*[17] impressively demonstrated by some elegant studies in an experimental model of myocardial infarction, the potential value of LI to distinguish between healthy and diseased tissue. In our present study, LI in high-voltage areas was higher than in low-voltage areas. This supports the concept that LI is useful to distinguish between healthy and scarred myocardium, also

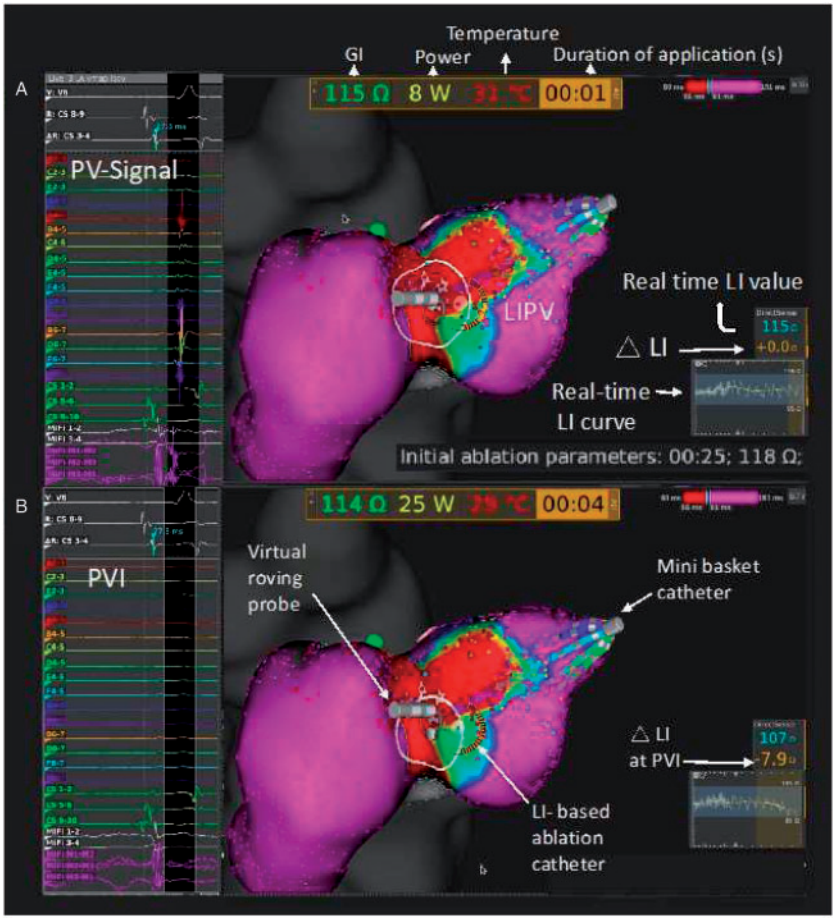

Figure 5 Local impedance measurement during ablation of a reconnected pulmonary vein. The Rhythmia™ activation map of a reconnected LIPV with an anterior gap is shown. On the top of each image, the information provided by the radiofrequency current generator is displayed; on the left, PV electrograms can be found and on the right, the LI information is provided. Image (*A*) shows the reconnected LIPV with a LI of 115 Ω and a GI of 118 Ω at the start of the RF application. The △LI is visualized right below the real-time LI value on the Rhythmia™ map in yellow. The lower image (*B*) demonstrates PVI occurring within 4 s with a 7.9 Ω-local impedance drop, which is shown in the real-time LI-curve in yellow. The drop in the generator was 4 Ω only. GI, generator impedance; LI, local impedance; LIPV, left inferior pulmonary vein; △LI = drop of local impedance; PVI, pulmonary vein isolation; RF, radiofrequency.

on the atrial level in humans. In addition, LI measurements by the ablation catheter were useful to distinguish healthy myocardium from blood pool, reflecting contact vs. non-contact. Noteworthy, mean baseline LI could only be used to reliably distinguish being in the blood pool vs. high voltage tissue, but not in intermediate or low voltage tissue. This finding could be explained by enrolment of patients undergoing re-do ablation procedures. Lang *et al.*[18] not only showed a difference in impedance between the LA and the PVs, but did also find lower impedances of the LA and PVs in patients undergoing repeat catheter ablation. Noteworthy, we found a slightly higher LI in low-/intermediate-voltage areas compared with the patients' individual blood pool. Therefore, LI might be an adjunct parameter in addition to the fluoroscopy, local electrograms and the 3D map to assess tissue contact in low-voltage areas. It remains unclear whether and how these findings might be influenced by different causes of myocardial scarring such as atrial fibrosis or low voltage due to prior ablation; different areas within the heart need to be explored in more detail.[17]

Regarding voltage measurements, further studies to determine LI cut-offs in different chambers and voltage areas are needed.

Up to now, real-time mechanical coupling during ablation is facilitated by the use of contact force (CF) sensing catheters.[19,20] A modest linear relationship between contact force over time (so called force-time-integral) and lesion depth has been shown.[21] However, in specific situations, such as ablation in the coronary sinus, CF can be misleading. While CF of the ablation catheter is low in the coronary sinus, the resistive load is high as more surface area of the electrode becomes enveloped by tissue rather than by blood.[5] Therefore, a large amount of RF energy could be delivered to the myocardium. In these kind of specific situations, LI alone or in combination with other parameters could be more informative about lesion formation than the sole use of CF, as CF is only of limited value to predict impedance drops during RFC delivery. LI could be a real-time measure for electrical coupling allowing an estimation of lesion size during ablation, as is supported by experimental evidence.

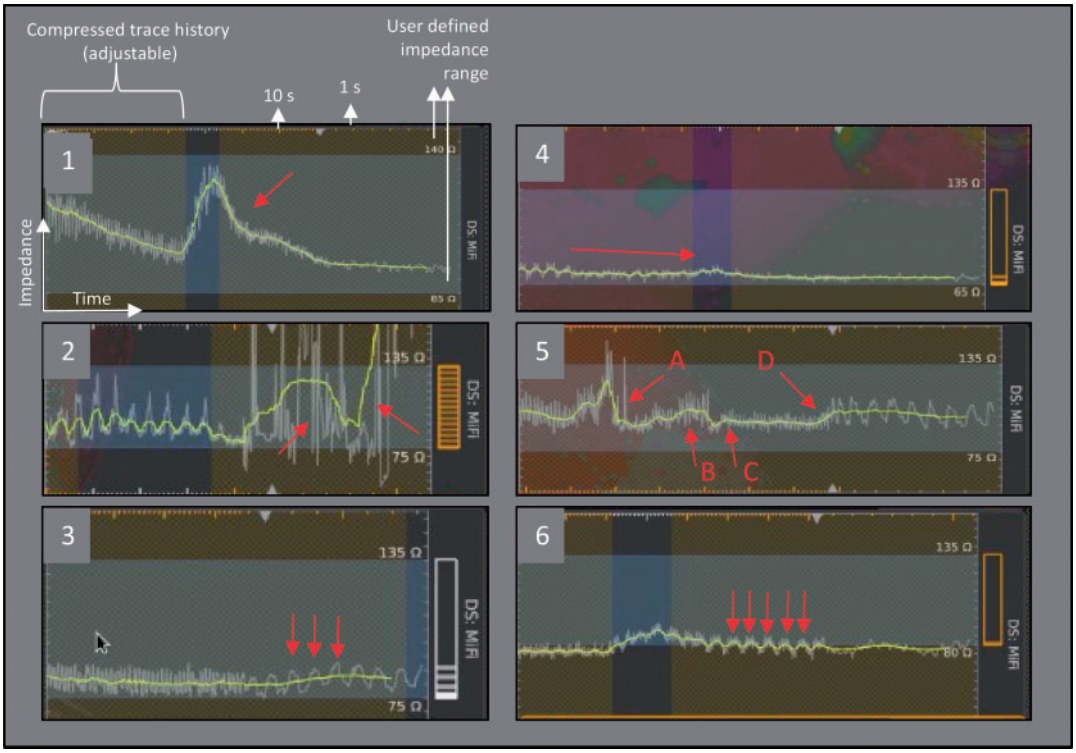

Figure 6 Different real-time local impedance curves during RF ablation. Different real-time curves of local impedances (LI) during RF ablation are shown. These LI-curves are exported from the Rhythmia™ map and show the mean LI as a yellow curve and the LI-standard deviation as a white curve. (1) A rapid and immense impedance drop of minus 33 Ω leading to premature stop of the ablation application for patients' safety (the LI at the start of the application was 128 Ω) is shown. (2) Placement of the ablation catheter next to the mini-basket catheter led to interference of the impedance measurement with implausible LI values (LI was 316 Ω and △ LI was 230 Ω during interference). (3) Instable catheter position led to systolic and diastolic movements of the catheter with rapid changes of the LI standard deviation shown by the white curves, around the yellow mean-LI curve. (4) Example of ablation in a low-voltage area: the start impedance (LI: 73 Ω) as well as △ LI (△ LI −2.8 Ω) were comparably low. (5) Example of a dragged ablation lesion: (*A*) shows the drop of the LI at the first ablation site, (*B*) then the catheter was moved and LI raised again due to movement of the catheter to an unablated tissue location, (*C*) followed by a second LI drop after the catheter was positioned at the second ablation site. (*D*) When the catheter was moved for the third time, LI raised again. (6) Example of local impedance fluctuations due to respiration. Notice the variability of the mean LI-curve (yellow).

Limitations

The present study has several limitations. First, the design of our study was explorative and we retrospectively analysed the real-time videos, exported from the electroanatomical mapping system. Next, we excluded RFC applications from the analysis to reliably include only solid and reproducibly quantifiable lesions. In consequence, only a limited sample size of 67 lesions was available to investigate the relationship of LI and voltage. Therefore, statistical power needs to be critically judged. Next, we only investigated LI in recurrent AF/AT ablation procedures. However, we present an early experience of LI-measurement and delivered specific details on >350 ablation lesions. Additional studies are warranted and underway to evaluate the safety of the here presented approach. Clinical implementation of this approach in other ablation procedures including catheter ablation of ventricular arrhythmias, in healthy and diseased myocardium needs to be studied in detail in the future. So far, the clinical results of this study show only a preliminary outcome. Noteworthy, we did not investigate effectiveness of RFC ablation guided by LI measurement. This is currently investigated in the LOCALIZE study (ELectrical COupling Information From The Rhythmia™ HDx Mapping System And DireCtSense™ Technology In The Treatment Of Paroxysmal AtriaL FibrIllation-A Non-RandomiZed, ProspEctive Study). In addition, no precise estimation of lesion size in humans is possible yet.

Finally, a limitation of the used catheter might be that there is currently no simultaneous combination of LI and contact force measurements available. Therefore, further studies are warranted to answer the question how precisely LI can indicate catheter–tissue contact in scared myocardium and to which extend it is able to guide catheter ablation in these situations.

Conclusion

Local impedance measurements are related to the voltage of the underlying tissue. Compared with the GI, baseline LI is a better predictor of impedance drops during ablation. Therefore, LI can be

monitored during ablation and may provide useful insights regarding catheter–tissue contact, catheter stability and lesion formation compared with the sole use of GI. Further studies are warranted to follow-up on our initial findings.

Supplementary material

Supplementary material is available at *Europace* online.

Acknowledgements

The authors thank Jake Laughner, PhD and Matt Sulkin, PhD (Boston Scientific Corp., St. Paul, MN, USA, 55112, Electrophysiology) for disclosing their previous findings on local impedance measurement to us, as well as for advise on data acquisition and engaging discussions/comments that greatly improved this article.

Funding

This work is supported by the DZHK (German Centre for Cardiovascular Research) [FKZ 81Z4710141 and 81X2710149].

Conflict of interest: L.M.: employee at Boston Scientific, Field Clinical Specialist Rhythmia™. C.E.: compensation for participation on speaker's bureau for Boston Scientific. C.M.: compensation for participation as consultant for Biotronik (also research grant), Biosense Webster, Boston Scientific, Medtronic, Philips Research Europe and on speaker's bureau for Abbott, Boston Scientific, Medtronic. S.W.: compensation for participation on speaker's bureau and consultant or on advisory board for: Boehringer Ingelheim, Bayer, Daiichi-Sankyo, BMS, Abbott. All other authors declared no conflict of interest.

References

1. Calkins H, Hindricks G, Cappato R, Kim Y, Saad EB, Aguinaga L *et al.* 2017 HRS/EHRA/ECAS/APHRS/SOLAECE expert consensus statement on catheter and surgical ablation of atrial fibrillation. *Europace* 2018;**20**:157–208.
2. Harvey M, Kim YN, Sousa J, El-Atassi R, Morady F, Calkins H *et al.* Impedance monitoring during radiofrequency catheter ablation in humans. *Pacing Clin Electrophysiol* 1992;**15**:22–7.
3. Reichlin T, Knecht S, Lane C, Kühne M, Nof E, Chopra N *et al.* Initial impedance decrease as an indicator of good catheter contact: insights from radiofrequency ablation with force sensing catheters. *Heart Rhythm* 2014;**11**:194–201.
4. Inaba O, Nagata Y, Sekigawa M, Miwa N, Yamaguchi J, Miyamoto T *et al.* Impact of impedance decrease during radiofrequency current application for atrial fibrillation ablation on myocardial lesion and gap formation. *J Arrhythm* 2018;**34**:247–53.
5. Zheng X, Walcott GP, Hall JA, Rollins DL, Smith WM, Kay GN *et al.* Electrode impedance: an indicator of electrode-tissue contact and lesion dimensions during linear ablation. *J Interv Card Electrophysiol* 2000;**4**:645–54.
6. Sulkin M, Laughner J, Hilbert S, Kapa S, Kosiuk J, Younan P *et al.* A novel measure of local impedance predicts catheter-tissue contact and lesion formation. *Circ Arrhythm Electrophysiol* 2018;**4**:e005831.
7. Ikeda A, Nakagawa H, Lambert H, Shah DC, Fonck E, Yulzari A *et al.* Relationship between catheter contact force and radiofrequency lesion size and incidence of steam pop in the beating canine heart: electrogram amplitude, impedance, and electrode temperature are poor predictors of electrode-tissue contact force and lesion. *Circ Arrhythm Electrophysiol* 2014;**7**:1174–80.
8. Piorkowski C, Sih H, Sommer P, Miller SP, Gaspar T, Teplitsky L *et al.* First in human validation of impedance-based catheter tip-to-tissue contact assessment in the left atrium. *J Cardiovasc Electrophysiol* 2009;**20**:1366–73.
9. van Es R, Hauck J, van Driel VJHM, Neven K, van Wessel H, Doevendans PA *et al.* Novelmethod for electrode-tissue contact measurementwithmulti-electrode catheters Rene. *Europace* 2018;**20**:149–56.
10. Gaspar T, Sih H, Hindricks G, Eitel C, Sommer P, Kircher S *et al.* Use of electrical coupling information in AF catheter ablation: a prospective randomized pilot study. *Heart Rhythm* 2013;**10**:176–81.
11. Gunawardene MA, Hoffmann BA, Schaeffer B, Chung D-U, Moser J, Akbulak RO *et al.* Influence of energy source on early atrial fibrillation recurrences: a comparison of cryoballoon vs. radiofrequency current energy ablation with the endpoint of unexcitability in pulmonary vein isolation. *Europace* 2018;**20**:43–9.
12. Vogler J, Willems S, Sultan A, Schreiber D, Lüker J, Servatius H *et al.* Pulmonary vein isolation versus defragmentation. *J Am Coll Cardiol* 2015;**66**:2743–52.
13. Schaeffer B, Hoffmann BA, Meyer C, Akbulak RÖ, Moser J, Jularic M *et al.* Characterization, mapping and ablation of complex atrial tachycardia: initial experience with a novel method of ultra high-density 3D mapping. *J Cardiovasc Electrophysiol* 2016;**27**:1139–50.
14. Frontera A, Takigawa M, Martin R, Thompson N, Cheniti G, Massoullié G *et al.* Electrogram signature of specific activation patterns: analysis of atrial tachycardias at high-density endocardial mapping. *Heart Rhythm* 2018;**15**:28–37.
15. Garcia-Bolao I, Ballesteros G, Ramos P, Menendez D, Erkiaga A, Neglia R *et al.* Identification of pulmonary vein reconnection gaps with high-density mapping in redo atrial fibrillation ablation procedures. *Europace* 2018;**20**:f351–8.
16. Nguyen DT, Zipse M, Borne RT, Zheng L, Tzou WS, Sauer WH. Use of tissue electric and ultrasound characteristics to predict and prevent steam-generated cavitation during high-power radiofrequency ablation. *J Am Coll Cardiol* 2018;**4**:491–500.
17. Fallert MA, Mirotznik MS, Downing SW, Savage EB, Foster KR, Josephson ME *et al.* Myocardial electrical impedance mapping of ischemic sheep hearts and healing aneurysms. *Circulation* 1993;**87**:199–207.
18. Lang CCE, Gugliotta F, Santinelli V, Mesas C, Tomita T, Vicedomini G *et al.* Endocardial impedance mapping during circumferential pulmonary vein ablation of atrial fibrillation differentiates between atrial and venous tissue. *Heart Rhythm* 2006;**3**:171–8.
19. Reddy VY, Shah D, Kautzner J, Schmidt B, Saoudi N, Herrera C *et al.* The relationship between contact force and clinical outcome during radiofrequency catheter ablation of atrial fibrillation in the TOCCATA study. *Heart Rhythm* 2012;**9**:1789–95.
20. Neuzil P, Reddy VY, Kautzner J, Petru J, Wichterle D, Shah D *et al.* Electrical reconnection after pulmonary vein isolation is contingent on contact force during initial treatment: results from the EFFICAS I study. *Circ Arrhythm Electrophysiol* 2013;**6**:327–33.
21. Shah DC, Lambert H, Nakagawa H, Langenkamp A, Aeby N, Leo G. Area under the real-time contact force curve (force-time integral) predicts radiofrequency lesion size in an in vitro contractile model. *J Cardiovasc Electrophysiol* 2010;**21**:1038–43.

ESC European Society of Cardiology

Europace (2019) **21**, i43–i53
doi:10.1093/europace/euy188

CLINICAL RESEARCH

An initial experience of high-density mapping-guided ablation in a cohort of patients with adult congenital heart disease

Sabine Ernst[1]*, Ilaria Cazzoli[1], and Silvia Guarguagli[1,2,3]

[1]Department of Cardiology, Royal Brompton and Harefield Hospital, Imperial College London, Sydney Street, SW3 6NP London, UK; [2]Division Of Cardiology, Fondazione IRCCS Policlinico San Matteo, Pavia, Italy; and [3]School of Cardiovascular Disease, University of Pavia, Fondazione IRCCS Policlinico San Matteo, Pavia, Italy

Received 8 April 2018; editorial decision 10 June 2018; accepted 31 October 2018

Aims In the management of both ventricular and supraventricular tachycardia in patients with congenital heart disease (CHD) catheter ablation has now been recognized as one of the mainstays.

Methods and results We review our initial experience of using the Rhythmia mapping system in a cohort of 12 adult CHD patients presenting with multiple arrhythmia substrates. A total of 78 arrhythmia maps were attempted in a total of 15 procedures, but possible due to the dilatation of the target chamber only 44% of maps were able to reconstruct the entire arrhythmia. All patients underwent pre-procedure 3D imaging (either cardiac magnetic resonance or computed tomography), but image integration was suboptimal. A median of two maps per patient were finally analysed and acquisition took in median 22 min with a median number of 12 574 (8230–18 167) mapping points. Procedural data with a total duration amounting to in median 285 (194–403) min, with a median total fluoroscopy exposure of 7.5 (5.2–10.7) min. After a median of 1.5 procedures [median of 12 (8–16 months)], nine patients remained in stable sinus rhythm or atrial paced rhythm, while three patients had further sustained recurrences. One of these passed away in end-staged heart failure.

Conclusion This initial experience of using high-density mapping for arrhythmia management in patients with CHD allowed rapid acquisition of multiple maps with high accuracy to identify surgical scars and fibrosis, however, it was limited by large atrial volumes and a high percentage of incomplete maps resulting in modest clinical success.

Keywords Catheter ablation • Multielectrode mapping • Congenital heart disease • Arrhythmias

Introduction

In the management of both ventricular and supraventricular tachycardia in patients with congenital heart disease (CHD) catheter ablation has now been recognized as one of the mainstays.[1–6] The majority of arrhythmia substrates in CHD patients is re-entrant in nature and frequently caused by the preceding surgical interventions, which result in scar tissue (e.g. atriotomy scars) that can create protected channels of conduction that can serve as critical isthmuses in re-entrant circuit tachycardia.[7–9] This was also convincingly demonstrated for the most frequent CHD Tetralogy of Fallot (ToF) with scar-defined re-entrant circuits that serve as the substrate for sustained ventricular tachycardia (VT).[10] However, also patients with non-palliated CHD can suffer from sustained arrhythmias, mostly caused by significant chamber dilatation. The success of atrial tachycardia (AT) ablation in CHD is largely influenced by the underlying cardiac anatomy and surgical repair, along with the current haemodynamic sequelae of the anatomy and repairs.

We review our initial experience of using the Rhythmia mapping system to a cohort of adult CHD patients presenting with arrhythmias in a single centre.

Methods

Patients with CHD and sustained arrhythmia were studied using the Rhythmia mapping system (Boston Scientific) from November 2015 to

* Corresponding author. Tel: +44 20 7351 8612; fax: +44 20 7351 8131. *E-mail address:* s.ernst@rbht.nhs.uk

What's new?

- First experience of high-density mapping in a cohort of complex patients with congenital heart disease.
- Rapid multi-electrode mapping of multiple arrhythmias.
- High-resolution depiction of scars after previous surgical and ablation intervention.

March 2018 at the Royal Brompton and Harefield NHS Foundation Trust. Patients were selected to be studied using the Rhythmia system if they were listed on the waiting list for ablation CHD and had no access obstruction that would necessitate remote magnetic navigation.

Pre-procedural preparation

All patients underwent careful and comprehensive assessment of their haemodynamic condition including transthoracic echocardiography (TTE) and 3D imaging. Surgical notes were reviewed whenever available to identify surgical scars from various surgical interventions. All arrhythmia documentations were reviewed to identify the dominant arrhythmia and possible additional arrhythmia substrates including atrial fibrillation (AF).

3D imaging for road mapping

In order to understand the individual 3D anatomy, 3D DICOM datasets were reviewed and reconstructed to allow the investigators to familiarize themselves with the case ahead of the invasive procedure. Imaging DICOM datasets were either contrast cardiac computed tomographies or non-contrast cardiac magnetic resonance images (CMR). Scans were reconstructed on the Rhythmia HDx DM mapping software and merged with the 3D chamber of interest (*Figure 1*).

Invasive catheter procedure

All patients were studied in a fasted state and after informed written consent had been obtained, under assisted sedation or general anaesthesia applied by a cardiac anaesthetist with continuous invasive arterial pressure and careful fluid monitoring. Decapolar catheters (Parahis, BARD) were positioned in the coronary sinus (CS) and/or in the free wall of the right atrium (RA) to serve as timing references for the high-density mapping. The 64-pole basket mapping catheter (IntellaMap Orion; Boston Scientific), which incorporates small unidirectional electrodes (0.4 mm^2; 2.5 mm spacing) was advanced into the RA using a steerable sheath (Agilis, St Jude Medical, medium or large curve) in all but the first patient (where only a short sheath was used). In case of suspicion of a left atrium (LA) origin, a double trans-septal puncture was performed after transoesophageal echocardiography excluded an LA thrombus or via an ASD if present. Using a double trans-septal access allowed to have both the ORION and the ablation catheter in the LA without the need for exchange (which could have increased the risk of e.g. air embolism). A bidirectional mapping and ablation catheter (IntellaNav, Boston Scientific) was used in all cases.

We studied all patients on continued oral anticoagulation and vascular access was gained using ultrasound guidance. After vascular access was gained, Heparin was applied in bolus IV applications with a target activated clotting time (ACT) of 300–350 s. The ACT was tested every 30 min and further Heparin was applied if necessary.

Acquisition of the sequential high-density map

Bipolar electrograms were automatically collected during stable rhythm using the following beat acceptance criteria: (i) cycle length stability, (ii) propagation DR [difference in time in activation between two electrodes of the reference catheter (mostly decapolar catheter in CS or RA free wall)], (iii) respiration phase allowing data acquisition at a constant respiratory phase, and (iv) catheter stability. Maps and intracardiac signals were acquired predominantly through the Orion, but additional mapping was added if necessary using the ablation catheter.

Ablation settings and endpoints

After the critical isthmus or focal origin was identified, irrigated tip radiofrequency (RF) ablation was applied using 30–45 W with a flow-rate of 17 ml/min for up to 120 s and a maximum temperature of 43°C. If a linear lesion was required, the catheter was dragged along the intended ablation line once local signal abatement was achieved. At sites of arrhythmia termination, a bonus RF application was applied to assure that the final blocking lesion was transmural and long lasting. For every linear lesion deployment, the criterion of bidirectional block was attempted by pacing from both sides of the intended line.[11–14] To test for other arrhythmias, further burst pacing was performed for up to 10 s with decreasing cycle length (CL) until atrial refractoriness or 200 ms CL was reached. At least four different sites in the right and left atrium (via the CS catheter) were tested and subsequently inducible ATs were mapped and ablated. In case of AF induction, direct current cardioversion (DCCV) was performed. If deemed clinically indicated, pulmonary vein isolation was performed using the Rhythmia system as described previously.[15,16] At the end of the procedure, all catheters and sheaths were removed, and the patient was carefully monitored in the recovery or high-dependency unit.

Follow-up

Patients were followed for clinical and asymptomatic recurrences by a team of electrophysiologists and CHD specialists with regular clinic visits. Holter recordings and a 12 lead electrocardiograms (ECGs) were assessed every 6 months. Monitoring from implanted devices was also regularly reviewed. Any recurring symptoms prompted immediate review and documentation of further arrhythmias was carried out. Any sustained AT was considered for repeat ablation procedure.

Statistical analysis

Continuous variables are expressed as mean ± standard deviation, or median values with 1st and 3rd quartiles in case of non-normal distribution. If clinically relevant, minimum and maximum values are also indicated. Comparisons were assessed using the Wilcoxon test for unpaired data and a *P*-value of <0.05 was deemed significant.

Results

3D map acquisition

A total of 15 procedures were carried out in 12 patients (7 female, mean age 49 ± 10.3 years) with a total of 78 attempted arrhythmia maps (*Table 1*). Underlying CHD condition consisted of patients with moderate CHD complexity in eight and great CHD complexity in four patients, ranging from sinus venous ASD (3 patients), Ebstein's anomaly (2 patients) to double outlet right ventricle (DORV, 2 patients), and mitral (1 patient) or tricuspid atresia (1 patient) (ref. *Table 2*). Nine out of 12 patients had undergone previous ablation

procedures using 3D electroanatomical mapping (CARTO) in all cases with a single mapping and ablation electrode. Five patients had previously undergone device implantation with a dual chamber pacemaker in four and an implantable cardioverter-defibrillator in 1 patient.

Arrhythmia substrates

Besides one patient with ToF and frequent ventricular ectopy (VE) after RV VT ablation, all other patients presented with atrial arrhythmias. In one patient with Ebstein's anomaly and surgical repair of the tricuspid annulus, 'pseudo regular' AF was confirmed only by intracardiac mapping, while in further two patients AT degenerated into AF at some point during the index map (one large RA in Ebstein's anomaly and one with common atrium). Due the atrial distension and excessive scaring, the P wave morphology during AF may impose as monomorphic and occasionally pseudo regular with close to fixed PP intervals. Intracardiac mapping however revealed irregular and chaotic activation with the area that dominates the P wave being in a bystander area. Eight patients were mapped in sustained AT with four index maps of the LA, three of the RA, and one for both RA and LA.

All patients presented with markedly dilated atria with a median 3D volume mapped using the ORION catheter of 199 mL (146–251 mL). However, in 7/15 procedures, the acquired 3D map was clearly smaller than the 3D reconstructed chamber anatomy (*Figure 1*). There was no difference between source data from CMR ($n = 8$) or CT ($n = 7$).

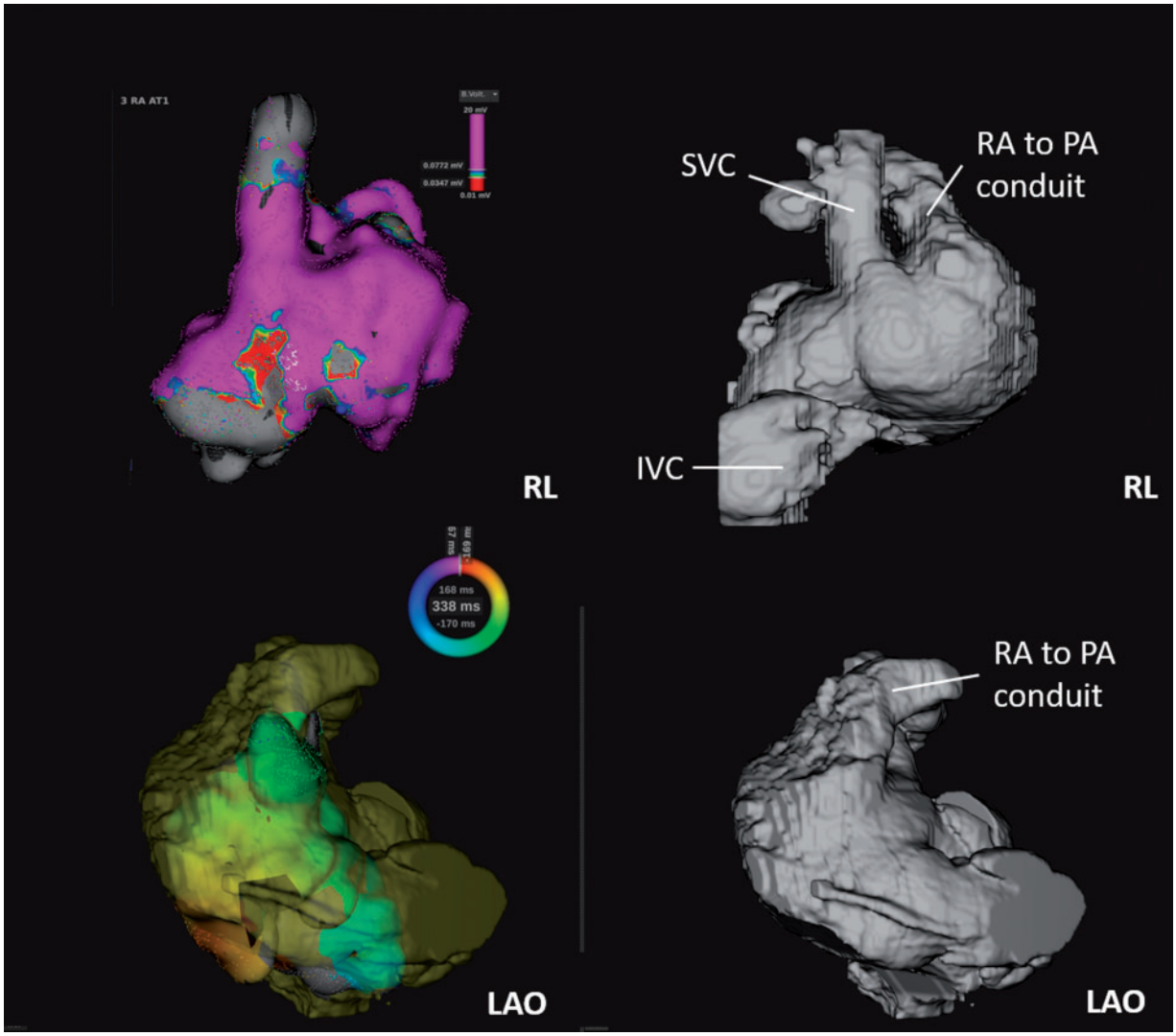

Figure 1 Example of a 3D reconstruction from cardiac magnetic resonance imaging of a patient with tricuspid atresia and modified RA to PA Fontan palliation. Right panel demonstrates reconstructions of 3D DICOM datasets to illustrate the underlying anatomy in RL and LAO projection. The left upper panel shows the electroanatomical mapping information and the left lower shows the same map superimposed on the 3D scan to illustrate the incomplete map. IVC, inferior caval vein; LAO, left anterior oblique; PA, pulmonary artery; RA, right atrium; RL, right lateral; SVC, superior caval vein.

The median CL of the mapped ATs was 345 ms (270–453 ms) with predominant 2:1 atrioventricular (AV) nodal conduction. Unfortunately, only 34/78 (44%) of maps attempted were deemed to be complete as arrhythmias were either non-sustained and terminated into sinus rhythm [(SR) 19, 24%; with mechanical termination in 9, 12%], degenerated into a different tachycardia (20, 24.5%), or into AF (5, 6%). Finally, a median number of two maps per patients were completed and analysed subsequently. Mapping time for these maps took in median 22 min with a median number of 12 574 (8230–18 167) mapping points. Index maps were typically covering the entire AT-CL when dealing with a re-entrant AT. Re-entrant mechanism was the most common AT substrate with previous atriotomy scars being the most frequently observed substrate. Cavotricuspid isthmus dependent arrhythmias were present in 4/15 procedures (*Figure 2*). We mostly observed re-entrant tachycardia but localized re-entry was also observed typically after previous ablation and/or at sites of cannulation scars (*Figure 3*).

The only patient with ventricular arrhythmia in our cohort presented with frequent monomorphic VE. The initial right ventricular (RV) map demonstrated the typical RV outflow tract patch scar and the result of a previously deployed ablation from the pulmonary valve to the tricuspid annulus (*Figure 4*). The ectopy was subsequently localized in the left ventricle close to the left ventricular (LV) summit area[17] and was mapped using the ablation catheter.

Table 1 Baseline characteristics

Patients, *n*	12
Female, *n* (%)	7 (63.6)
Age at ablation procedure (years), mean ± SD	49 ± 10.3
Previous ablations, *n* (%)	12/15 (80)
Systemic ventricular systolic function, *n* (%)	Normal, 8/12 (66.6) Mildly impaired, 2/12 (18.2) Moderately impaired, 2/12 (25)
CHD complexity score, *n*	Moderate complexity, 8/12 Great complexity, 4/12
Previous surgeries, median (IQR)	2 (1.5–2.5)
Age at first surgery (years), median (IQR)	6 (1–22)
Time surgery to first arrhythmia (years), median (IQR)	16 (2–25)
Previous device implantation, *n* (%)	PM, 4/12 (33.3) ICD, 1/12 (8.3)

Scar identification by voltage mapping

Using an initial bipolar cut-off of 0.3 mV and 0.05 mVs all maps were assessed in order to identify the previously created surgical scars and any further acquired fibrosis. This can be individualized further depending on the noise level of the local electrograms in an area of interest. The median scar area identified ranged from none to 50 cm^2. *Figure 5* illustrates the impact of different confidence levels to eliminate the low voltage area from the automatic analysis in a patient with common atrium.

Table 2 Description of congenital condition(s) and corresponding surgical procedures

Congenital conditions	Surgical procedure	Surgical scars
Ebstein's anomaly	Bidirectional Glenn, TVR	Right atriotomy, by-pass cannulation
DORV, VSD, PS	Rastelli procedure, RV to PA conduit and re-do	Right ventriculotomy, by-pass cannulation, VSD closure patch, valved homograft conduit
MA, DORV, PS and sub-PS, non-restrictive VSD, bilateral SVCs	Atrial septostomy, open PV valvotomy, PA banding	Atriotomy, RVOT, by-pass cannulation
TOF	TOF repair (open valvotomy, pericardial patch to RVOT and Dacron patch to VSD) PVR	RVOT patch and VSD closure patch, by-pass cannulation
TA, non-restrictive-VSD, bilateral SVCs, aberrant origin of left subclavian artery from aorta	Modified Fontan	Right atriotomy, by-pass cannulation, suture RAA to PA
Hypoplastic RV, ASD, VSD, PA, hypoplastic PA	Waterston shunt	(Extra-pericardial), by-pass cannulation
CoA, BAV, sub-AS	Konno procedure, AVR, CoA repair	Aortic root and LVOT, RVOT, by-pass cannulation
Complete Atrioventricular septal defect (AVSD with common atrium)	AVSD repair, LAVV repair followed by replacement	By-pass cannulation, left atriotomy
ASD, BAV	Surgical ASD closure, AVR	By-pass cannulation, right atriotomy, aortic root
ALCAPA	Takeuchi procedure	By-pass cannulation, aorta and PA
Ebstein's anomaly, PFO	Bidirectional Glenn, PFO closure, TVR	Right atriotomy, by-pass cannulation
Fenestrated sinus venosus ASD with left to right shunt	None	None

ASD, atrioseptal defect; AVSD, atrioventricular septal defect; BAV, bicuspid aortic valve; CoA, Coarctation of the Aorta; IVC, inferior caval vein; LAVV, left atrioventricular valve; LVOT, left ventricular outflow tract; PFO, persistent foramen ovale; RA, right atrium; RV, right ventricular; RVOT, right ventricular outflow tract; SVC, superior caval vein; TOF, Tetralogy of Fallot; VSD, ventricular septal defect.

In the 34 complete maps, a total of 30 critical targets were identified and subsequently successfully ablated using a median RF delivery duration of 39 (29–58.1) min. In the remaining four maps, no clear ablation target was identified, and RF ablation did not terminate the arrhythmia. Non-inducibility was achieved in 9/15 procedures and atrial fibrillation was induced as the last atrial arrhythmia in three cases. Finally, DCCV was performed in a total of four cases. Typically, the CL of the subsequently inducible arrhythmias was shorter than the index AT. Localized re-entry was typically seen only secondary to an initial re-entrant AT.

Table 3 summarizes the procedural data with a total duration amounting to in median 285 (194–403) min, with a median total fluoroscopy exposure of 7.5 (5.2–10.7) min, and 408.5 (195–1196) μGym^2 dose area product.[18]

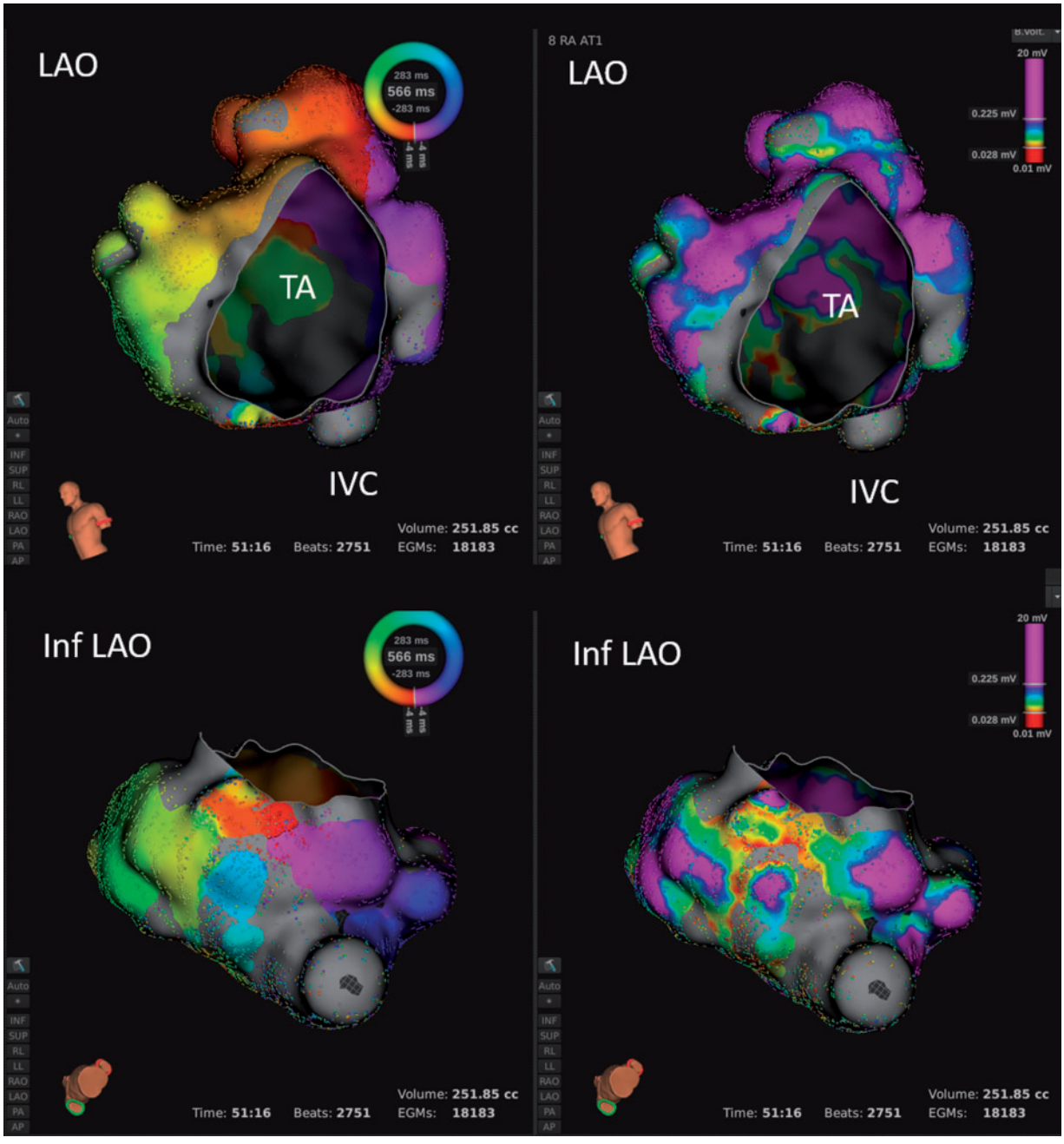

Figure 2 Example of cavotricuspid isthmus re-entry in a patient with previous ablation and common atrium (mitral atresia). Clockwise activation around the TA was confirmed and ablation terminated the slow re-entry into SR. Left panels show the local activation information, while the right panels demonstrate voltage amplitude information. IVC, inferior caval vein; LAO, left anterior oblique; TA, tricuspid annulus.

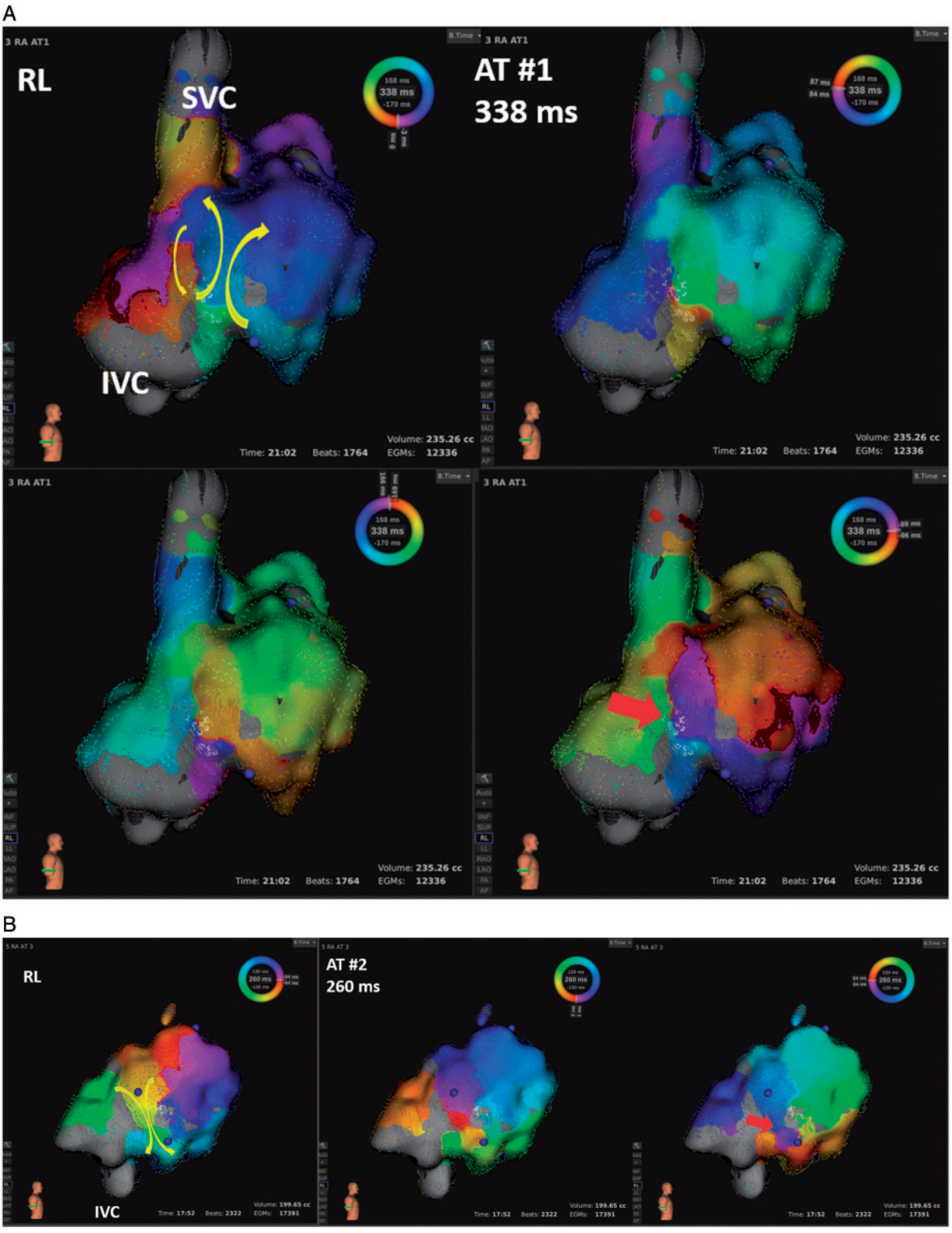

Figure 3 Multiple tachycardias in a single patient (same as in *Figure 1*) to depict various scar-related substrates. (*A*) Activation map of AT#1 with 338 ms CL showing a figure of eight re-entry with a small isthmus (red arrow). RF at this site terminated the AT into SR. (*B*) Burst pacing in the same patient induced AT#2 with a CL of 260 ms, which is remapped (please note the missing SVC). Now the figure of eight re-entry mechanism is travelling through the corridor between the two scars and ablation again terminated at the red arrow. (*C*) Further burst pacing induced AT #3 with 240 ms CL. Remap of the RA demonstrates a localized re-entry around a small central scar area more posterior than the previous scar areas (oblique posterior anterior PA projection). Again termination at the red arrow. AT, atrial tachycardia; CL, cycle length; IVC, inferior caval vein; PA, pulmonary artery; RA, right atrium; RF, radiofrequency; RL, right lateral; SR, sinus rhythm; SVC, superior caval vein.

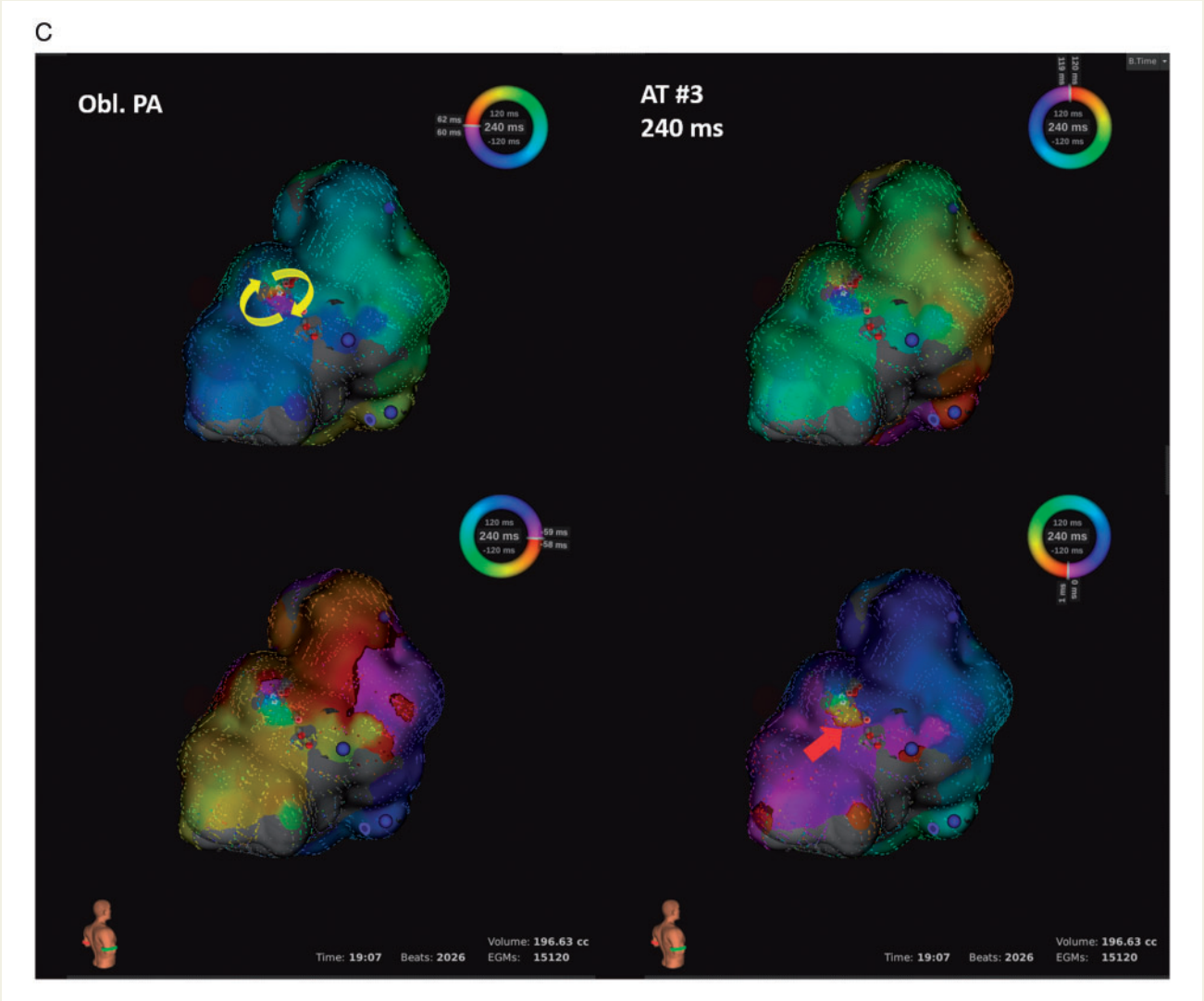

Figure 3 Continued.

Follow-up results

After the procedures all patients underwent immediate follow-up investigations which ruled out any acute complication or damage to intracardiac structures out by TTE. During a median follow-up of 12 (8–16) months, eight patients suffered from recurrent arrhythmia (66%) necessitating further invasive ablation procedures in six of them. Repeat ablation was carried out with either the Rhythmia mapping ($n = 3$) or the CARTO mapping system ($n = 3$). After a median of 1.5 procedures [median follow-up duration of 12 (8–16) months)], nine patients remained in stable SR or atrial paced rhythm, while the remaining three patients experienced further sustained arrhythmia. Antiarrhythmic medication was continued with beta-blockers in eight patients and/or Amiodarone in five patients.

One patient died 8 days after a second Rhythmia-guided AT ablation in end-stage heart failure and after initially achieving SR by RF delivery. During the short-time follow-up, this 44 years old patient had further sustained AF despite being continued on amiodarone. In the presence of a hypoplastic left ventricle with double outlet right ventricle (DORV) the right-sided AV valve was severely regurgitant but was deemed inoperable.

Predictors of success/failure

Due to the inhomogeneous cohort and the various underlying surgical settings, we were unable in this small sample size to identify factors for success or failure. Interestingly, the volume of the atrial chambers mapped or the complete vs. incomplete merge with the 3D image reconstruction did not seem to predict a more difficult procedure.

Complications

We observed no acute or late complications in any of the patients. Specifically, we did not observe any damage to valvular structures or thrombo-embolic events.

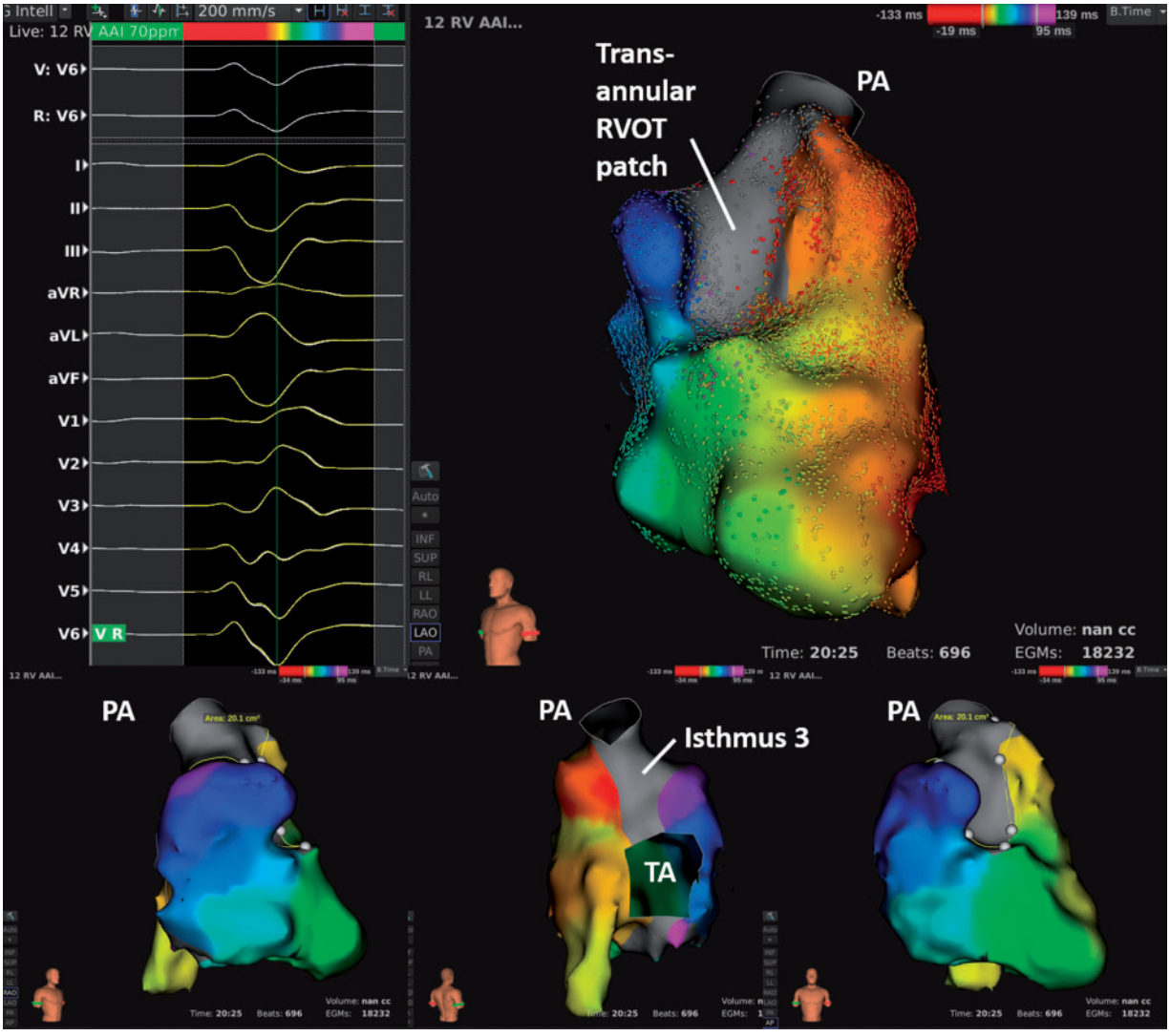

Figure 4 RV map in a patient with Tetralogy of Fallot in permanent atrial pacing. The left upper panel shows the SR with the typical right bundle branch block like QRS complex. Please note the colour range above the ECGs that is reproduced on the right upper panel as well. The outflow tract patch is transannular, and therefore, there is no Isthmus 1 (surgically created between the outflow tract patch and the pulmonary valve) and the patch area is 20.1 cm^2. Isthmus 3 (surgically created isthmus between the ventricular septum patch and the pulmonary valve) is also blocked as this patient had undergone previous VT ablation and presented now with LV ectopy. The lower three panels demonstrated three projections from RAO, oblique PA, and PA, respectively. ECG, electrocardiogram; LV, left ventricular; RAO, right anterior oblique; RV, right ventricular; SR, sinus rhythm; VT, ventricular tachycardia.

Discussion

We report on our initial experience of using the Rhythmia mapping system in a highly selected cohort of CHD patients with re-entrant or focal arrhythmia. Despite initial successful ablation, we observed a relatively high recurrence rate of 66% after the index ablation using the high-density mapping system. Clinical success after repeat ablations was achieved finally in 75% of patients during a median of 12 months follow-up period, mostly on continued anti-arrhythmic medication. This outcome is comparable to other 3D mapping systems in similar settings and demonstrates that the optimal ablation strategy for this challenging patient cohort is not necessarily depending on the 3D mapping system.[4,5,19] The specific challenges included the complete sequential acquisition of the entire target chamber, access to all regions including areas 'behind' structures such as Eustachian ridge, deployment of complete ablation lesions, and finally multiple substrates.

Advantages of multielectrode high-density mapping for CHD substrates

As reported by a number of groups previously, the major advantage of the Rhythmia system is the fast acquisition of multiple mapping points with the mini-basket and its' small electrodes.[20–23] This allows

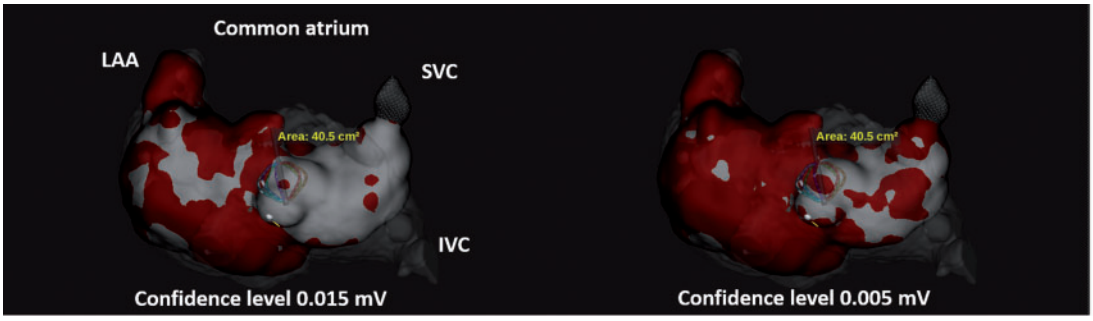

Figure 5 Example of different confidence levels (left: 0.015 mV, right: 0.005 mV), which excludes scar areas from the automatic analysis in a patient with common atrium. Please note that with the higher setting, nearly the entire RA area is depicted as scar making bystander activation most likely. This setting however needs to be individually adjusted and depends on the signal to noise ratio (ref Latcu *et al.*[22]). IVC, inferior caval vein; LAA, left atrial appendage; RA, right atrium; SVC, superior caval vein.

Table 3 Procedural data

Ablation procedures, total	15
Oral anticoagulation, *n* (%)	Warfarin, 12/15 (80%)
	NOAC, 2/15 (13.3%)
INR pre-procedure, median (IQR)	2.5 (1.9–2.7)
Baseline ECG, *n* (%)	SR, 2/15 (13.3)
	Paced, 4/15 (26.6)
	AT, 7/15 (46.6)
	AF, 2/15 (13.3)
GA, *n* (%)	12/15 (80)
Intra-procedural TOE, *n* (%)	7/15 (46.6)
Procedure time (min), median (IQR)	285 (194–403)
Fluoroscopic time, (min) median (IQR)	7.5 (5.2–10.7)
DAP (cGym^2), median (IQR)	408.5 (195–1196)

AF, atrial fibrillation; AT, atrial tachycardia; DAP, dose area product; ECG, electrocardiogram; IQR, interquartile range, SR, sinus rhythm; TOE, transoesophageal echocardiography.

depiction of scars and low voltage areas that surpass large electrode sequential mapping resolution. Especially for previously ablated areas, surgical scars, and atrial fibrosis due to chamber dilatation, this information is very valuable. Being able to 'pre-set' the confidence level allows adjusting the 'field of view'. In addition, using the rowing electrode to identify local conduction in detail is equally important in the post-processing phase. Detailed analysis is needed however to understand and interpret the acquired maps.

Disadvantage of multielectrode mapping system in its' current version

As with all novel tools, the operators needed to overcome a learning curve to get familiar with this mapping system. Especially the steerability of the mini-basket and the lack of direction indicators made the 3D mapping process challenging. Possibly, this resulted in the large amount of terminations/changes of arrhythmia in our cohort. Especially in very enlarged and abnormally formed chambers, the differentiation between scar and non-contact is difficult to make and may result in non-mapped areas. The need for a stable arrhythmia that lasts long enough to be completely mapped is an obvious further limitation for any sequential mapping system. With regard to this, the only system capable of overcoming this limitation at present is the non-invasive multielectrode mapping system ecVUE (CardioInsight),[24] which has been however limited by the 'blind spot' of septal activation with surrogate right and left atrial break-out activation.[25] Multiple maps were acquired in a very short acquisition time, but the experience in CHD patients is still limited so far.

Incomplete 3D image integration

The use of 3D image integration is a standard during CHD ablation procedures using various 3D mapping systems. The 3D roadmap helps to ascertain that all parts of a given target chamber have been mapped, such that critical isthmuses cannot be overlooked by not having mapped a given region. This is of great importance in grossly enlarged chambers. One of the established 'tricks' is to map e.g. the aortic arch to allow 'merging' of the 3D scan over this essentially non-moving structure. However, the Rhythmia system in its' current version does not allow to move all 3D reconstructions in a 'linked' fashion but moves each chamber independently. The only alternative is to merge each target chamber separately, therefore the roadmap 'guidance' nature of the pre-acquired scans is somewhat diminished. In our cohort, this resulted in incompletely merged maps in nearly half of the procedures. An incomplete map may miss a critical part of a given arrhythmia, while the 'registered' roadmap may also help to avoid pushing the mini-basket to aggressively against the myocardium, thereby avoiding mechanical ectopy and in the worst-case termination or changing the arrhythmia.

Accessibility of target chambers is another well recognized problem in CHD patients. Due to our experience with remote magnetic navigation we elected not to use the Rhythmia mapping system in patients with atrial switch for transposition of the great arteries (TGA, such as Mustard or Senning operation) or total cavo pulmonary connections (TCPC).[5] This would have required transbaffle access, resulting possibly in a higher resolution of the acquired mapping information, but most likely resulting in substantially higher radiation

exposure and procedure times. Theoretically, the ORION catheter could be advanced also in a retrograde fashion across the aortic and subsequent AV valve, but again most likely on the expense of radiation and procedure duration.[21]

Atrial fibrillation as an important clinical arrhythmia

Catheter ablation of sustained AT is an established ablation strategy which is greatly facilitated using high-density 3D mapping as shown in our experience. However, a subset of our patients also presented with sustained AF which occasionally looked pseudo-regular on the surface ECG. This is a growing clinical problem in the CHD population as patients survive longer and present with larger atrial chambers.[26]

Future outlook for high-density multielectrode mapping in congenital heart disease patients

This is our very initial experience using the Rhythmia mapping system in CHD patients, and it is obviously not yet a fully evolved strategy. Having struggled much with changing arrhythmias and multiple substrates, we would propose a different approach: In a first attempt, a complete map of the target chamber in stable sinus or paced rhythm could identify all conduction barriers (previous surgical scars or previous ablation lines). This should be followed by 'closure' of potential conduction gaps through obvious pathways such as the cavotricuspid isthmus, corridors between atriotomy scars, and Crista terminalis or the AV annulus and finally from cannulation scars to the inferior or superior caval veins. These ablations should be carried out with the best possible prediction of complete trans-murality (e.g. contact force), which is currently not available for this mapping system. As CHD patients may present with much thicker myocardium even in the atria, direct visualization may even be needed to achieve durable transmural lesions. Once all ablation targets have been completed during stable rhythm, pacing attempts should be made to identify additional sustained arrhythmias. Focussed mapping in the region of interest alone during short lasting arrhythmia, as demonstrated elegantly by the Bordeaux group in two cases,[27,28] could potentially avoid mapping the entire and most likely grossly dilated chamber. A multicentre approach is therefore proposed to acquire enough data for the various CHD conditions to make firm recommendations.

In summary, high resolution mapping is definitely helpful when addressing the complex cohort of CHD patients. However, the system needs to undergo substantial improvements with regards to image integration and especially implementation of contact force measurements to assure best lesion deployment.

Limitations

This is a retrospective analysis of the use of the Rhythmia mapping system in a highly selected patient cohort with complex CHD conditions that mostly had failed previous ablation attempts. Moreover, the cohort itself is very heterogeneous and especially the size of the target chamber made complete mapping a substantial challenge. The operators' learning curve with both the manipulation of the mini-basket catheter and the map settings need to be taken into consideration when judging the outcome of these ablations, aiming at mapping sustained arrhythmia which may not be the optimal strategy given the current limitations.

Conclusions

This initial experience of using high-density mapping for arrhythmia management in patients with CHD allowed rapid acquisition of multiple maps with high accuracy to identify surgical scars and fibrosis. It was limited by the large atrial volumes, a high percentage of incomplete maps and a median of six arrhythmias per patient, resulting in a modest clinical success and need for re-ablation. Further improvements such as full 3D image integration and contact force assessment will make this novel multielectrode sequential mapping system hopefully a game changer in the near future.

Acknowledgements

The authors wish to thank Jeff Cooper (Boston Scientific) for his expert technical support.

Conflict of interest: none declared.

References

1. Khairy P, Van Hare GF, Balaji S, Berul CI, Cecchin F, Cohen MI *et al.* PACES/HRS Expert Consensus Statement on the Recognition and Management of Arrhythmias in Adult Congenital Heart Disease: developed in partnership between the Pediatric and Congenital Electrophysiology Society (PACES) and the Heart Rhythm Society (HRS). Endorsed by the governing bodies of PACES, HRS, the American College of Cardiology (ACC), the American Heart Association (AHA), the European Heart Rhythm Association (EHRA), the Canadian Heart Rhythm Society (CHRS), and the International Society for Adult Congenital Heart Disease (ISACHD). *Heart Rhythm* 2014;**30**:e1–65.
2. Page RL, Joglar JA, Caldwell MA, Calkins H, Conti JB, Deal BJ *et al.* 2015 ACC/AHA/HRS guideline for the management of adult patients with supraventricular tachycardia: executive summary: a report of the American College of Cardiology/American Heart Association Task Force on Clinical Practice Guidelines and the Heart Rhythm Society. *Circulation* 2016;**133**:e471–505.
3. Baumgartner H, Bonhoeffer P, De Groot NM, de Haan F, Deanfield JE, Galie N *et al.* ESC Guidelines for the management of grown-up congenital heart disease (new version 2010). *Eur Heart J* 2010;**31**:2915–57.
4. Yap SC, Harris L, Silversides CK, Downar E, Chauhan VS. Outcome of intra-atrial reentrant tachycardia catheter ablation in adults with congenital heart disease: negative impact of age and complex atrial surgery. *J Am Coll Cardiol* 2010;**56**:1589–96.
5. Ueda A, Suman-Horduna I, Mantziari L, Gujic M, Marchese P, Ho SY *et al.* Contemporary outcomes of supraventricular tachycardia ablation in congenital heart disease: a single-center experience in 116 patients. *Circ Arrhythm Electrophysiol* 2013;**6**:606–13.
6. Hernandez-Madrid A, Paul T, Abrams D, Aziz PF, Blom NA, Chen J *et al.* Arrhythmias in congenital heart disease: a position paper of the European Heart Rhythm Association (EHRA), Association for European Paediatric and Congenital Cardiology (AEPC), and the European Society of Cardiology (ESC) Working Group on Grown-up Congenital heart disease, endorsed by HRS, PACES, APHRS, and SOLAECE. *Europace* 2018;**20**:1719–53.
7. Ueda A, Adachi I, McCarthy KP, Li W, Ho SY, Uemura H. Substrates of atrial arrhythmias: histological insights from patients with congenital heart disease. *Int J Cardiol* 2013;**168**:2481–6.
8. Walsh EP, Cecchin F. Arrhythmias in adult patients with congenital heart disease. *Circulation* 2007;**115**:534–45.
9. Nakagawa H, Shah N, Matsudaira K, Overholt E, Chandrasekaran K, Beckman KJ *et al.* Characterization of reentrant circuit in macroreentrant right atrial tachycardia after surgical repair of congenital heart disease: isolated channels between scars allow "focal" ablation. *Circulation* 2001;**103**:699–709.
10. Zeppenfeld K, Schalij MJ, Bartelings MM, Tedrow UB, Koplan BA, Soejima K *et al.* Catheter ablation of ventricular tachycardia after repair of congenital heart disease: electroanatomic identification of the critical right ventricular isthmus. *Circulation* 2007;**116**:2241–52.
11. Shah D, Haissaguerre M, Takahashi A, Jais P, Hocini M, Clementy J. Differential pacing for distinguishing block from persistent conduction through an ablation line. *Circulation* 2000;**102**:1517–22.

12. Miyazaki S, Shah AJ, Jadidi AS, Scherr D, Wilton SB, Hocini M *et al*. Instantaneous electrophysiological changes characterizing achievement of mitral isthmus linear block. *J Cardiovasc Electrophysiol* 2011;**22**:1217–23.
13. Ernst S, Ouyang F, Clausen C, Goya M, Ho SY, Antz M *et al*. A model for *in vivo* validation of linear lesions in the right atrium. *J Interv Card Electrophysiol* 2003;**9**: 259–68.
14. Ernst S, Ouyang F, Lober F, Antz M, Kuck KH. Catheter-induced linear lesions in the left atrium in patients with atrial fibrillation: an electroanatomic study. *J Am Coll Cardiol* 2003;**42**:1271–82.
15. Anter E, Tschabrunn CM, Contreras-Valdes FM, Li J, Josephson ME. Pulmonary vein isolation using the Rhythmia mapping system: verification of intracardiac signals using the Orion mini-basket catheter. *Heart Rhythm* 2015;**12**:1927–34.
16. Rottner L, Metzner A, Ouyang F, Heeger C, Hayashi K, Fink T *et al*. Direct comparison of point-by-point and rapid ultra-high-resolution electroanatomical mapping in patients scheduled for ablation of atrial fibrillation. *J Cardiovasc Electrophysiol* 2017;**28**:289–97.
17. Enriquez A, Malavassi F, Saenz LC, Supple G, Santangeli P, Marchlinski FE *et al*. How to map and ablate left ventricular summit arrhythmias. *Heart Rhythm* 2017; **14**:141–8.
18. Heidbuchel H, Wittkampf FH, Vano E, Ernst S, Schilling R, Picano E *et al*. Practical ways to reduce radiation dose for patients and staff during device implantations and electrophysiological procedures. *Europace* 2014;**16**:946–64.
19. Wasmer K, Eckardt L. Management of supraventricular arrhythmias in adults with congenital heart disease. *Heart* 2016;**102**:1614–9.
20. Frontera A, Takigawa M, Martin R, Thompson N, Cheniti G, Massoullie G *et al*. Electrogram signature of specific activation patterns: analysis of atrial tachycardias at high-density endocardial mapping. *Heart Rhythm* 2018;**15**:28–37.
21. Viswanathan K, Mantziari L, Butcher C, Hodkinson E, Lim E, Khan H *et al*. Evaluation of a novel high-resolution mapping system for catheter ablation of ventricular arrhythmias. *Heart Rhythm* 2017;**14**:176–83.
22. Latcu DG, Bun S-S, Viera F, Delassi T, El Jamili M, Al Amoura A *et al*. Selection of critical isthmus in scar-related atrial tachycardia using a new automated ultra-high resolution mapping system. *Circ Arrhythm Electrophysiol* 2017;**10**:e004510.
23. Anter E, McElderry TH, Contreras-Valdes FM, Li J, Tung P, Leshem E *et al*. Evaluation of a novel high-resolution mapping technology for ablation of recurrent scar-related atrial tachycardias. *Heart Rhythm* 2016;**13**:2048–55.
24. Ernst S, Saenen J, Rydman R, Gomez F, Roy K, Mantziari L *et al*. Utility of noninvasive arrhythmia mapping in patients with adult congenital heart disease. *Card Electrophysiol Clin* 2015;**7**:117–23.
25. Shah AJ, Hocini M, Xhaet O, Pascale P, Roten L, Wilton SB *et al*. Validation of novel 3-dimensional electrocardiographic mapping of atrial tachycardias by invasive mapping and ablation: a multicenter study. *J Am Coll Cardiol* 2013;**62**: 889–97.
26. Labombarda F, Hamilton R, Shohoudi A, Aboulhosn J, Broberg CS, Chaix MA *et al*. Increasing prevalence of atrial fibrillation and permanent atrial arrhythmias in congenital heart disease. *J Am Coll Cardiol* 2017;**70**:857–65.
27. Hooks DA, Yamashita S, Capellino S, Cochet H, Jais P, Sacher F. Ultra-rapid epicardial activation mapping during ventricular tachycardia using continuous sampling from a high-density basket (Orion(TM)) catheter. *J Cardiovasc Electrophysiol* 2015;**26**:1153–4.
28. Takigawa M, Frontera A, Thompson N, Capellino S, Jais P, Sacher F. The electrical circuit of a hemodynamically unstable and recurrent ventricular tachycardia diagnosed in 35 s with the Rhythmia mapping system. *J Arrhythm* 2017;**33**: 505–7.

EP-614903-AA